Addendum

Synthesis and metabolism of Δ^5-cholestene-3β,12α-diol. Bile acids and steroids 113.

Arkiv för Kemi *17*, 381 (1961)

By Henry Danielsson

Add to line 39 on page 382: Calculated for $C_{27}H_{44}O_2$: C, 80.9 %; H, 11.1 %. Found: C, 81.1 %; H, 11.2 %.

ARKIV FÖR KEMI Band 17 nr 26

Communicated 7 December 1960 by KARL MYRBÄCK and ARNE FREDGA

Acid-induced aromatic hydrogen exchange. V

Discussion of reaction mechanism

By LARS MELANDER

With 7 figures in the text

1. Introduction

From recent work on the electrophilic aromatic hydrogen exchange and related phenomena it seems that the Zucker–Hammett hypothesis using the h_0 scale [1] does not hold for this type of acid-catalyzed reaction. Kresge and Chiang [2] have shown that a compound such as 1,3,5-trimethoxybenzene is not a good Hammett base, as the formation of a conjugate acid by the addition of a proton from aqueous perchloric acid at a nuclear carbon atom follows an acidity function very close to $h'_R = h_R \cdot a_{H_2O}$ rather than h_0. This means that rough parallelism of a reaction rate to any other function which rises less steeply with increasing acidity (e.g. h_0 or the concentration of H_3O^+ ion) is likely to indicate incomplete transfer of the proton in the transition state. Such a behaviour has been observed for the acid-induced hydrogen exchange of trimethoxybenzene.

Eaborn and Taylor [3] have recently found that the rate of hydrogen exchange of benzene and toluene in strong sulphuric acid is much more accelerated by increasing acidity than expected. In the strongest acid used (up to 84 %) the rate of the detritiation of benzene follows approximately

$$\frac{d \log_{10} k}{d(-H_0)} = 2.2$$

which means an acidity dependence steeper than the function h'_R or even the function h_R.

With benzene and toluene we do not know the true acidity dependence of the conjugate-acid formation. Gold and Tye [4] found with di- and triarylethylenes in the heterogeneous system of cyclohexane and aqueous sulfuric acid of concentrations comparable to those used with benzene and toluene that

$$\frac{d \log_{10} (c_{HB^+}/c'_B)}{d(-H_0)} \approx 2.2$$

in the region 84–89 % acid and up to 2.7 in 95–98 % acid (c_{HB+} denotes the concentration of conjugate acid in the acid phase, c'_B that of the corresponding hydrocarbon in the cyclohexane phase). They assumed that the hydrocarbons in question behaved as true Hammett bases and accounted for the excess slope by a salting-in effect, i.e., by a decrease of the activity coefficient of the neutral hydrocarbon in the acid phase. In view of the results of Deno and Perizzolo [5] such a large variation of the activity coefficient now seems unlikely, a more reasonable value being something like a tenth of the slope observed. Olsson's [6] values on the solubility of toluene in roughly 70 and 80 % sulphuric acid indicate the same order of magnitude of the variation.

In this connection it should also be mentioned that Olsson [7] reported a value

$$\frac{d \log_{10} k_{obs}}{d(-H_0)} = 1.97$$

in preliminary experiments on the dedeuteration of toluene-3-*d* in heterogeneous experiments with 81 % aqueous sulphuric acid. The variation of k_{obs} includes that of the true rate and that of the solubility. If the latter is fairly small, the agreement with the results of Eaborn and Taylor is good.

From these results it is obvious that neither the rate of the hydrogen exchange of toluene and benzene nor the protonation of arylethylenes follows the Hammett acidity function. On the other hand, the acidity dependence of the two phenomena seems to be the same, and if the two groups of compounds are actually comparable, a complete transfer of the proton in the transition state of the exchange is indicated. The reasoning carried through by Melander and Myhre [8] is still applicable to the new findings if the acidity scale is now thought of as defined by the arylethylenes instead of Hammett indicators, which are not useful for the present purpose. In any case, the very strong acceleration of the hydrogen exchange of benzene and toluene by increasing acidity seems to be most easily explained if water could be excluded from the transition state, because any inclusion of water tends *per se* to decrease such an acceleration.

The possible absence of the conjugate base of the attacking acid from the transition state has been made intelligible in terms of a rapid pre-equilibrium [9], but, as shown by Melander and Myhre [8], such a pre-equilibrium is neither required nor proved by the kinetics. It seems that there have been difficulties in conceiving a single-step proton transfer having a transition state without interaction between the proton and the base that delivered it or is going to accept it, respectively. There are points of view, however, according to which such a behaviour might seem fairly reasonable and also the difference in behaviour between more and less reactive aromatic compounds is conceivable. According to the same picture the existence of a pre-equilibrium is reduced to a question of secondary importance. However the true experimental behaviour may be, the following principles should be kept in mind in discussions of the mechanism of hydrogen exchange, and to a considerable extent they are also applicable to other types of aromatic substitution reactions.

One important point must be kept in mind on dealing with kinetics. As long as we believe in the principles of the transition-state theory we have also to admit that a study of the reaction rate gives us a single picture of the transition state rather than a full movie of the course of the atomic rearrangement. It follows that pre-equilibria, which adjust themselves rapidly or bond breakings and bond formations, which are not begun in the transition state, have to be revealed in some other way.

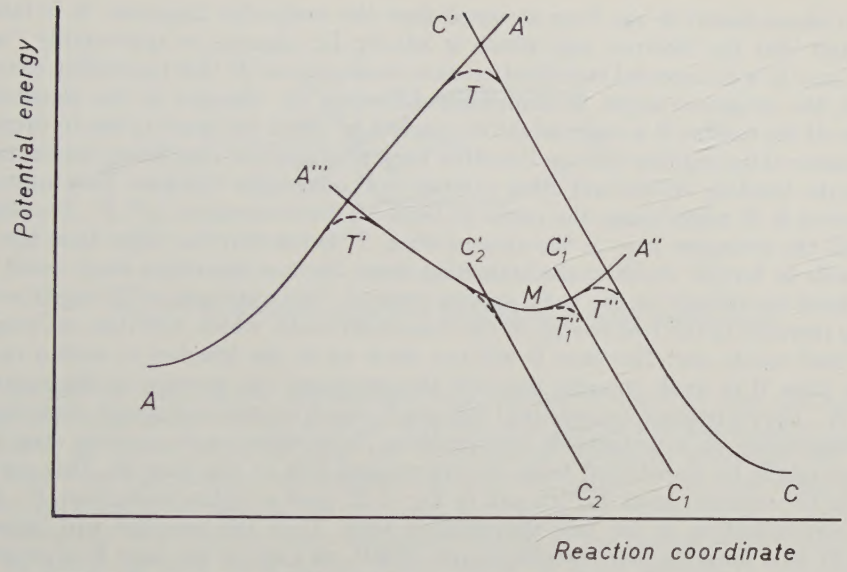

Fig. 1. Potential-energy diagram for hypothetical hydrogen transfer reactions.

2. Kinetic consequences of the possibility of internal stabilization in one of the reactants

What has caused considerable trouble in the understanding of hydrogen-cation transfer reactions is the general feeling that naked hydrogen nuclei cannot possibly have any independent existence in solutions but must be associated with some basic species. An equivalent statement would be that the free energy of solvation of the proton is so high that it pays energetically for it to join with almost any other molecule and certainly with those having lone electron pairs.

All this is certainly true, and in an ordinary transfer the reaction path could be represented by the curve ATC in Fig. 1. The branch AA' represents the dissociation energy of the reactant RH into R^- and H^+. If no base intervenes a very high potential energy level will be reached before the dissociation is complete. If there is a basic species B, however, which will act as an acceptor, a transition state, i.e., a potential energy maximum T along the reaction coordinate, might be reached at a reasonable potential energy, because the proton will never need to be entirely free. The branch CC' represents the corresponding dissociation of BH^+ into B and H^+, and in the transition state the situation might be described as one of resonance:

$$R{-}H \quad :B \quad \longleftrightarrow \quad R\ddot{:} \quad H{-}B^+$$

which resonance rounds off the curve at T.

In the present case B certainly stabilizes the transition state which, in the absence of B, would come at higher energy levels. The transition state of the lowest possible free energy compatible with the composition of the system will generally be responsible for the formation of the major part of the products. Thus the base B will be involved in the kinetics.

In the above model it has been assumed that the molecular fragment R is fairly simple and that the electron pair which is left by H^+ cannot be appreciably "absorbed" into R with internal stabilization as a consequence. If this possibility exists, however, the situation might be somewhat different. By changes in the electronic structure of the residue R a stage might be reached in which the bond to the hydrogen has lost some of its stability but, on the other hand, an incipient stabilizing interaction between the bonding orbital and other orbitals in R outweighs this loss. This internal stabilization in R might cause the curve to bend off downwards as $AT'A''$. Provided R^- is still the strongest base in the system when T' is reached, no other base like B will be able to further stabilize the transition state. Such a transition state could be said to have no affinity to the basic species present. The approach of B might even cause an increase in the free energy of the transition state, which will then no longer be the most stable one. The base B will not show up in the kinetics in such a case.

If the base B is weak enough, but still the strongest one present in the system besides R^-, the rearranged (isomerized) RH might reach a potential energy minimum, M, corresponding to a metastable intermediate. In a subsequent reaction step the hydrogen might be transferred from the rearranged RH to the base B. This corresponds to the reaction path $MT''C$, and in Fig. 1 T' is at a higher level than T'', the former corresponding to the rate-determining step. Thus the reaction will behave kinetically as a unimolecular rearrangement of RH, as long as the base B is present in sufficient concentration. The reaction path $AT'MT''C$ corresponds simply to a two-stage reaction with a rate-determining first step.

If we add to the system a stronger base $B_{(1)}$, the dissociation energy curve of $B_{(1)}H^+$ might be represented by the curve branch C_1C_1' below CC' and the second transition state will come at T_1''. The reaction is still two-stage.

When the strength of the base increases beyond a certain limit, the base dissociation curve might cut the curve $AT'M$ between T' and M, as does the dissociation curve C_2C_2' of $B_{(2)}H^+$. The sequence represents a smooth transition from a two-stage to a single-stage mechanism. The reaction path $AT'C_2$ has but one transition state and no intermediate. Still the base $B_{(2)}$ does not stabilize the transition state and will not be involved in the kinetics as long as it is present in a sufficient concentration.

Perhaps the best way to explain the bending downwards of the curve $AT'M$ is to say that RH exists in two isomeric forms, corresponding to the curves AA' and $A'''A''$, and that these are in resonance at T'.

In the case represented by the reaction path $AT'C_2$ the intermediate M will never exist in its equilibrium conformation and it could be referred to as a "virtual intermediate", since a real intermediate should be able to exist in its equilibrium conformation for a couple of thermal collisions, or, at least, correspond to a minimum in the actual reaction path.

3. Electronic behaviour in aromatic molecules during the electrophilic hydrogen exchange reaction

It is now generally agreed that the ordinary electrophilic aromatic substitution reactions proceed according to an additive two-stage mechanism. The first step involves the addition of an electrophilic entity to a pair of electrons which are localized from the π-electron system of the molecule onto one of the carbon atoms.

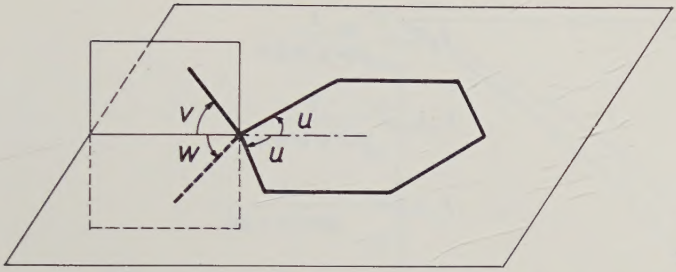

Fig. 2. The different angles at a hybridizing aromatic carbon atom.

In the second step, which corresponds to a reversal of the first one, the hydrogen attached to the same carbon atom is expelled as a proton and the π-electron system restored. It seems probable that the electrophilic hydrogen exchange will follow the same reaction pattern, the entering electrophilic entity in this case being another hydrogen nucleus, isotopic to the one being replaced if the reaction is to be observable.

During the two reaction steps the hybridization at the carbon atom changes from sp^2 to about sp^3 and back again. There might be some interest in following this change somewhat more in detail, although, it should be admitted, a treatment including only s and p orbitals implies certainly a fairly rough simplification. Nevertheless the salient features of the changes could be expected to be reflected by the following simple picture.

It seems reasonable to confine the directions of the two carbon–hydrogen bonds to a plane perpendicular to the ring plane and bisecting the angle between the bonds from the carbon atom to the two neighbouring carbon atoms. There seems to be little reason to expect the ring to be other than planar during the reaction. If some particular value is assigned to the C–C–C angle, the orthogonality conditions will deliver a relation between the principal directions of the extra-annular carbon orbitals as well as expressions for the fractional s and p character of each orbital as a function of one of these directions.

Fig. 2 shows the two perpendicular planes, the large one containing the aromatic ring, the small one the carbon–hydrogen bonds. Thus the angles u are measured within the large plane, the angles v and w within the small one. An angle zero means that the respective bond coincides with the line of intersection of the two planes, or its extension.

Following Coulson [10] we write the (normalized) hybrid which has its maximum in the direction denoted by i as

$$\frac{s+\lambda p_i}{\sqrt{1+\lambda^2}}$$

where s is the $2s$ orbital and p_i the particular $2p$ orbital which has the positive direction of its symmetry axis pointing in the direction i. λ is a parameter.

The condition of orthogonality between the different pairs of hybrids gives

$$\lambda_u^2 = -\frac{1}{\cos 2u}$$

$$\lambda_u \lambda_v = \frac{1}{\cos u \cos v}$$

$$\lambda_u \lambda_w = \frac{1}{\cos u \cos w}$$

$$\lambda_v \lambda_w = -\frac{1}{\cos (v + w)}$$

where the λ's are indexed by the respective angle notations. These equations give the following relation between the angles:

$$\cot v \cot w = 1 - \cot^2 u$$

The parameters λ can be determined from the expressions

$$\lambda_u = \frac{1}{\sqrt{-\cos 2u}}$$

$$\lambda_v = \frac{\sqrt{\text{tang}^2 u - 1}}{\cos v}$$

$$\lambda_w = \frac{\sqrt{\text{tang}^2 u - 1}}{\cos w}$$

If reasonable values are assigned to the angle u during the changes in v and w, the orbitals v and w can be followed as to direction and fractional s character, these magnitudes being regarded as functions of, say, the angle v.

In the unperturbed benzene molecule u is 60°, but when both directions v and w deviate considerably from 90° the conjugation will certainly be decreased between the carbon atom concerned and its neighbours. It seems natural to assume that the corresponding carbon–carbon bonds are somewhat lengthened and have the s character of their σ bonds slightly decreased, the angle u decreasing somewhat. This will also allow some increase in other ring angles, and carbon atoms engaged in the formation of bonds with high double-bond character will have the possibility of increasing the s character of the σ bonds concerned. Such changes within the ring are likely to decrease the overall energy and hence they are likely to occur.

It seems reasonable to study the interrelation of the directions v and w and the different λ's for $u = 60°$ and for u equal to half the tetrahedral angle, $u = 54°7$, the latter representing the lower values that u might acquire when the bonds to the adjacent carbon atoms have lost a considerable part of their double-bond character. The qualitative conclusions to be drawn below are not particularly dependent on the details of these assumptions.

Fig. 3 shows the interrelation of the angles v and w. Fig. 4 gives the fractional s character, $(1 + \lambda^2)^{-1}$, of the orbitals v and w as functions of the angle v. The two lines outside the right-hand frame indicate the corresponding magnitude for the orbitals u, these quantities being dependent only on the choice of the angle u. Fig. 5 shows in the same way the Pauling–Sherman bond strength P, i.e., the maximum

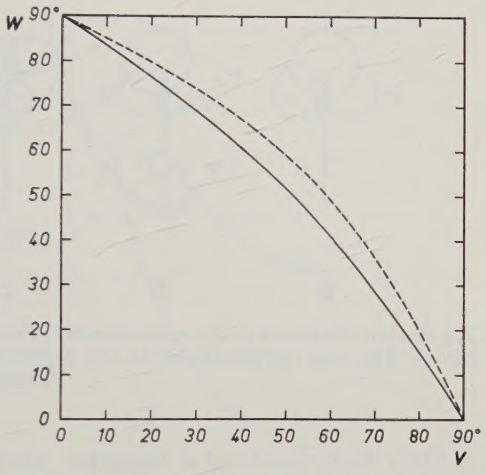

Fig. 3. Interrelation of the angles v and w. Full curve, $u = 60°$; dashed curve, $u =$ half tetrahedral angle.

value of the wave function when the components of the latter are represented by their angular part, normalized to 4π (see, for instance, ref. [10]),

$$P = \frac{1 + \lambda\sqrt{3}}{\sqrt{1 + \lambda^2}}$$

The interrelation between the amount of s character or the "strength" of a carbon orbital and the actual energy of bond formation with hydrogen is far from simple.

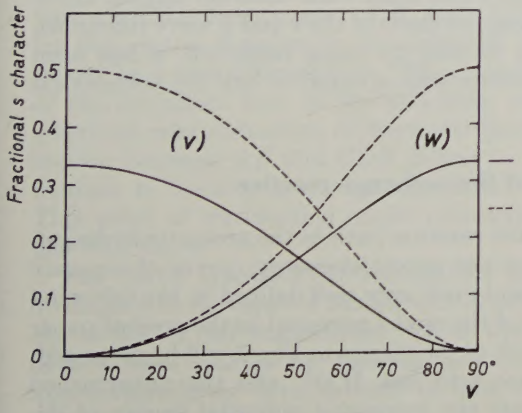

Fig. 4.

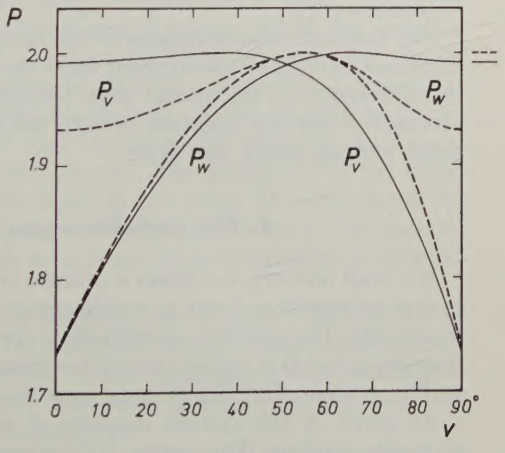

Fig. 5.

Fig. 4. Fractional s character of orbitals v and w as functions of the angle v. The corresponding value for the orbitals u indicated outside the frame. Full curve, $u = 60°$; dashed curve, $u =$ half tetrahedral angle.

Fig. 5. Bond strengths of orbitals v and w as functions of the angle v. The corresponding value for the orbitals u indicated outside the frame. Full curve, $u = 60°$; dashed curve, $u =$ half tetrahedral angle.

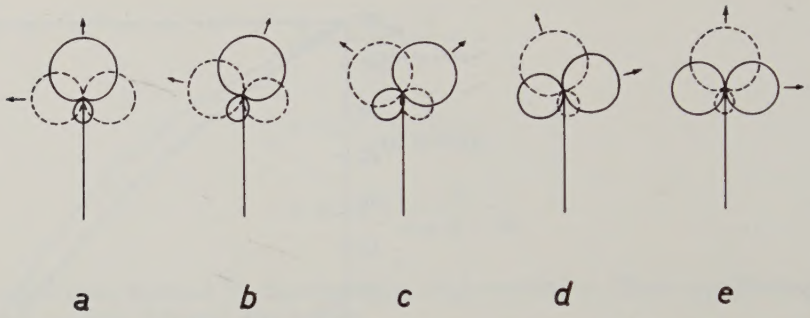

Fig. 6. Polar diagrams of the extra-annular orbitals in the v,w-plane at different stages of hybridization. The ring (perpendicular to the paper) indicated by vertical line; u assumed to be 60° throughout.

A fairly high fractional s character, about 0.5, seems to give the best bond [10], but experience from aromatic and aliphatic compounds shows that sp^2 and sp^3 orbitals give quite stable bonds, too. Thus the carbon–hydrogen bond could be expected to be quite stable as long as it does not deviate more from the ring plane than it does in the symmetric intermediate. On the other hand, it is quite obvious that the bond will lose very much in stability in approaching a position perpendicular to the ring plane. This will result from the fact that the last traces of s character are lost from the carbon orbital and that the previous hyperconjugation between the carbon–hydrogen bond and the electron-deficient π-electron system gradually turns into ordinary aromatic conjugation and probably deprives the bond of some of its electronic density. The π-complexes are known to be unstable under ordinary conditions [11].

Fig. 6 shows polar diagrams of the orbitals v and w for some different angles. These diagrams have been constructed from the angular parts of the s and p wave functions, the difference in the radial part between $2s$ and $2p$ being neglected. u has been assumed to remain constant at 60°, the picture with u equal to half the tetrahedral angle looking much the same.

4. The probable course of the exchange reaction

We shall now try to obtain a picture of the reaction path in the aromatic hydrogen exchange reaction from a consideration of the potential energy curves of separate structures. The reaction coordinate is certainly not very well defined in the following reasoning, but it is hoped that the outlines of the model proposed in the present paper will be evident. In the following each branch of the curves in Fig. 7 will be discussed.

At point A the system consists of some acid, say H_3O^+, and the unperturbed aromatic nucleus. The curve AB represents the increasing potential energy of detaching H^+ from the conjugate base of the acid, H_2O. The point D represents the conjugate acid of the aromatic molecule and is probably best thought of as a π-complex in the sense of Brown and Brady [11] rather than that of Dewar [12]. The curve DE represents the increasing energy when the π-complex is rearranged towards a σ-complex [11], and the need for energy is due to the decreasing conjugation within the aromatic π-electron system, caused by the rehybridization at the carbon.

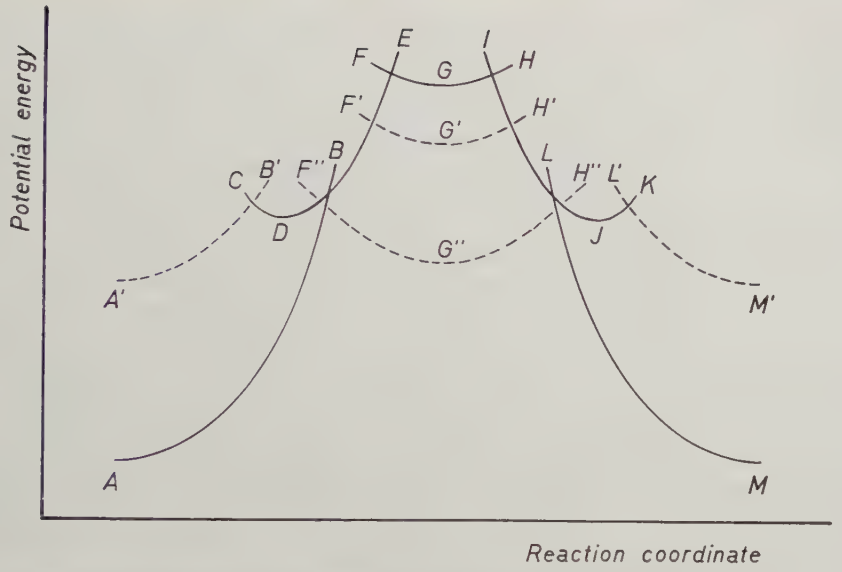

Fig. 7. Potential-energy diagram for different structures involved in aromatic hydroge n exchange Rounding off by resonance at intersections omitted for the sake of simplicity.

The relative position of curves AB and DE is such as to indicate that the π-complex in its equilibrium conformation is a stronger acid than the attacking acid. Were the attacking acid stronger, its incipient dissociation would perhaps correspond to the curve $A'B'$.[1] The curve DC represents the energy of dissociation of the π-complex into the corresponding neutral aromatic molecule and a proton. With the reaction path resulting from curves $A'B'$ and CDE, there would be some activation energy for the proton donation to the aromatic molecule, and the unperturbed π-complex would be a true intermediate. These relationships depend on the relative basicities of the conjugate base of the attacking acid and the aromatic molecule at a stage where no rehybridization of the latter has yet occurred. The possibility of the intersection between AB and CDE falling to the right of the point D comes from the increase in basicity of the carbon orbital during the rehybridization at the carbon. This point of intersection might correspond to a stage of hybridization somewhat like *b* in Fig. 6.

The curve branch FGH corresponds to an intermediate of type *c* in Fig. 6 or a σ-complex in the sense of Brown and Brady [11], and the energy increase corresponding to GF or GH comes from one or the other of the hydrogen atoms tending to detach itself (partly by bending, see below) from the carbon-hydrogen bond of approximately sp^3 type in order to form a π-complex.

[1] In the diagram of Fig. 7 we prefer to represent the π-complex structure by a single curve, CDE, for all aromatic positions and all acids discussed. The curve CDE obviously shows the energy of a π-complex plus the lone conjugate base of the attacking acid. The curves of the type AB or $A'B'$, which represent the aromatic compound plus the acid molecule, will then lie at higher levels with increasing strength (decreasing stability) of the acid. The curves of type FGH or $F'G'H'$, etc., representing a σ-complex plus the lone conjugate base of the attacking acid will be at a lower level the more stable the σ-complex, i.e., the lower the localization energy of the aromatic position in question.

Little has been said about what happens to the hydrogen which was originally present at the aromatic position in question when we pass from A to G. From a comparison with Fig. 6 it is evident that its bond to carbon undergoes a transition from the sp^2 type to something of less s character. According to the discussion in Section 3, however, it is evident that the change should not mean too much from the point of view of energetics. The absence of an isotope effect in several types of aromatic substitution [13] indicates that the vibrational characteristics do not undergo any appreciable change either, at least not when the entering substituent is heavy.

When the point G has been reached the same course repeats itself in the reverse direction with the roles of the hydrogens changed. The curve IJ represents the energy gain in restoring the conjugation within the aromatic ring (it corresponds to the curve $A'''M$ in Fig. 1). Before the aromatic structure is fully restored, the basicity of the carbon orbital might sink below that of the most basic species present, and thus the hydrogen will move over to the latter base before the π-complex J is reached. The point of intersection between the curves IJ and LM corresponds to a stage like d in Fig. 6. The curve LM will finally be followed. If the energy gained from increasing aromatic resonance more than outweighs the one required to transfer the hydrogen, no minimum will be passed. With a less basic acceptor for the proton, the π-complex corresponding to J will be an intermediate, and there will be some activation energy before the final decrease in energy along the curve $L'M'$.

Increased reactivity of the aromatic molecule will correspond to a lowering of the curve FGH, for instance to the position $F'G'H'$. The reason is that FGH corresponds to a chemical entity with electron localization at the pertinent carbon atom, while the other curves correspond to "fully aromatic" structures, and increased reactivity means decreased localization energy of the π-electrons (cf. footnote on p. 299). It is evident that the over-all transition states (the intersections between the top curve and the π-complex curves) will come at points of the reaction coordinate which are more distant from the symmetric intermediate the more reactive the aromatic position. This means that the transition state will obtain more of the π-complex character with increasing reactivity.

An interesting possibility arises when the reactivity of the aromatic position goes so far that the top curve intersects the two curves AB and LM below the intersections of the latter with the π-complex curves, as with curve $F''G''H''$ in Fig. 7. This means that the electron localization meets so little resistance that the maximum energy is reached already at the moment the proton is transferred. In such a case the conjugate base of the attacking acid will be a member of the transition state. From the work of Kresge and Chiang [2, 14] it seems that 1,3,5-trimethoxybenzene is such a reactive aromatic compound. With strong acids and highly reactive aromatic positions it might possibly happen that the formation of the π-complex is the rate-determining step.

It might be useful to reconsider these statements in the light of the hybridization at the carbon atom (cf. Section 3), which gives a better continuity than the necessarily discontinuous representation in terms of resonating structures.

When the curve AB runs into the curve DE, the approach of the acid changes the hybridization at the carbon atom concerned from about a to b in Fig. 6, and at some stage like b the proton affinity of the orbital might have become sufficient for the proton to be transferred. The rehybridization proceeds further in the same direction, and the transition state is reached when the rate of energy gain from the stabilizing new carbon–hydrogen bond just balances the rate of energy loss from the

less and less efficient conjugation of the same carbon orbital with the remainder of the π-electron system.

The question whether there will ever be such a balance before the symmetrical structure *c* in Fig. 6 or *G* in Fig. 7 is reached is, of course, the question of the very existence of a metastable symmetrical intermediate or σ-complex. The energy of conjugation of the carbon orbitals with the remaining π-electron system passes through a minimum in the symmetrical intermediate, because at that point the two orbitals have equivalent positions. Both of them partaking in carbon–hydrogen bonds, one of them is on its way from the favourable *p* state while the other one is on its way towards it. It seems likely that the carbon–hydrogen bonding energy, which simultaneously goes through a maximum, varies somewhat more rapidly, the resulting energy of the entity being at a minimum.

Much independent evidence is known nowadays that speaks for the existence of a metastable intermediate in aromatic substitution reactions in general. This evidence will not be reviewed here, but mention may be made of one particular experimental result which is generally not cited in such discussions and to which the writer's attention was recently drawn by Professor R. B. Woodward in a personal discussion.

When the optically active ketone

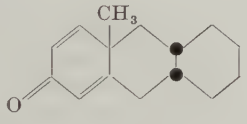

is rearranged to the phenol

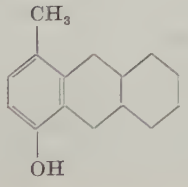

the optical activity is lost [15]. This can hardly be explained in any other way than that the symmetrical intermediate

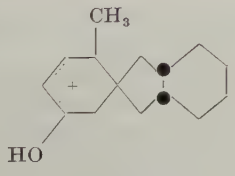

is formed and survives long enough (at least a couple of thermal motions) for the two bridges to become entirely equivalent.

Returning to the hydrogen exchange reaction, it seems likely that the hybridization at the carbon in the transition state should be of some type intermediate between, say, *b* and *c* in Fig. 6.

After the intermediate has been passed through the same course repeats itself in the reverse direction, the other hydrogen now playing the main role.

With a stronger acid (curve $A'B'$ in Fig. 7), the hydrogen is transferred to the π-electron cloud with some activation energy, and a rehybridization to increase the basicity of the carbon orbital is not necessary to effect this transfer. The π-complex (in the sense of Brown and Brady [11]) afterwards reorganizes, the hybridization at the carbon following the path *a–b–c–d–e* of Fig. 6 and the other hydrogen finally being transferred to a base with some activation energy.

When the curve FGH of Fig. 7 is replaced by $F'G'H'$, i.e., the aromatic position is somewhat more reactive, the first transition state comes somewhat earlier in the sequence *a–b–c* because the resistance of the π-electron system against breaking up is weaker. The second transition state will come correspondingly later in the sequence *c–d–e*, because the decisive energy gain from "healing" the aromatic π-electron system sets in at a later stage, owing to the lower "healing tendency". The same is still more advanced in the case of the curve $F''G''H''$ of Fig. 7, the maximum potential energy being reached already as the acid approaches (first transition state) or the aromatic π-electron system not healing until a base removes the proton (second transition state). With very strong acids and highly reactive aromatic positions the formation of the π-complex might be rate-determining, corresponding to a rate-determining removal of the hydrogen from the π-complex in the second step.

From the foregoing discussion it should be evident that the reaction coordinate at the stage *c* of Fig. 6 or the point *G* of Fig. 7 is partly a rehybridization bending of the two carbon–hydrogen bonds at the reaction centre like the "rocking" vibration of an ordinary methylene group. The reaction coordinate leading from the symmetric intermediate through the transition state cannot possibly be expected to consist exclusively of a carbon–hydrogen stretching movement, because this would not correspond to the "easiest" reaction path for the detachment of the hydrogen. A bending movement, on the other hand, will certainly involve expenditure of energy because of the increasing p character of the carbon orbital of the carbon–hydrogen bond, but simultaneously also an energy gain from the gradual change of the hyperconjugation between the carbon–hydrogen orbital and the remainder of the π-electron system into conjugation of ordinary aromatic strength. The bending is probably accompanied by some increase in bond length. When, finally, it is energetically convenient for the proton to switch over to the base, the movement becomes more of a stretching.

5. Comparison with experimental facts

Acidity dependence. The present situation concerning the acidity dependence of the hydrogen exchange has been reviewed in the Introduction (Section 1). It seems that relatively unreactive aromatic positions, as those in benzene and toluene, behave as if their σ-complexes correspond to the curves FGH and $F'G'H'$ in Fig. 7. The rate-determining transition state has little or no affinity to the conjugate base of the attacking acid. Whether a potential-energy minimum corresponding to a π-complex is passed or not might be a question of the strength of the attacking acid and is without kinetic significance.

With highly reactive aromatic positions, as those in 1,3,5-trimethoxybenzene, the σ-complex curve is at a low energy level, like $F''G''H''$ in Fig. 7, or still lower. The conjugate base of the attacking acid will then generally be involved in the rate-determining transition state.

Brönsted relationship. According to a private communication, Dr. A. J. Kresge has found that the hydrogen exchange of 1,3,5-trimethoxybenzene follows the Brönsted relationship within a very large interval and with a parameter $\alpha = 0.518$. This should be so if the transition state is determined simply by the intersection of two curves of the type AB and $F''G''$. If the curve AB is moved vertically, the transition-state level will move in the same direction by a smaller amount, as determined by the two slopes. (It must be assumed that all intersections concerned fall beneath the curve DE and hence are not disturbed by resonance with it.) Aromatic positions of low reactivity should give a Brönsted parameter $\alpha = 1$ if the proton transfer is complete already in the transition state.

Basicity and localization energy. The basicity should vary as the height of the point G in Fig. 7 for different aromatic positions. The geometry shows that the activation energy for the hydrogen exchange should vary in a similar way but somewhat less rapidly. Such a behaviour has been observed [16, 17], although in media where the mechanism could be different and the entropy of activation has been found to vary from one compound to another.

In the same way as with all mechanisms postulating a metastable σ-complex, the reaction rate should be expected to follow the quantum mechanically computed localization energy of the π-electrons. This seems to be the case with the hydrogen exchange as well as with most related aromatic substitutions. An irregularity might arise with very strong acids and very reactive aromatic positions if the formation of the π-complex happened to be rate-determining.

It has been pointed out by Dr. Philip C. Myhre in a private discussion that the behaviour of the cyclopentadiene molecule fits well into the present scheme. The neutral molecule itself corresponds to the intermediate in the exchange reactions, and its conjugate base, $C_5H_5^-$, is truly aromatic. In this case the G-type point falls on a lower energy level than even the point A, the "intermediate" being the stable entity in an equilibrium system of the present type.

Isotope effects. Owing to the complicated nature of the reaction coordinate, the discussion of the isotope effect is an intricate matter. It is hoped that this can be treated in a future paper. At present, at least, no evidence from this field seems to be in conflict with the model discussed in the present paper.

SUMMARY

The main purpose of the present paper is to introduce into the current discussion a model for the electrophilic aromatic hydrogen exchange which seems to be in agreement with most known experimental facts. Some new pieces of evidence concerning the acidity dependence of the reaction rate indicate that there is still use for a model according to which the conjugate base is not involved in the rate-determining transition state of relatively unreactive aromatic positions.

The possible kinetic consequences of internal stabilization in one of the reactants of a bimolecular reaction are discussed and it is pointed out that this might cause the reaction to be zero-order with respect to the other reactant.

The hybridization at the carbon atom at the reaction centre is discussed in simple terms of *s-p*-hybridization.

The probable course of the reaction is described in terms of potential-energy curves for separate, resonating structures as well as in terms of the rehybridization at the carbon atom.

The proposed mechanism is compared with the general experimental facts except isotope effects.

Nobel Institute of Chemistry, Stockholm 50, Sweden.

REFERENCES

1. HAMMETT, L. P., Physical Organic Chemistry (1st ed.), New York and London 1940, pp. 273–277.
3. KRESGE, A. J., and CHIANG, Y., to be printed.
2. EABORN, C., and TAYLOR, R., J. Chem. Soc. (London) *1960*, 3301.
4. GOLD, V., and TYE, F. L., J. Chem. Soc. (London) *1952*, 2181.
5. DENO, N. C., and PERIZZOLO, C., J. Am. Chem. Soc. *79*, 1345 (1957).
6. OLSSON, S., Arkiv Kemi *15*, 259 (1960).
7. OLSSON, S., Arkiv Kemi *14*, 85 (1959).
8. MELANDER, L., and MYHRE, P. C., Arkiv Kemi *13*, 507 (1959).
9. GOLD, V., and SATCHELL, D. P. N., J. Chem. Soc. (London) *1955*, 3609, 3619.
10. COULSON, C. A., Valence, Oxford 1952, pp. 193 ff.
11. BROWN, H. C., and BRADY, J. D., J. Am. Chem. Soc. *74*, 3570 (1952).
12. DEWAR, M. J. S., The Electronic Theory of Organic Chemistry, Oxford 1949, pp. 168 ff.
13. MELANDER, L., Isotope Effects on Reaction Rates, New York 1960, pp. 107 ff.
14. KRESGE, A. J., and CHIANG, Y., J. Am. Chem. Soc. *81*, 5509 (1959).
15. WOODWARD, R. B., pp. 177 ff. in TODD, A., (editor), Perspectives in Organic Chemistry, New York–London 1956.
16. MACKOR, E. L., SMIT, P. J., and VAN DER WAALS, J. H., Trans. Faraday Soc. *53*, 1309 (1957).
17. DALLINGA, G., VERRIJN STUART, A. A., SMIT, P. J., and MACKOR, E. L., Z. Elektrochemie *61*, 1019 (1957).

Tryckt den 14 april 1961

Uppsala 1961. Almqvist & Wiksells Boktryckeri AB

ARKIV FÖR KEMI Band 17 nr 27

Communicated 25 January 1961 by Sven Hörstadius and Per-Erik Lindahl

On the *in vitro* metabolism of the plant estrogen biochanin A in rumen fluid

By Anna Nilsson

Introduction

Natural estrogens in plants have been given considerable attention since the demonstration of their presence in forages. Besides their suggested beneficial effects in milk production [1] and meat production [2] they are probably also responsible for several breeding disorders reported from Australia [3], Germany [4] and USA [5].

In Trifolium pratense the principal active estrogen is biochanin A [6] and to a lesser extent genistein [7], both of them isoflavones. Recently coumestrol, a coumarin derivative, has been isolated from white clover, Trifolium repens, ladino variety [8]. The estrogenic potency of these plant estrogens is low, approximately 10^{-5} that of estradiol or stilbestrol. The biological effect can, however, be considerable because they are present in important quantities, in red clover, e.g., equivalent to 0.5–8 μg estradiol per 100 g of dry matter [9, 10]. The estimations of the estrogenic activity of forage are based on assays with mice and rats and nothing is known about the true biological effect in ruminants. It is possible that the isoflavones already by microbial processes in the rumen are transformed into more potent estrogens or inactive compounds.

The present communication deals with isotopic and chromatographic studies on the metabolism of biochanin A *in vitro* in rumen fluid from sheep and cattle.

Experimental

Materials. Biochanin A (4′methyl-genistein) and genistein were synthesized according to methods of Yoder *et al.* [11] and Baker *et al.* [12]. Tritium labelled biochanin A (specific activity 3.5 mc/g) was prepared by exposure to tritium gas [13]. Details of the labelling with tritium will be published elsewhere.

Radioactivity measurements were carried out in a liquid scintillation counter Ekco N6 12 operating at a temperature of −20°C. Samples were counted with an internal reference of a known amount of labelled biochanin A of high activity. Sufficient counts were taken to give a counting error less than 4 %.

Incubation procedure. Rumen fluid was taken from three fistulated sheep maintained on a diet of chopped hay, prepared from clover and grass, concentrates and periodically fodder beats. Rumen content was also taken from slaughtered sheep and cows to complete the results from the experiments mentioned above.

The rumen fluid was strained through gauze and used without delay. The biochanin A samples were dissolved in diluted sodium hydroxide. The solution was neutralized by diluted hydrochloric acid in order to make it correspond osmotically to physiological saline. Biochanin A was thereby distributed in the medium as a very fine suspension. To a rumen sample of 20 ml 2 mg biochanin A, suspended in 2 ml saline, was added.

In the control experiments the rumen liquor was boiled for 10 minutes before being added to the isolflavone.

The incubations were performed in Erlenmeyer flasks at 39° in a water bath for 3 hours. In anaerobic experiments the flasks were closed with rubber stoppers fitted with tubes for gassing, and tubes provided with a water valve allowing the escape of fermentation gases. The flasks were gassed with carbon dioxide.

The ability of the rumen fluid to metabolize glucose was followed in rumen samples both with and without biochanin A. Glucose determinations were performed by methods of M. Somogyi [14] modified by I. Sperber.

All reactions were stopped by adding twice as much ethanol as the volume of the samples, and heating to boiling. The solution was filtered and the residue on the filter was extracted twice with small volumes of boiling ethanol. After washing the pooled extracts with half a volume of heptane, the aqueous alcohol solution was evaporated to dryness. The residue was dissolved in ether and washed with a small amount of 5 % aqueous $NaHCO_3$.

Chromatography of biochanin A and its metabolites was carried out on sheets of Whatman paper no 3. The chromatograms were developed with two solvent systems: I, benzene–acetic acid–water (165:34:1), and II, isopropanol–ammonia–water (200:10:20). The isoflavones were located by their absorption in ultraviolet or stained with diazotized sulphanilic acid or with 2,6-dibromchinonchlorimid. Unstained spots were eluted with 80 % ethanol.

Aliquots of the eluates were analyzed for radioactivity. The radioactive eluates were rechromatographed in solvent system II to ascertain the homogeneity of the compounds in another solvent system.

For isolation purpose the procedure described above was performed on a larger scale. The eluates from the bands containing the metabolites were lyophilized. The residue was further purified through repeated recrystallizations from 50 % ethanol and cold ether.

Results

In vivo the rumen content is essentially an anaerobic system being under a gas phase of carbon dioxide, methane and nitrogen. Biochanin A was however metabolized to the same extent under anaerobic and aerobic conditions *in vitro*. All diagrams except that of exp. 2 Fig. 2 represent anaerobic incubations. The chromatograms illustrated were developed in solvent system I.

In the diagrams the radioactivity of the eluates is expressed as percentages of the sum of recovered activity and indicated on the ordinata. The distance of the eluted bands from the starting point is plotted along the abscissa.

The first diagram in Fig. 1 represents one of seven anaerobic incubations with rumen fluid from three fistulated sheep. The other experiments illustrated in this figure are performed with rumen fluid from slaughtered animals: sheep (exp. 2 and 3), cows (exp. 4, 7 and 8) and veal calves (exp. 5 and 6). Besides the biochanin A band

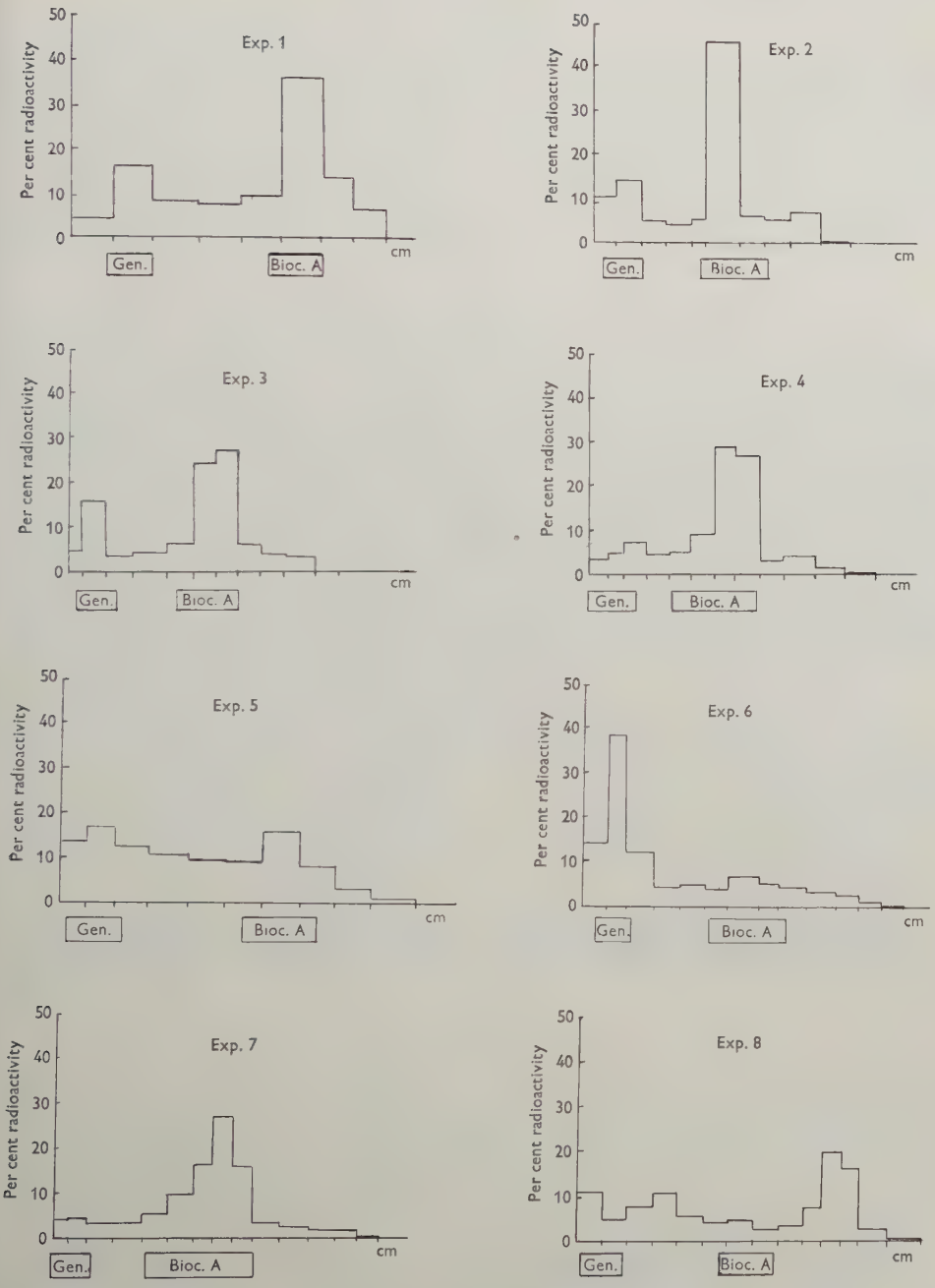

Fig. 1. The distribution of radioactivity in paper chromatograms with biochanin A, anaerobically incubated with rumen fluid. In experiment 1 the rumen fluid is taken from three fistulated sheep, in 2 and 3 from slaughtered sheep, in 4–8 from cattle. The chromatographic position of the test substances are indicated below the diagrams.

Table 1.

Rf values in solvent systems:	Compound A	Genistein	Biochanin A
I benzene – acetic acid – water (165 : 34 : 1)	0.15	0.15	0.65
II isopranol – ammonia – water (200 : 10 : 20)	0.28	0.28	0.43
butanol – acetic acid – water (1 : 1)	0.87	0.87	0.91
butanol – 2*N* ammonia (1 : 1)	0.45	0.45	0.54
70% aqueous ethanol	0.94	0.94	0.91

there appeared another ultraviolet absorbing and stainable band with a peak in radioactivity in the experiments 1–6 and indistinct in exp. 7. This metabolite, called A, coincides with genistein in five solvent systems.

The ultraviolet and infrared absorption curves of the metabolite and synthetic genistein were identical. The melting point and mixed melting point of the metabolite and genistein was the same, 292–294°C.

Two new metabolites, B and C, predominated in exp. 8 (Fig. 1). The compound B was probably identical with the metabolite having the same chromatographic position in the experiments with rumen fluid from one fistulated sheep, illustrated in diagram 1–3, Fig. 2. It was located between genistein and biochanin A in both solvent systems I (*Rf* 0.25) and II (*Rf* 0.33). The compound C appeared in solvent I above the genistein and biochanin A spots (*Rf* 0.76), in solvent II between them (*Rf* 0.29).

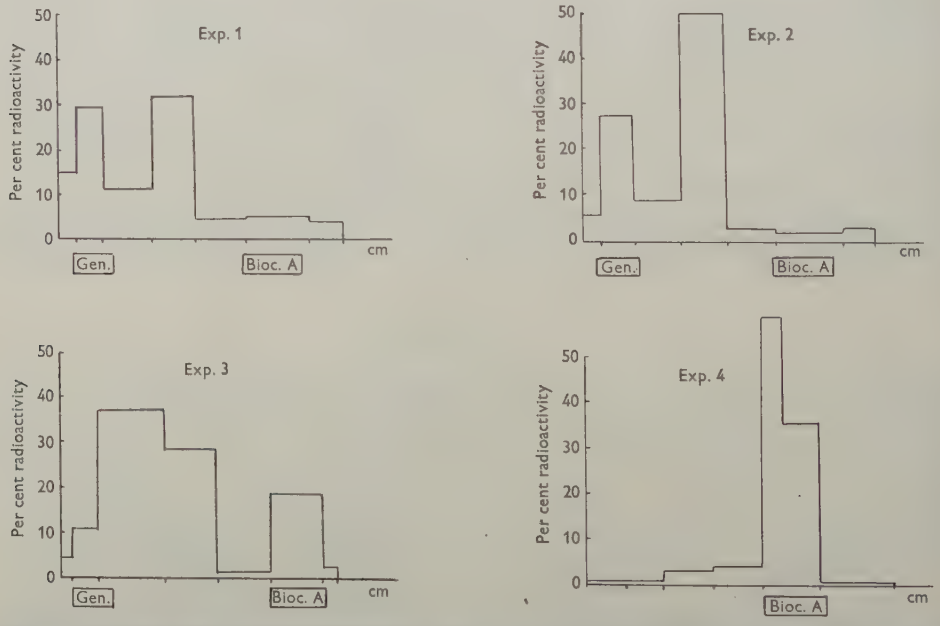

Fig. 2. The distribution of radioactivity in paper chromatograms with biochanin A, incubated anaerobically (exp. 1 and 3) and aerobically (exp. 2). All incubations were performed in rumen fluid from one fistulated sheep. Exp. 4 illustrates an experiment with boiled rumen fluid from the same sheep. The chromatographic position of the test substances are indicated below the diagrams.

Traces of the metabolite C was also found in exp. 4, Fig. 1. Both compounds were stained with sulfanilic acid, but only C absorbed ultraviolet light. The experiments illustrated in Fig. 2 were performed with an interval of only one month. Compound B did not appear again in incubations with rumen fluid from the same sheep performed two months later. The amount of material used in the two oncubations was too small to allow an isolation of the compounds.

Chromatograms of boild rumen fluid incubated with biochanin A showed only one peak in radioactivity and one ultraviolet absorbing or stained band at the place of biochanin A (diagram 4 in Fig. 2).

Discussion

The types of rumen organisms and their fermentation activities change in response to changes in the diet. No attempt was, however, undertaken to adopt the fistulated sheep to a diet especially rich in red clover. As to the slaughtered animals nothing was known about their diet. No special precautions were taken to maintain normal conditions for the microbial population in the *in vitro* incubations performed. By limiting the incubation time it was hoped to preserve within certain limits normal rumen conditions. One criterion of normal function of the rumen microorganisms was that glucose disappeared from the samples as rapidly in the end as in the beginning of the experiment. The addition of biochanin A had no influence on the ability of the microorganisms to utilize glucose. After 24 hours' incubation a rumen fluid sample was still able to demethylate biochanin A and metabolize glucose. The pH values of the incubates were within the range 6.4–5.4.

In vitro experiments of this type may yield results which are not directly applicable to *in vivo* conditions. The results presented here indicate that the plant estrogen in red clover, biochanin A, to some extent is metabolized already in the rumen before passing on into the intestines of the animal. Demethylation of biochanin A to the slightly more potent estrogen genistein is thus a possible degradation step in the rumen.

The two unknown metabolites have not appeared regularly in the experiments accounted for here. Nothing is known so far about their estrogenic potency or chemical properties. Insufficient amounts of material have been available to admit any analysis.

SUMMARY

Studies on the metabolism *in vitro* of the plant estrogen biochanin A, 4′methylgenistein, labelled with tritium have been performed in rumen fluid from sheep and cattle. Demethylation to genistein, a slightly more potent estrogen, occurred in fifteen experiments out of sixteen. Two unknown metabolites appeared in some of the incubations.

ACKNOWLEDGEMENTS

The author is greatly indebted to Dr. S. Gronowitz for invaluable advice and support in the synthesizing work. My thanks are also due to Professor N. Hellström in whose laboratory I was allowed to work with the first synthesis of the isoflavones used. To Professors S. Nordfeldt, P. E.

Lindahl and I. Sperber I wish to express my gratitude for the kind interest they have shown in my work. The investigation has been supported by a grant from the N.J.F. committee for forage quality.

The National Animal Experiment Station.

REFERENCES

1. Hutton, J. B., J. Endocrinol. *17*, 8, 121–133 (1958).
2. Hammond, J., Outlook on Agriculture *I*, 6 (1957).
3. Bennets, H. W., Underwood, E. Y., and Shier, F. L., Austral. Vet. J. *22*, 2 (1946).
4. Schoop, G., Fortpflanzung und Besammung der Haustiere *2*, 73 (1952).
5. Chiang, T. S., Nature 4643, 1175 (1958).
6. Pope, G. S., Elcoate, P. V., Simpson, S. A., and Andrews, D. G., Chem. & Ind. Lond. 1902 (1953).
7. Bradbury, R. B., and White, D. E., J. Chem. Soc. 3447 (1951).
8. Bickhoff, E. M., Booth, A. N., Leyman, R. L., Livingston, A. L., Thompson, C. R., and De Eds, A., Science *120*, 3119, 575 (1954).
9. Pope, G. S., Dairy Sci. Abstr. *16*, 334 (1954).
10. Nilsson, A., Kgl. Lantbrukshögskol. Ann. *26*, 19 (1960).
11. Yoder, L., Cheng, E., and Burroughs, W., Iowa Acad. Sci. Proc. *61*, 271 (1954).
12. Baker, W., Chadderton, J. B., and Ollis, W. D., J. Chem. Soc. *11*, 1852 (1953).
13. Wilzbach, K. E., J. Am. Chem. Soc. *79*, 1013 (1957).
14. Somogyi, M. J., Biol. Chem. *160*, 69 (1945).

Tryckt den 14 april 1961

Uppsala 1961. Almqvist & Wiksells Boktryckeri AB

ARKIV FÖR KEMI Band 17 nr 28

Communicated 25 January 1961 by The Svedberg

Diffusion in porous media

By Hans Vink

In an earlier paper [1] the author considered the effect of solute diffusion through membranes in connection with osmotic experiments. The flow equations used there had previously been used by Kirkwood in a discussion of ion transport through membranes [2] but their derivation can be traced back to earlier work, notably to the treatment of De Groot [3]. This original derivation of the equations assumed conditions that are valid for free diffusion. Here the derivation will be modified, so as to take explicitly into account the presence of a fixed lattice in the diffusing system.

To define our system we consider a fluid consisting of $n+1$ components numbered $0, 1, 2, \ldots, n$, and let one of the components, say 0, represent the lattice. For the bulk motion of the fluid ordinary hydrodynamic arguments apply. The lattice component can then be fixed in space by introducing constraints in the form of an appropriate external field of force.

The derivation is close to that given by De Groot and will therefore only be briefly stated. We use mass units as in [3], with the following notations:

ϱ_k, mass of component k per unit volume

ϱ, total mass per unit volume

$v = \dfrac{1}{\varrho}$, specific volume

$c_k = \varrho_k/\varrho$, concentration (mass fraction) of k

$\mathbf{v}_k$, velocity of k

$\mathbf{v} = \sum_0^n \varrho_k \mathbf{v}_k/\varrho$, center of mass velocity

$\mathbf{J}'_k = \varrho_k \mathbf{v}_k$, mass flow of substance k per unit area

$\mathbf{J} = \varrho \mathbf{v}$, total mass flow per unit area

$\mathbf{J}_k = \varrho_k (\mathbf{v}_k - \mathbf{v})$, mass flow of substance k with respect to center of mass movement.

Using material (barycentric) derivatives we have the following fundamental equations.

The equation of motion,

$$\varrho \frac{d\mathbf{v}}{dt} = -\operatorname{grad} P + \sum_0^n \mathbf{F}_k \varrho_k, \tag{1}$$

where P is the pressure and $\mathbf{F}_k$ the external force per unit of mass acting on substance k.

The equation of conservation of energy,

$$\varrho \frac{d\left(\frac{1}{2} v^2 + u\right)}{dt} = -\operatorname{div}\left(P\,\mathbf{v} + \mathbf{J}_q\right) + \sum_0^n \mathbf{F}_k \cdot \mathbf{v}_k\, \varrho_k, \tag{2}$$

where u is the energy per unit mass with exclusion of the barycentric kinetic energy and $\mathbf{J}_q$ is the heat flow per unit of area.

The entropy equation, as given by Gibbs equation and assumed to be valid along the center of mass movement,

$$T \frac{ds}{dt} = \frac{du}{dt} + P \frac{dv}{dt} - \sum_0^n \mu_k \frac{dc_k}{dt}. \tag{3}$$

Here s, u, v, and μ are the specific entropy, energy, volume and chemical potential respectively.

We further make use of the equation for conservation of total mass and mass of component k,

$$\frac{\partial \varrho}{\partial t} = -\operatorname{div} \varrho\, \mathbf{v} \tag{4}$$

and

$$\frac{\partial \varrho_k}{\partial t} = -\operatorname{div} \varrho_k \mathbf{v}_k. \tag{5}$$

From the relation for the material derivative

$$\frac{d}{dt} = \frac{\partial}{\partial t} + \mathbf{v}\ \operatorname{grad} \tag{6}$$

it follows

$$\frac{d\varrho}{dt} = -\frac{1}{v^2}\frac{dv}{dt} = -\varrho\ \operatorname{div}\ \mathbf{v} \tag{7}$$

and

$$\frac{d\varrho_k}{dt} = -\operatorname{div}\ \mathbf{J}_k' + \mathbf{v}\ \operatorname{grad}\ \varrho_k = -\operatorname{div}\ \mathbf{J}_k - \varrho_k\ \operatorname{div}\ \mathbf{v}. \tag{8}$$

As

$$\varrho_k = \varrho\, c_k \tag{9}$$

equation (8) gives, with the help of (7)

$$\varrho \frac{dc_k}{dt} = -\operatorname{div}\ \mathbf{J}_k. \tag{10}$$

Multiplying equation (1) by $\mathbf{v}$ and substracting from (2) we get the variation of the specific energy

$$\varrho \frac{du}{dt} = -P\ \operatorname{div}\ \mathbf{v} - \operatorname{div}\ \mathbf{J}_q + \sum_0^n \mathbf{F}_k \cdot \mathbf{J}_k. \tag{11}$$

We may now deduce the entropy balance by introducing (11) into (3) and using (7) and (10):

$$\varrho T \frac{ds}{dt} = -\operatorname{div} \mathbf{J}_q + \sum_0^n \mathbf{F}_k \cdot \mathbf{J}_k + \sum_0^n \mu_k \operatorname{div} \mathbf{J}_k. \tag{12}$$

We will now proceed to solve equation (12) under steady state conditions. The steady state is defined by

$$\frac{d\mathbf{v}}{dt} = 0. \tag{13}$$

Then (1) yields

$$\operatorname{grad} P - \sum_1^n \mathbf{F}_k \varrho_k = \mathbf{F}_0 \varrho_0. \tag{14}$$

This equation defines the external force on the lattice component. It may be considered as brought about by an elastic deformation of the lattice and is balanced by the frictional force between the lattice and the moving fluid, and the pressure gradient. We further introduce the condition of a fixed lattice by setting $\mathbf{v}_0 = 0$, or

$$\mathbf{J}_0 = -\varrho_0 \mathbf{v}. \tag{15}$$

Introducing (14) and (15) into (12) we get

$$\varrho T \frac{ds}{dt} = -\operatorname{div} \mathbf{J}_q + \sum_1^n \mathbf{F}_k \cdot \mathbf{J}'_k + \sum_0^n \mu_k \operatorname{div} \mathbf{J}_k - \mathbf{v} \operatorname{grad} P. \tag{16}$$

This can be rearranged to

$$\varrho \frac{ds}{dt} = -\operatorname{div} \frac{\mathbf{J}_q - \sum_0^n \mu_k \mathbf{J}_k}{T} + \frac{1}{T}\left\{ -\mathbf{J}_q \cdot \frac{\operatorname{grad} T}{T} + \sum_1^n \mathbf{F}_k \cdot \mathbf{J}'_k - \mathbf{v} \cdot \operatorname{grad} P - \sum_0^n \mathbf{J}_k \cdot T \operatorname{grad} \frac{\mu_k}{T} \right\}. \tag{17}$$

To simplify further we observe that

$$\mathbf{J}_k = \mathbf{J}'_k - c_k \mathbf{J} \tag{18}$$

and thus

$$\sum_0^n \mathbf{J}_k \cdot T \operatorname{grad} \frac{\mu_k}{T} = \sum_0^n \mathbf{J}'_k \cdot T \operatorname{grad} \frac{\mu_k}{T} - \mathbf{J} \cdot \sum_0^n c_k T \operatorname{grad} \frac{\mu_k}{T}. \tag{19}$$

As μ_k is a function of temperature, pressure and concentration, we have

$$T \operatorname{grad} \frac{\mu_k}{T} = -h_k \frac{\operatorname{grad} T}{T} + v_k \operatorname{grad} P + \frac{\partial \mu_k}{\partial c_k} \operatorname{grad} c_k, \tag{20}$$

where $h_k = \mu_k + T s_k$ is the specific enthalpy of component k. With (20) the sum in the last term in (19) becomes

$$\sum_0^n c_k T \text{ grad } \frac{\mu_k}{T} = -\sum_0^n c_k h_k \frac{\text{grad } T}{T} + \sum_0^n c_k v_k \text{ grad } P + \sum_0^n c_k \frac{\partial \mu_k}{\partial c_k} \text{ grad } c_k$$

$$= -h \frac{\text{grad } T}{T} + v \text{ grad P}, \tag{21}$$

where h and v are the specific enthalpy and volume respectively. In (21) we have also used the Gibbs-Duhem equation. With (20) and (21) inserted into (19) we get

$$\sum_0^n \mathbf{J}_k \cdot T \text{ grad } \frac{\mu_k}{T} =$$

$$\sum_1^n \mathbf{J}'_k \cdot \left[\frac{\partial \mu_k}{\partial c_k} \text{ grad } c_k + v_k \text{ grad } P + (h - h_k) \frac{\text{grad } T}{T} \right] - \mathbf{v} \cdot \text{grad } P. \tag{22}$$

Introducing (22) into (17) we get finally

$$\varrho \frac{d s}{d t} = -\text{div} \frac{\mathbf{J}_q - \sum_0^n \mu_k \mathbf{J}_k}{T} + \frac{\mathbf{J}_q \cdot \mathbf{X}_u + \sum_1^n \mathbf{J}'_k \cdot \mathbf{X}_k}{T} = -\text{div } \mathbf{J}_s + \sigma, \tag{23}$$

where

$$\mathbf{X}_u = -\frac{\text{grad } T}{T} \tag{24}$$

$$\mathbf{X}_k = \mathbf{F}_k - \frac{\partial \mu_k}{\partial c_k} \text{ grad } c_k - v_k \text{ grad } P - (h - h_k) \frac{\text{grad } T}{T}. \tag{25}$$

Note that in (25) the chemical potentials of the different components are interconnected by the Gibbs-Duhem equation

$$\sum_0^n c_k d \mu_k = 0, \tag{26}$$

where the lattice component is also included.

According to (23) the change of entropy is due to two causes, the negative divergence of an entropy flow $\mathbf{J}_s$ and the entropy production with a source strength

$$\sigma = \frac{1}{T} \left(\mathbf{J}_q \cdot \mathbf{X}_u + \sum_1^n \mathbf{J}'_k \cdot \mathbf{X}_k \right). \tag{27}$$

From the equation for the entropy source strength the following phenomenological equations are obtained

$$\left.\begin{aligned} \mathbf{J}_i' &= \sum_{k=1}^{n} L_{ik}\mathbf{X}_k + L_{iu}\mathbf{X}_u, \\ \mathbf{J}_q &= \sum_{k=1}^{n} L_{uk}\mathbf{X}_k + L_{uu}\mathbf{X}_u. \end{aligned}\right\} \tag{28}$$

For the coefficients the Onsager relations exist

$$L_{ik} = L_{ki} \quad \text{and} \quad L_{iu} = L_{ui}. \tag{29}$$

Equations (28) give a general representation of flows in a medium with a fixed lattice. It should be observed that the flows and forces are somewhat different from those used by De Groot in his treatment of free diffusion. In particular the reference frame for the flows is fixed in the lattice and does not move along with the center of mass of the fluid. In order to bring out the importance of the choice of the reference frame and to make possible a direct comparison with free diffusion, we refer the flows in (27) to the center of mass velocity of the mobile fluid. Denoting it by $\mathbf{v}$ (we now consider the mobile fluid only) we have

$$\mathbf{J}_k = \varrho_k(\mathbf{v}_k - \mathbf{v}) = \mathbf{J}_k' - c_k\mathbf{J}. \tag{30}$$

Introducing this into (27) we get

$$T\sigma = \mathbf{J}_q \cdot \mathbf{X}_u + \sum_{1}^{n} \mathbf{J}_k \cdot \mathbf{X}_k + \mathbf{J} \cdot \sum_{1}^{n} c_k \mathbf{X}_k. \tag{31}$$

Using (14) and the Gibbs-Duhem equation, the last term in (31), which represents the entropy production due to the center of mass movement, can be written

$$\begin{aligned} T\sigma_J &= \mathbf{J} \cdot \sum_{1}^{n} c_k \mathbf{X}_k \\ &= -\mathbf{v} \cdot \left[\mathbf{F}_0\varrho_0 - v_0\varrho_0 \operatorname{grad} P - \varrho_0 \frac{\partial \mu_0}{\partial c_0} \operatorname{grad} c_0 - \varrho_0 (h - h_0) \frac{\operatorname{grad} T}{T}\right]. \end{aligned} \tag{32}$$

At a uniform temperature and with a uniform lattice concentration the remainder in the brackets of (32) is equal to the frictional forces between the moving fluid and the lattice, and hence the entropy production due to the center of mass movement equals the work done by the dissipative forces, devided by the temperature.

The total mass flow $\mathbf{J}$, along with the individual mass flows $\mathbf{J}_k'$ $(k = 1, \ldots, n)$ are thus completely determined by the forces $\mathbf{X}_k$ $(k = 1, \ldots, n)$ through the equations (28).

A different situation is encountered in free diffusion. This is clearly obtained from the above treatment of diffusion in a lattice as a limiting case by setting $\varrho_0 = 0$ and $\varrho_0\mathbf{F}_0 = 0$ in the above equations. From (32) it then follows that

$$\sum_{1}^{n} c_k \mathbf{X}_k = 0 \tag{33}$$

and thus the entropy production due to the center of mass movement vanishes.

The mass flows obtained from the expression for the entropy production (27) are now indeterminate. If $\mathbf{J}'_k\,(k=1,\ldots,n)$ are a set of flows consistent with (27), then so are

$$\mathbf{J}'_k + c_k\mathbf{J}' \quad (k=1,\ldots,n)$$

with $\mathbf{J}'$ being arbitrary. The total mass flow

$$\mathbf{J}=\sum_1^n \mathbf{J}'_k$$

is therefore not determined by the forces $\mathbf{X}_k\,(k=1,\ldots,n)$ and can be fixed only from additional boundary conditions.

Equation (33) shows that the forces $\mathbf{X}_k$ are not independent, and this has to be considered when writing down the phenomenological equations (28). Introducing (33) into the expression for the entropy source strength (27), we get

$$T\sigma=\mathbf{J}_q\cdot\mathbf{X}_u+\sum_1^{n-1}\mathbf{X}_k\cdot\left(\mathbf{J}'_k-\frac{c_k}{c_n}\mathbf{J}'_n\right). \tag{34}$$

We may now introduce the new mass flows

$$\mathbf{J}''_k=\mathbf{J}'_k-\frac{c_k}{c_n}\mathbf{J}'_n. \tag{35}$$

Hereby the indeterminacy in the flows has been removed and they are uniquely determined by the $n-1$ independent forces $\mathbf{X}_k\,(k=1,\ldots,n-1)$ The phenomenological equations now take the form

$$\left.\begin{aligned}\mathbf{J}''_i&=\sum_{k=1}^{n-1}L_{ik}\mathbf{X}_k+L_{iu}\mathbf{X}_u,\\ \mathbf{J}_q&=\sum_{k=1}^{n-1}L_{uk}\mathbf{X}_k+L_{uu}\mathbf{X}_u,\end{aligned}\right\} \tag{36}$$

with

$$\left.\begin{aligned}&L_{ik}=L_{ki}\quad\text{and}\quad L_{iu}=L_{ui},\\ &i,\,k=1,\ldots,n-1.\end{aligned}\right\} \tag{37}$$

The phenomenological equations thus reduce in this case to a system consisting of the heat flow and $n-1$ mass flows, and thus contain only $\frac{1}{2}\,n\,(n+1)$ independent coefficients. When the phenomenological equations are written in the form of (28), a number of new relations must exist among the phenomenological coefficients, in addition to the Onsager relations, so that the number of independent coefficients is reduced (cf. [3]). In the case of diffusion in a lattice, all the $n+1$ forces are independent and therefore the number of independent coefficients is $\frac{1}{2}\,(n+1)\,(n+2)$.

There is a further point that clearly brings out the difference between the two kinds of diffusion. In the case of free diffusion, it follows from (14) that

the hydrostatic pressure is completely determined by the external forces and is therefore not an independent variable. Especially, when external forces are absent the pressure is uniform. In the case of diffusion in a lattice, however, the hydrostatic pressure is obviously an independent variable.

SUMMARY

Flow equations for diffusion in porous media are deduced, based on the principles of irreversible thermodynamics. The diffusion processes are considered to take place in a multicomponent system where one of the components is fixed in space by the introduction af appropriate constraints and thus is made to form a lattice, which represents the porous medium.

Institute of Physical Chemistry, University of Uppsala, Sweden.

REFERENCES

1. Vink, H., Arkiv Kemi *15*, 149 (1959).
2. Kirkwood, J. H., Ion Transport Across Membranes, ed. H. T. Clarke, Academic Press Inc. Publishers, New York 1954, p. 119.
3. De Groot, S. R., Thermodynamics of Irreversible Processes, North-Holland Publishing Company, Amsterdam 1951.

Tryckt den 14 april 1961

Uppsala 1961. Almqvist & Wiksells Boktryckeri AB

ARKIV FÖR KEMI Band 17 nr 29

Communicated 7 December 1960 by Arne Fredga

The kinetics of the hydrolytic fission of the γ-lactone ring of terpenylic acid

By Rune Sandberg

With 5 figures in the text

The acid and basic hydrolyses of γ-lactones have been the subject of several quantitative investigations, and in recent years the mechanisms of these reactions have been fully established as far as the simplest lactone, γ-butyrolactone, is concerned. Long *et al.* showed by a mass spectrometric method (using O^{18}) that both the acid and basic hydrolysis of this lactone involved splitting of the acyl-oxygen bond [1]. They also showed [2] that in an aqueous medium the rate for the acid-catalyzed hydrolysis was proportional to the concentration of strong acid, but that the lactonization rate varied with the acidity as measured by the Hammet acidity function, h_0. This means, according to the Hammet theory [3, 4], that the reaction transition state for the hydrolysis contains a water molecule in addition to a proton, while for the reverse reaction the water molecule is omitted.

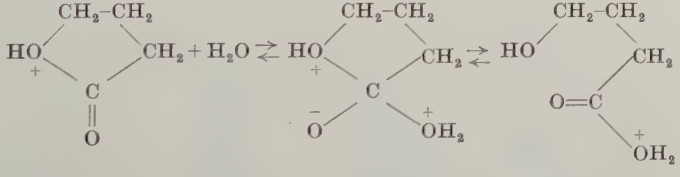

Thus, using Ingold's classification [5], the operating mechanism in this reversible process is $A_{Ac}2$.

The position of terpenylic acid as a key substance in the oxidative degradation of (+)-Δ^3-carene to (−)-terebic acid made it necessary to investigate its ring stability [6]. Optically active terpenylic acid can conveniently be used for such a study because the corresponding hydroxy acid is symmetric; accordingly the hydrolysis of the lactone ring can be easily followed by the rate of racemization.

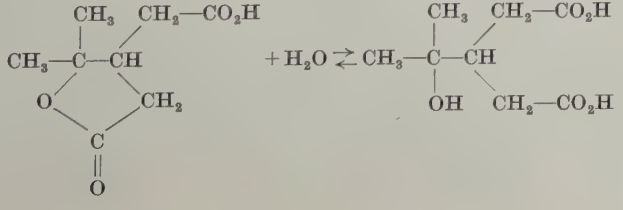

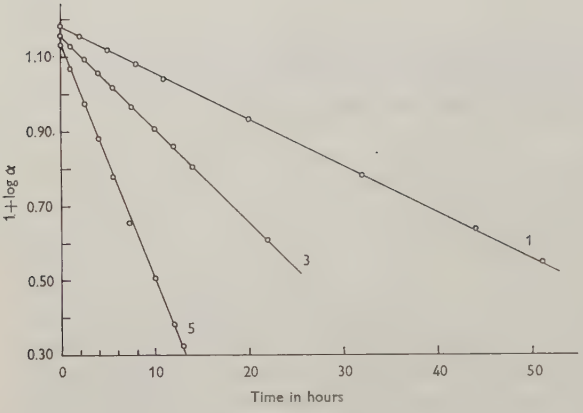

Fig. 1 a.

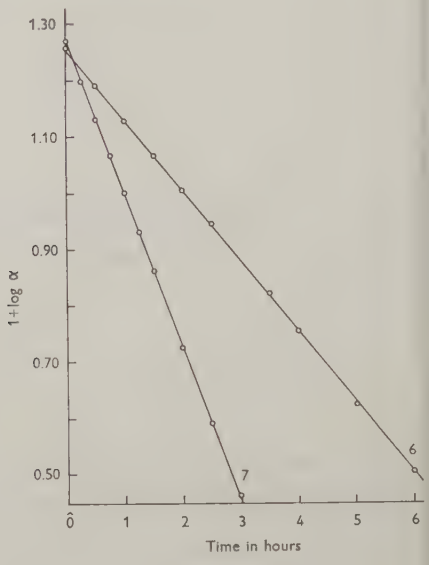

Fig. 1 b.

Fig. 1. Log α *versus* time for racemization of terpenylic acid in hydrochloric acid solutions. The numbering refers to Table 1.

Table 1. Rate constants for racemization of terpenylic acid (TA) in aqueous hydrochloric acid at 25.0±0.1°C.

No.	C_{HCl}	C_{TA}	k'_{10} · tim^{-1}	$10^3 k$ (l · mole^{-1} · min^{-1})
1	0.0997	0.0809	0.0125	4.81
2	0.1001	0.0579	0.0125	4.79
3	0.1986	0.0785	0.0249	4.81
4	0.1994	0.0539	0.0250	4.81
5	0.497	0.0988	0.0623	4.81
6	1.002	0.1008	0.125	4.79
7	2.07	0.1031	0.270	5.01
8	2.07	0.1035	0.272	5.04

A few results of importance for the study of the stereochemistry of terpenylic acid have been reported in this connection [6]. The kinetic investigations described in the present paper involve a more thorough study of the hydrochloric acid catalysed hydrolysis and also an extension to the alkaline side.

The measurements in aqueous hydrochloric acid were performed in solutions ranging from 0.1 to 2.0 molar. In each case the reactions were strictly first-order as shown by the plots of log α *versus* time given in Fig. 1. The slope of the straight lines thus obtained gives the first-order rate constant (k'_{10}).

The result, including duplicated runs, is summarized in Table 1, where the second-order rate constant k for the reaction of lactone with acid is obtained from the relation $k = (\ln 10/60) \cdot (k'_{10}/C_{HCl})$.

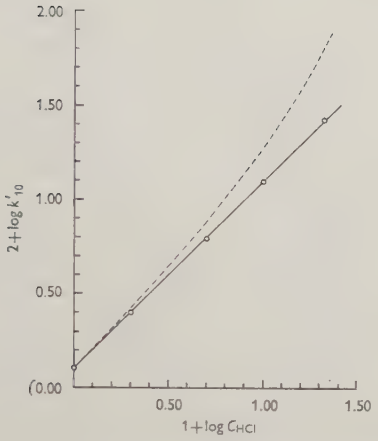

Fig. 2. Log k'_{10} *versus* log C_{HCl} for racemization of terpenylic acid in aqueous hydrochloric acid. The dotted line is a predicted curve for dependence on H_0. This curve is calculated using the values of H_0 for hydrochloric acid solutions given by Paul and Long [7].

Table 2. Racemization of terpenylic acid in dioxan solution at $25.0° \pm 0.1°$. $C_{TA} = 0.193$. $C_{HCl} = 0.0480 \pm 3 \times 10^{-4}$.

No.	1	2	3	4	5	6[a]	7
C_{H_2O}	0.160	0.193	0.213	0.240	0.319	0.319	0.508
$10^5 k' \cdot \text{min}^{-1}$	5.56	7.37	8.83	10.1	16.4	27.1	33.3

[a] $C_{HCl} = 0.0760$.

From Table 1 it is obvious that the values of k are practically constant in the range of hydrochloric acid concentrations investigated. In other words, the rate of hydrolysis is proportional to the concentration of hydrochloric acid. This is clearly demonstrated in Fig. 2 by a plot of log k'_{10} *versus* log C_{HCl} together with a predicted curve for dependence on the Hammet function H_0. ($H_0 = -\log h_0$.)

The result accordingly indicates a bimolecular mechanism of hydrolysis, that is a transition state containing both a proton and a water molecule. In order to confirm this, the reaction was studied in dioxan solution, keeping the lactone and hydrochloric acid concentrations constant at 0.20 and 0.05 molar respectively, but varying the water concentration in the range 0.16 to 0.51 molar. Again the reactions were strictly first order for each of the concentrations of water chosen, as shown by the plots of log α *versus* time for some selected runs given in Fig. 3. This fact is noticeable although not surprising; it merely implies that the equilibrium lactone $\rightleftharpoons$ hydroxy acid lies practically completely on the lactone side. The result is summarized in Table 2.

As the concentrations of lactone and acid were kept constant, a plot of log k' *versus* log C_{H_2O} should give a straight line with a slope representing the order of proportionality between rate and C_{H_2O}. An examination of Fig. 4 shows that

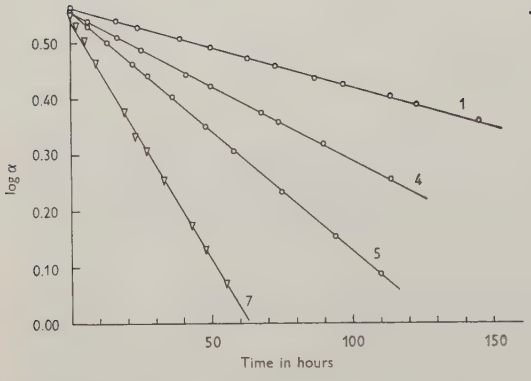

Fig. 3. Log α *versus* time for racemization of terpenylic acid in dioxan solution. The numbering refers to Table 2.

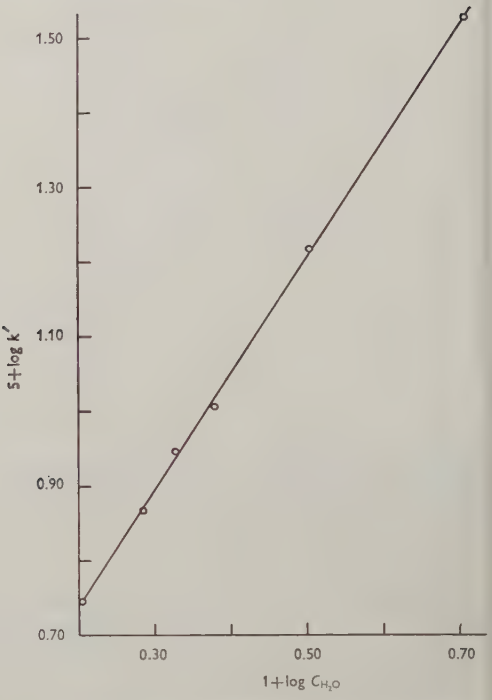

Fig. 4. Log k' *versus* log C_{H_2O} for racemization of terpenylic acid in dioxan solution.

this order is approximately 1.5 (1.54). A single run (No. 6 in Table 2) further indicated a direct proportionality between rate and hydrogen chloride concentration. The anomaly is not easily explained; it may be caused by the nonpolar solvent. In any case it can be stated that the acid-catalyzed hydrolysis of the γ-lactone ring of terpenylic acid proceeds by a *bimolecular mechanism involving one molecule of water.*

In the introduction it was pointed out that γ-butyrolactone is hydrolyzed by the $A_{Ac}2$ mechanism. The rates of lactonization of γ-hydroxyacids have, however, been shown to increase as the hydroxyl group changes from primary to secondary to tertiary [8, 9]. Sebelius [8] found, that in the series of γ-butyrolactone, γ-valerolactone, γ-isocaprolactone the relative rates of formation were 1 : 3.4 : 12.3, while the rates for the reverse reaction appeared to decrease slowly. As it can be assumed that γ-isocaprolactone and terpenylic acid behave very similarly, these facts together with the result of the present investigation might imply a continuous change in mechanism from a bimolecular acyl-oxygen to a bimolecular alkyl-oxygen cleavage ($A_{Al}2$). On a consideration of the polar effects, it could be expected that alkyl substituents in the γ-position would, if anything, retard hydrolysis by the former mechanism and accelerate hydrolysis by the latter. On the other hand, lactonization and hydrolysis by an $A_{Al}2$ mechanism ought to be very sensitive to steric hindrance, and in fact this effect might be assumed to suppress the polar one to a large extent. Besides, such a drastic change in mechanism as

Table 3. Constant pH-titration at 25.0°C. pH 12.02. Volume at zero time (v_0) 15.66 cc. Time (t) in minutes.

t	v_t' ml NaOH	$t+5$	v_{t+5}' ml NaOH	$10^2(v_{t+5}-v_t)$
0	0	5	0.2630	1.652
0.5	0.0306	5.5	0.2860	1.598
1.0	0.0614	6.0	0.3080	1.537
1.5	0.0900	6.5	0.3270	1.474
2.0	0.1180	7.0	0.3466	1.417
2.5	0.1450	7.5	0.3664	1.369
3.0	0.1680	8.0	0.3840	1.333
3.5	0.1928	8.5	0.3992	1.270
4.0	0.2192	9.0	0.4160	1.207
4.5	0.2432	9.5	0.4320	1.155

that indicated seems in itself rather improbable. These considerations point to a different explanation. It is well known that alicyclic compounds are often stabilized by alkyl groups [10]. Actual examples are the great facility with which the tetramethylsuccinic and β,β-dimethylglutaric acids form anhydrides, and while adipic anhydride is converted to cyclopentanone only in a low yield when distilled at 300°, alkylsubstituted cyclopentanones are formed almost quantitatively [11, 12, 13]. It can be assumed that the same stabilizing effect operates also in the case of γ-lactones. Moreover, in the reversible conversion of a γ-lactone to a hydroxy acid the reaction complex is also a five-membered ring. A stabilization of the ring system should thus cause a decrease of the energy content of the reaction complex, that is an increase of the lactonization rate. Consequently there is no need to propose a change in mechanism: the γ-lactones are most probably all formed and hydrolyzed by acyl-oxygen cleavage, independent of the number of alkylsubstituents.

It was not found possible to determine the kinetics of the alkaline hydrolysis polarimetrically. The method of constant pH-titration was adopted instead. The titrations were performed in solutions of strengths 0.06 molar in terpenylic acid and 0.26 molar in potassium chloride in order to keep the ionic strength approximately constant. A recorder gave a curve in the form of a plot of the amount of alkali added *versus* time. Because of some difficulties in determining the zero point the rate constants were evaluated by the Guggenheim method [14], using the rate equation

$$k \cdot t_i + \log (v_i' - v_i) = \text{constant}.$$

The procedure is illustrated in Table 3 which shows one run in detail. The figures in the four first columns are obtained directly from the curve registered and the expression $(v_{t+5}-v_t)$ from the relation

$$v_{t+5}-v_t = \frac{v_{t+5}'}{v_0+v_{t+5}'} - \frac{v_t'}{v_0+v_t'},$$

thus representing the relative concentrations of the amount of lactone reacted within the actual time interval.

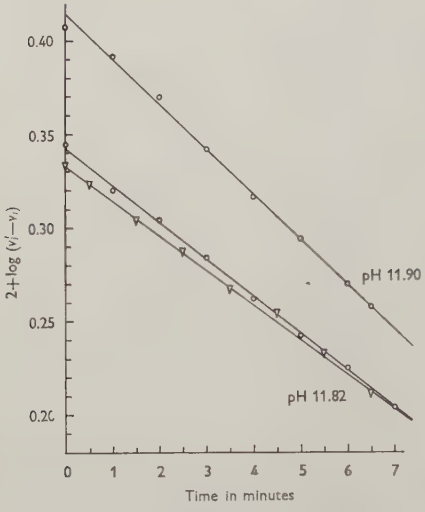

Fig. 5 a.

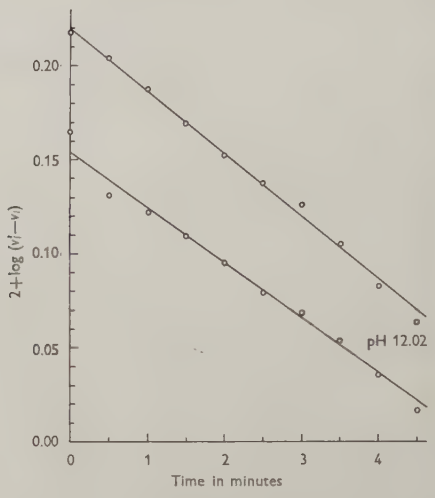

Fig. 5 b.

Fig. 5. Plots of log $(v_i' - v_i)$ *versus* time for hydrolysis of the γ-lactone ring of terpenylic acid by constant pH titration.

Table 4. Alkaline hydrolysis of the γ-lactone ring of terpenylic acid (TA) at 25.0°C. $C_{TA} = 0.061$ *M*. $C_{KCl} = 0.26$ *M*.

pH	$10^2 k' \cdot \text{min}^{-1}$	k $(\text{l} \cdot \text{mole}^{-1} \cdot \text{min}^{-1})$
11.82	4.26	6.4
11.82	4.50	6.8
11.90	5.53	7.0
12.02	6.79	6.5
12.02	7.71	7.4
		Mean value 6.8

The slope of the straight line obtained by plotting log $(v_i' - v_i)$ *versus* t_i gives the first-order rate constant. Such plots for the runs described are shown in Fig. 5.

The result is given in Table 4. The second order rate constant 6.8 $\text{l} \cdot \text{mole}^{-1} \cdot \text{min}^{-1}$ agrees fairly well with those obtained for γ-isocaprolactone by Sebelius [8] and by Stevens and Tarbell [15]. An examination of the data from an investigation by Sircar [16] of paraconic acids gave the rate constant 5.6 $\text{l} \cdot \text{mole}^{-1} \cdot \text{min}^{-1}$ for terebic acid, the lower homologue of terpenylic acid.

Finally, it may be noted that for a 0.1 molar solution of optically active terpenylic acid, in pure water (pH 2.6) or approximately neutralized (pH ~ 8), the decrease in rotation is about 1 % in 24 hours. Half-life periods of about 200 hours can be calculated for pH 2 and 9. The lactone ring is thus remarkably stable within a wide pH range.

Experimental

Racemization reactions. Dioxan (samples for chromatographic use) was refluxed over and distilled from sodium hydride. Solutions of water in dioxan were prepared by making up weighed amounts of water to measured volumes. Solutions containing hydrogen chloride were prepared by first drying the gas by passing it through concentrated sulphuric acid and phosphorous pentoxide and then dissolving it. The solutions of hydrogen chloride were always checked before use and never stored for long before being renewed.

Weighed amounts of optically active terpenylic acid were dissolved in 10 or 15 ml of the actual solutions. The concentrations of the reagents were corrected for the amount of terpenylic acid. The measurements were performed in a polarimeter thermostat described by Ramberg and Hedlund [17], using a 2 dm polarimeter tube. The time for the first reading was taken as zero time.

Alkaline hydrolysis. The experiments were carried out with a difunctional titrator as described by Neilands and Cannon [18]. A combined Metrohm glass-electrode type EA 120 U was used and the pH-scale was calibrated against a $Ba(OH)_2$–$CaCl_2$ buffer (pH 11.82) as described by Tuddenham and Anderson [19]. The titrations were performed in a 25 ml water-jacketed beaker with constant stirring. The titrating fluid was 1.018–*N* NaOH. In one typical run 0.1057 g of terpenylic acid was dissolved in 0.65 ml of 4.0–*M* KCl solution, 1.50 ml of water and about 5 ml of 0.1–*N* NaOH (less than one equivalent). Then an additional amount of 0.1–*N* NaOH was rapidly added from the buret. The titrator, previously set for titration at pH 11.82, was started immediately this value was reached, when a total of 7.80 ml had been added.

SUMMARY

The kinetics of the acid catalyzed and the alkaline hydrolysis of the γ-lactone ring of terpenylic acid have been studied by the rate of racemization and by constant pH titration respectively. In the former case it has been shown that the hydrolysis proceeds by a bimolecular mechanism involving one molecule of water. The significance of this has been discussed considering the fact that alkylsubstitution in the lactone ring causes an increase in its rate of formation and a decrease in the hydrolysis rate. It is proposed that γ-lactones are formed and hydrolyzed by the $A_{Ac}2$ mechanism regardless of the number of alkylsubstituents.

The γ-lactone ring of terpenylic acid has been found to be remarkably stable within a wide pH range.

ACKNOWLEDGEMENTS

The author is indebted to Professor Arne Fredga, for his interest in this work and to Dr. Andreas Rosenberg for his inestimable help in connection with the constant pH titrations.

A grant from the *Swedish Natural Science Research Council* is gratefully acknowledged.

Department of Organic Chemistry, Chemical Institute, University of Uppsala, November 1960.

REFERENCES

1. Long, F. A., and Friedman, L., J. Am. Chem. Soc. *72*, 3692 (1950).
2. Long, F. A., Dunkle, F. B., and McDevit, W. T., J. Phys. Chem. *55*, 829 (1951).
3. Hammet, L. P., Physical Organic Chemistry, p. 273. New York 1940.

4. PAUL, M. A., and LONG, F. A., Chem. Rev. *57*, 935 (1957).
5. INGOLD, C. K., Structure and Mechanism in Organic Chemistry, pp. 752–782. New York 1953.
6. SANDBERG, R., Arkiv Kemi *16*, No. 23 (1960).
7. PAUL, M. A., and LONG, F. A., Chem. Rev. *57*, 12 (1957).
8. SEBELIUS, H., Dissertation. Lund 1927.
9. KAILAN, A., Z. physik. Chem. *94*, 111 (1920); *101*, 63 (1922).
10. NEWMAN, M., Steric Effects in Organic Chemistry p. 114. New York 1956. See also WHELAND, G. W., Advanced Organic Chemistry, pp. 366 ff. New York 1949.
11. BLANC, H. G., Compt. rend. *144*, 1356 (1907).
12. FALTIS, F. and WAGNER, H., Ann. *433*, 103 (1923).
13. FUSON, R. C., in GILMAN, H., Organic Chemistry, Vol. I. 65, p. 80. New York 1944.
14. GUGGENHEIM, E. A., Phil. Mag. [7], *2*, 538 (1926).
15. STEVENS, C. M., and TARBELL, D. S., J. Org. Chem. *19*, 1996 (1954).
16. SIRCAR, S. S. G., J. Chem. Soc. *129*, 1257 (1927).
17. RAMBERG, L., and HEDLUND, J., Arkiv Kemi, Mineral. Geol. *13* A No. 1 (1938).
18. NEILANDS, J. B., and CANNON, M. D., Anal. Chem. *27*, 29 (1955).
19. TUDDENHAM, W. M., and ANDERSSON, D. H., *Color Control Dept. Report A-49*, New York 1949, from BATES, R. G., Electrometric pH Determinations. New York 1954.

Tryckt den 14 april 1961

Uppsala 1961. Almqvist & Wiksells Boktryckeri AB

ARKIV FÖR KEMI Band 17 nr 30

Communicated 7 December 1960 by Arne Fredga

On the resolution and the racemization of 4-methyl-Δ^3-cyclohexenecarboxylic acid

By Rune Sandberg

With 3 figures in the text

In the study of the stereochemistry of terpenylic acid [1], it was originally intended to resolve 4-methyl-Δ^3-cyclohexenecarboxylic acid into its optical antipodes for conversion to optically active homoterpenyl methyl ketone via α-terpineol. Fisher and Perkin [2] were the first to synthesize optically active α-terpineol by this route, but they obtained an alcohol of less than 50 % activity. Apparently the acid was far from completely resolved, as the esterification and the following Grignard synthesis hardly could cause an extensive racemization. In spite of great efforts the present author could not find a satisfactory procedure for the resolution, and as the necessary amount of optically active acid was not obtained by the method finally adopted, an alternative approach was made to the original problem [1]. The resolving bases used in the present investigation were brucin in methanol ((−)-acid) and (+)-α-(2-naphthyl)-ethylamine in acetone ((+)-acid). The resolution was interrupted at values of $[\alpha]_D^{25}$ of -58° and $+99^\circ$ respectively (abs. alcohol); the latter value was reached after thirteen recrystallizations but it is doubtful if this is the maximum activity. Fisher and Perkin obviously believed they had obtained the pure antipodes with values of $[\alpha]_D$ of -58° and $+56^\circ$ respectively. It is notable that they reported melting points "about 99°C".

It is not clear wheather the sluggish course of the resolution, illustrated by Fig. 1, is due to a partial racemization. The influence of the resolving base might cause a transformation of the double bond from one side of the methyl group to the other. Another possibility would be a protonation of the double bond during the isolation of the optically active acid. It was, however, found that when the acid obtained from the mother liquor of a recrystallization of the amine salt was tested for optical activity, the calculated value was obtained. Furthermore, it could be shown that the optically active acid did not racemize in 2-*N* sodium hydroxide solution, and as will be seen later, the hydration of the double bond is so slow that it is unlikely to be the operative process. Instead, the explanation may be that the difference between the solubilities of the diastereomeric salts is unusually small, since the enantiomers can be said to differ only in the position of a double bond. Consequently the separation difficulties may be further complicated by the formation of mixed crystals.

Interest was now centered upon the general reactivity of the ethylenic linkage

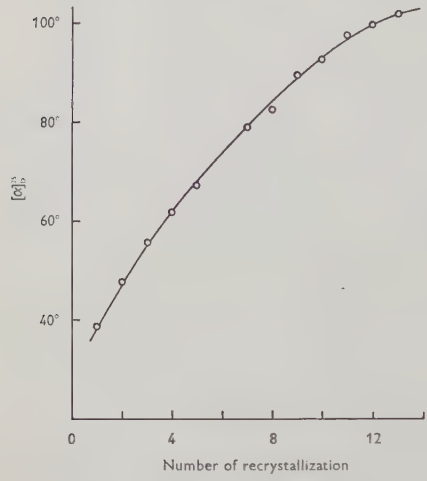

Fig. 1. $[\alpha]_D^{25}$ of (+)-acid against number of recrystallization of the salt with (+)-α-(naphthyl)-ethylamin.

towards reagents obeying Markownikoff's rule. The addition of such a reagent gives a symmetrical molecule and can accordingly be followed kinetically as a racemization reaction.

The position of the double bond in 4-methyl-Δ^3-cyclohexenecarboxylic acid is the same as that in Δ^3-carene and that of the ring double bond in limonene. It has previously been pointed out [1] that under anhydrous conditions limonene does not add more than one molecule of hydrogen chloride to give the optically active limonene monohydrochloride. A striking parallelism is now found in the reaction of the above mentioned acid with hydrogen chloride in dioxan solution: the rate of racemization in dry dioxan is almost unmeasurably slow while the presence of only a small amount of water accelerates the reaction considerably. With concentrated hydrochloric acid in a polar solvent such as acetic acid, 4-chloro-4-methylcyclohexancarboxylic acid is produced in quantity. A similar catalytic influence by water has also been reported for the addition of hydrogen chloride to dicyclopentadiene to form the monohydrochloride [3]. In a recent investigation on the addition of hydrogen chloride to isobutene [4] it was proposed that the halogen acids cannot as such protonate the olefine but must first set their protons relatively free in pre-equilibrium. The need for the presence of a protonizing agent, such as water, indicates that in the cases mentioned the effective reagent in the formation of the intermediate carbonium ion is H_3O^+ rather than H^+ in some free state.

The hydration reaction was studied in some detail, in view of the possible hydration, or isomerization, of Δ^3-carene discussed in the previous paper [1]. The rate of hydration of the ethylenic bond in aqueous solution has been shown to be directly proportional to the Hammet acidity function h_0 [5, 6]. As the cyclohexenecarboxylic acid is very slightly soluble in water, a mixed aqueous solvent (24.4 moles % of ethanol) with known values of H_0 for different concentrations of hydrochloric acid [7] was selected as a reaction medium. The acidity range investigated was 0.64–2.53 molar. In each case the reaction was accurately first order. Plots of log α against time gave straight lines from which the values of k were ob-

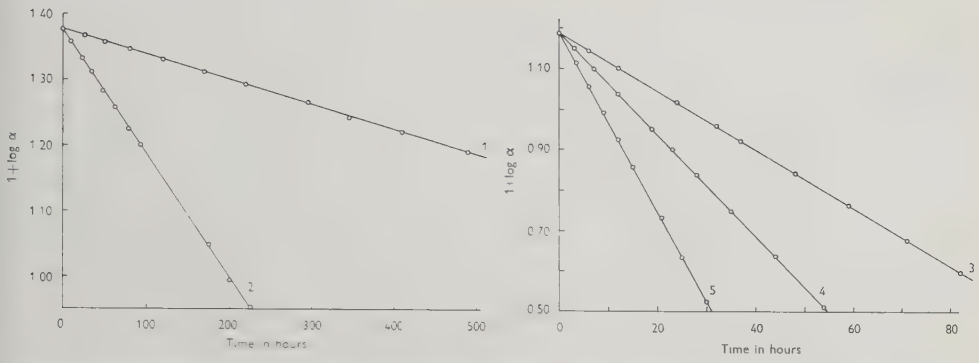

Fig. 2. Log α *versus* time for racemization of 4-methyl-Δ^3-cyclohexenecarboxylic acid in hydrochloric acid solutions. The numbering refers to Table 1.

Table 1. Hydrochloric acid catalyzed hydration of 4-methyl-Δ^3-cyclohexenecarboxylic acid in 24.4 moles % of ethanol in water at 25°C. Concentration of unsaturated acid 0.101 molar.

No.	1	2	3	4	5
C_{HCl}	0.639	1.27	1.90	2.22	2.53
$10^5 k \cdot min^{-1}$	1.44	7.22	27.7	48.0	84.4
H_0	1.12	0.61	0.25	0.06	−0.11

tained (Fig. 2). The result is summarized i Table 1. It may be observed that the rate constant for the hydration in 0.64 molar hydrochloric acid $1.44 \cdot 10^{-5} \cdot min^{-1}$ implies a half-life period of 850 hours.

The use of mixed aqueous solvents in diagnostic investigations of different acid-catalyzed reactions has recently been strongly criticized by Satchell [7]. He found that for a reaction the rate of which in water solution was proportional to $C_{H_3O^+}$ the dependence of rate on acidity in ethanol-water mixtures changed from $C_{H_3O^+}$ to h_0 with increasing ethanol contents. In the present case a plot of log k against H_0 gives a straight line which however has a slope of 1.44 (Fig. 3). This result is thus in accordance with that of Satchell in that it indicates that with increasing ethanol contents and for a given acid concentration, the increase in rate is greater than the change in H_0.

Simonsen stated [1, 8] that Δ^3-carene is not affected by 5 % sulphuric acid even when it is heated at 100° in a closed container for seven days. This seems quite plausible in view of the half life period calculated for the hydration of the cyclohexenecarboxylic acid in 0.64 molar hydrochloric acid and the above interpretation.

Experimental

Racemic 4-methyl-Δ^3-cyclohexenecarboxylic acid. The methyl ester was prepared according to Alder and Vogt [9] and hydrolyzed in methanolic potassium hydroxide

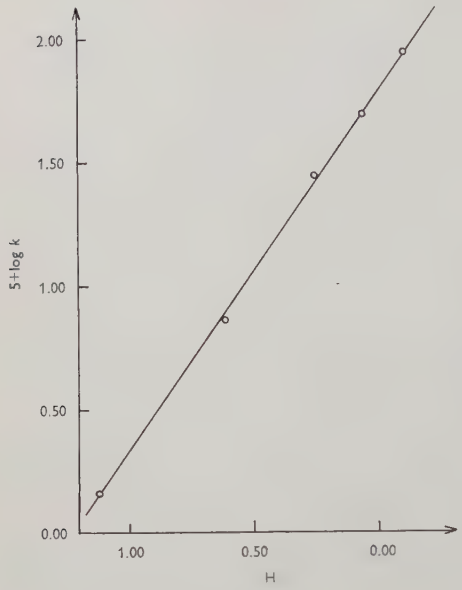

Fig. 3. The dependence of the rate of hydration on the acidity function H_0 in ethanol–water mixture.

solution. On recrystallization from light petrol-ether the acid melted at 97–99° (lit. [10], m.p. 99°).

Attempted resolution. The alkaloids brucine, cinchonidine, morphine, quinidine, quinine and strychnine, the synthetic bases (+)-α-phenyl-ethylamine and (+)-α--(2-naphthyl)-ethylamine and (−)-α-phenylethylthiuronium chloride [11] were all tested in the solvents acetone, methanol, ethanol and ethyl acetate. Significant results were obtained only with brucine in methanol and ethanol ($[\alpha]_D^{25}$ of acid $-27°$ and $-20°$ respectively), with naphthylethylamin in all solvents ($[\alpha]_D^{25}$ ranging from $+15°$ to 25°) and with the thiuronium chloride in methanol ($-20°$).

50.0 g (0.357 mole) of the racemic acid and 141 g (0.357 mole) of brucine were dissolved by warming in 1400 ml of methanol. After several hours at room temperature and one night in the refrigerator 111 g of salt were obtained. The acid from this had $[\alpha]_D^{25} = -21.5°$. The salt was recrystallized from methanol eight times, after which 53.5 g remained. The acid was liberated and recrystallized twice from light petrol, yield 8.3 g m.p. 96–99°. Equiv. wt. calc. 140.2, found 140.6 $[\alpha]_D^{25} = -58.2°$.

The mother liquor from the first crystallization was evaporated to dryness and the acid liberated, yielding 17.8 g with $[\alpha]_D^{25} = +29.0°$.

This acid was dissolved in ether and mixed with an ethereal solution of (+)--α-(2-naphthyl)-ethylamine obtained from 31 g of the neutral sulphate. The salt obtained was recrystallized from mixtures of acetone with methanol (5–10 % by volume) the latter being omitted for the last four recrystallizations. The course of the resolution is shown in Fig. 1. After the thirteenth recrystallization only 2.0 g of salt remained, and the acid from this was liberated and recrystallized from *n*-heptane. It then had $[\alpha]_D^{25} = +99.2°$ with m.p. 98–99°. All optical activities were measured in absolute alcohol.

4-Chloro-4-methyl-cyclohexanecarboxylic acid. 1.4 g (0.01 mole) of racemic 4-methyl-Δ^3-cyclohexenecarboxylic acid was dissolved in 10 ml of glacial acetic acid and 3 ml of concentrated hydrochloric acid was added. The mixture was left over night at room temperature and then poured into 30 ml of water. The acid precipitated was filtered by suction and dried in a vacuum desiccator over sodium hydroxide pellets. Recrystallization from light petrol yielded 0.7 g melting at 100–102°. For analysis the acid was recrystallized from the same solvent once more, the melting point remaining unchanged.

Anal. $C_8H_{13}O_2Cl$ Calc. equiv. wt. 88.3; Cl 20.07.
Found equiv. wt. 89.1; Cl 19.94.

Kinetics. The experimental method was the same as that described in a previous paper [12]. The 4-methyl-Δ^3-cyclohexenecarboxylic acid used in the measurements had $[\alpha]_D^{25} = -58°$.

In the experiments on addition of hydrogen chloride a solution of dioxan (15.00 ml), 0.200 molar in cyclohexenecarboxylic acid and 0.486 molar in halogen acid showed a decrease in rotation of 1.5 % in 24 hours. The addition of 5.00 ml of a 0.333 molar solution of water in dioxan increased the racemization rate to 5 % in the same time.

The hydration reactions were all followed to about 70 % completion except that conducted in 0.64 molar hydrochloric acid which was interrupted after 490 hours when 35 % had reacted. The H_0 values were obtained by interpolation from those reported by Satchell [7].

SUMMARY

Attempts have been made to resolve 4-methyl-Δ^3-cyclohexenecarboxylic acid into its optical antipodes. The partially active acid was utilized for kinetic measurements of additions to the double bond. The very slow addition of hydrogen chloride was found to be catalyzed by water, and the increase in rate of hydration in ethanol-water mixture to be greater than the change in the acidity function h_0 with increasing concentration of the catalyzing acid. The result was discussed with reference to the reactivity of the ring double bonds in limonene and Δ^3-carene.

ACKNOWLEDGEMENTS

The author is indebted to Professor Arne Fredga for his stimulating interest in this work. A grant from *the Swedish Natural Science Research Council* is gratefully acknowledged.

Department of Organic Chemistry, Chemical Institute, University of Uppsala, November 1960.

REFERENCES

1. Sandberg, R., Arkiv för Kemi *16*, No. 23 (1960).
2. Fisher, K., and Perkin, Jr., W. H., J. Chem. Soc. *93*, 1871 (1908).
3. Bruson, H. A., and Riener, T. W., J. Am. Chem. Soc. *67*, 1178 (1945).
4. de la Mare, P. B. D., Hughes, E. D., Ingold, C. K., and Pocker, J., J. Chem. Soc. *1954*, 2930.
5. Taft, Jr., R. W., J. Am. Chem. Soc. *74*, 5372 (1952).

6. LONG, F. A., and PAUL, M. A., Chem. Rev. *57*, 935 (1957).
7. SATCHELL, D. P. N., J. Chem. Soc. *1957*, 2878.
8. SIMONSON, J. L., J. Chem. Soc. *117*, 574 (1920).
9. ALDER, K., and VOGT, W., Ann. *564*, 118 (1949).
10. LEHMANN, E., and PAASCHE, W., Ber. *68*, 1068 (1935).
11. KLÖTZER, W., Monatsh. *87*, 346 (1956).
12. SANDBERG, R., Arkiv för Kemi *17*, 319 (1961).

Tryckt den 18 april 1961

Uppsala 1961. Almqvist & Wiksells Boktryckeri AB

ARKIV FÖR KEMI Band 17 nr 31

Vorgelegt am 7. Dezember 1960

Elektrophoretische Versuche an einem γ-Globulin-Präparat sowie an Seren normaler, sarkomtragender und sarkom-immuner Ratten

Von Hans von Euler und Hans Hasselquist

Mit 4 Figuren im Text

Wie wir schon in vorhergehenden Arbeiten hervorgehoben haben, werden bei der Implantation eines Tumors in normale Ratten viele und mannigfache Wirkstoffe eingeführt. Unter diesen kann man [1] drei Hauptgruppe unterscheiden, nämlich 1) cancerogene Stoffe. 2) antitumorale Faktoren, 3) Enzymsysteme, die an der Immunisierung eines Wirtstieres beteiligt sind.

Die Gegenwart eines — vermutlich mit Desoxyribonukleinsäure verknüpften — karyolytischen Prinzips in Seren normaler und sarkomatöser Ratten wurde schon von H. v. Euler und Leo Heller [2] betont.

Die Tumor-Abwehr ist wiederholt vom serologischen Gesichtspunkt aus als Wirkung von Antikörpern behandelt worden. In neuerer Zeit wurde auch auf Tatsachen hingewiesen, welche die Existenz spezifischer Tumor-Antikörper sehr wahrscheinlich machen (Waterman [3], Zilber [4]). Über serologische Organspezifität beim Buttergelb-Tumor der Ratte hat E. Weiler [5] bemerkenswerte Angaben gemacht. Andere (nicht serologische) Tumor-Abwehr-Reaktionen wurden neuerdings von Druckrey und Mitarb. [6] besprochen.

In Fortsetzung unserer Arbeiten über die in Tumoren enthaltenen Wirkstoffe und Abwehr-Faktoren [7] haben wir [8]

einerseits versucht, durch Einführung geeigneter Mengen von Tumorgeweben oder Tumorextrakten eine endgültige Abwehr gegen den gleichen Tumor (eventuell gegen homologes Krebsgewebe) hervorzurufen ohne den normalen Organismus durch cancerogene Effekte zu schädigen,

andererseits begonnen [9], das Verhalten von γ-Globulin als Wirkstoff-Komponenten in normalen und in cancerösen Blutseren zu studieren.

I. Elektrophorese des γ-Globulin-Präparates Kb

Zur Prüfung des bei unseren Arbeiten verwendten γ-Globulin-Präparates Kb, das wir der Chem. Fabrik Kabi Stockholm, verdanken, wurde dasselbe mit dem Apparat LKB 3276-S4 der Elektrophorese unterworfen, und zwar mit dem Hochauflösungspuffer von Aronson-Grönwall. Wir haben hierzu verwendet:

Fig. 1.

Papier: Schleicher u. Schüll Nr. 2043 b.
Pufferlösung pH 8,9: 0,5-m Trioxymethyl-Aminomethan, TRIS, 0.021-m Äthylendiamin-tetraessigsäure, EDTA, 0,75-m Borsäure.
Konz. des γ-Globulins: 10 mg/ml.
Spannung: 200 Volt. Stromstärke: 1 mA. Zeit 5 Stunden.

Die Wanderungsgeschwindigkeit betrug unter den angegebenen Bedingungen 2 mm (5 Stunden) gegen die Anode. W. Grassman u. Mitarb. [10] beobachteten eine Wanderung sämtlicher Komponenten zur Anode.
Unser Versuch zeigte die Einheitlichkeit des γ-Globulin-Präparates Kb; er liess keine fremden Komponenten erkennen (Fig. 1).

II. Seren normaler, sarkomtragender und sarkomimmuner Ratten

Die im Folgenden zu beschreibenden Versuche stehen in Zusammenhang mit den bei der Transplanation von Tumoren auftretenden Abwehrkräften, die in Regressionen zum Ausdruck kommen und Immunität hervorrufen können.
Die normale Ratte kann sich gegen die Bildung und Ausbreitung eines von einem gleichstammigen Tier transplantierten Tumors auf verschiedene Weise schützen besonders

1. durch die Ausbildung cancerostatischer Faktoren und Enzymsysteme, die zum Teil als „Antikörper" bezeichnet werden,
2. durch Vermehrung und Aktivierung ihrer normalen Hormone, Coenzyme und Wuchsstoffe.

Die Voraussetzung für weitere Fortschritte auf diesem zentralen Gebiet besteht in der Isolierung und chemischen Aufklärung der einzelnen im Serum auftretenden Komponenten.
Wir nehmen diese Aufgabe in Angriff durch Versuche zur elektrophoretischen Trennung der Serumkomponenten, zunächst der Globuline, die zu den Antikörpern in unser Beziehung zu stehen scheinen.

Elektrophorese der Seren

Versuchsreihe I

Papier: Schleicher u. Schüll Nr. 2043 b.
Pufferlösung: Veronal pH 8,6; Ionenstärke 0,1.
Spannung, Stromstärke und Zeit:

I	II	III
200 Volt	100 Volt	50 Volt
2 mA	1 mA	0,5 mA
1 St.	5 St.	18 St.

Nach Schluss der Versuchszeiten wurden die Papierstreifen bei 100° getrocknet und nach Grassmann [10] mit Amidoschwarz 10 B entwickelt.

1. Serum einer Normalratte 0,005 ml.
2. Serum einer Jensensarkom-tragenden Ratte 0,005 ml (grosser Tumor).

Sämtliche Komponenten wandern zur *Anode*.
Die Albumin-Koncentration ist höher im Normal-Serum als im cancerösen Serum.

Bei Kontroll-Versuchen mit zwei anderen Seren einer Normalratte und einer ein kleines Sarkomtragenden Ratte ergab sich zwichen den Elektrogrammen kein Unterschied.

Versuchsreihe II

Papier: Schleicher u. Schüll Nr. 2043 b
Pufferlösung: pH 8,9 mit TRIS, EDTA und Borsäure.
Spannung: 200 Volt. Stromstärke 1 mA. Zeit: 16 Stunden.
Entwickler: Amidoschwarz 10 B in Methanollösung, enthaltend 15 Vol.% Eisessig.
Normalserum und Serum einer sarkomtragenden Ratte mit grossem Tumor 0,005 ml.
Ergebnis: Das Normalserum zeigt eine β-Globulin-Komponente k, die im Serum der sarkomtragenden Ratte zu fehlen scheint (Fig. 2).

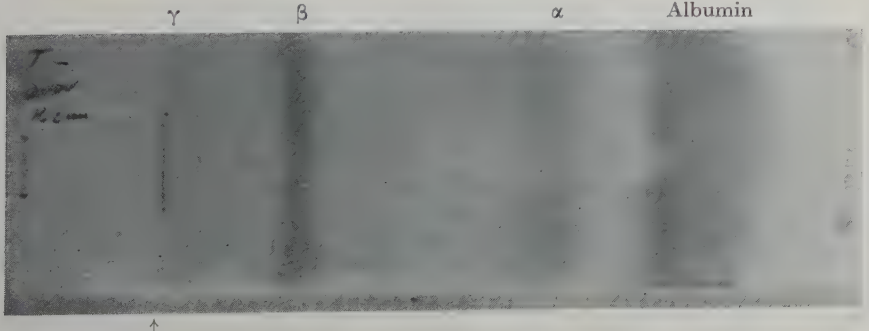

Fig. 2 a.

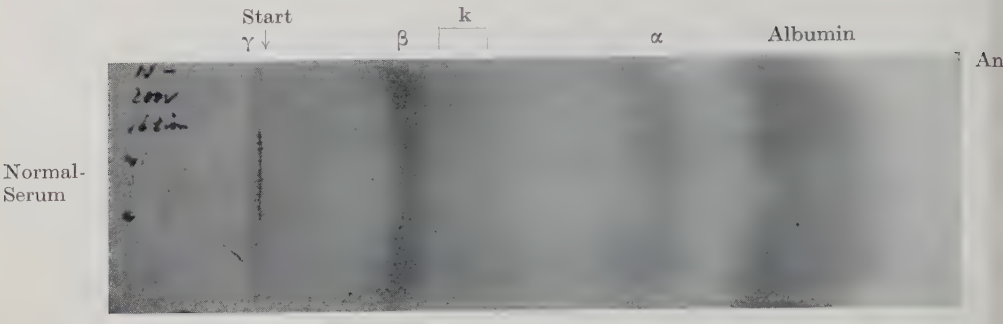

Fig. 2 b.

Versuchsreihe III

Pufferlösung: pH 8.9. Hochauflösungspuffer mit TRIS, EDTA und Borsäure nach Aronson-Grönwall.

Spannung: 200 Volt. Stromstärke: 1 mA. Zeit: 5 Stunden.

Diese kürzere Zeit (5 St.) wurde in dieser Versuchsreihe gewählt um die Feinstruktur der Seren schärfer beobachten zu können. Bei längerer Elektrophorese wird ein Teil der Komponenten, die anfangs in niedrigen Konzentrationen vorhanden sind, über eine grössere Oberfläche ausgebreitet; diese Komponenten können deshalb nicht mit Sicherheit nach der Färbung mit Amidoschwarz 10 B erkannt werden.

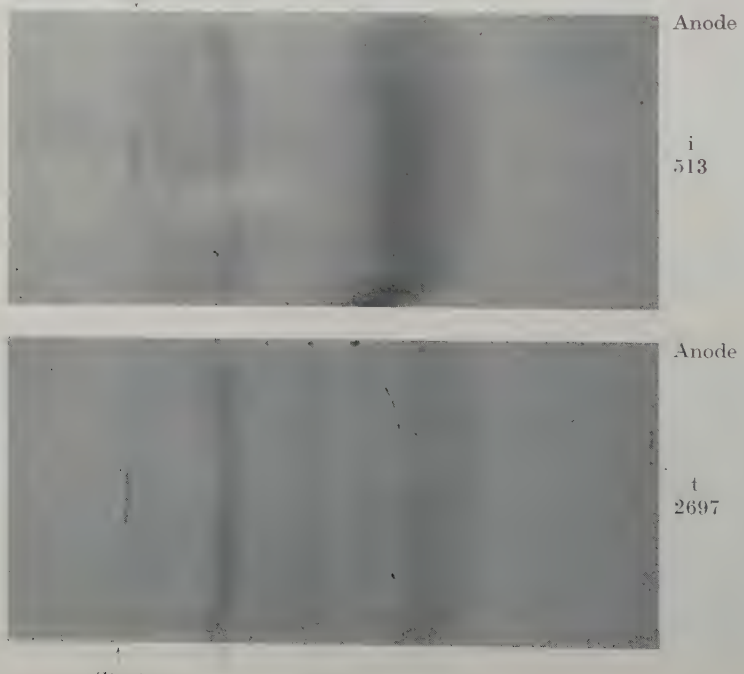

Fig. 3.

Seren von: 1. Immunratte BdI Nr. 513 (i)
2. Immunratte BDI Nr. 515
3. Tumorratte BDI Nr. 2697 (kleines Tier) (t)
4. Tumorratte BDI Nr. 2680 (kleines Tier).

Die Elektrogramme wurden verglichen mit den an Normalseren hergestellten.

Ergebnisse an den Seren 1–4

1. Normal- und Immunratten lassen keinen Unterschied in der Struktur erkennen, abgesehen von dem Umstand, dass Normalserum anscheinend noch eine β-Komponente abscheidet. Prä-Albumin, Albumin, α_1-Globulin sowie γ-Globulin sind im Elektrophoretogramm deutlich sichtbar.

2. Die beiden Immunseren 1 und 2 zeigen keinen Struktur-Unterschied. Prä-Albumin, Albumin, α_1-Globulin treten deutlich hervor, γ-Globulin aber nur schwach. Zwei weitere Komponenten (α oder β) werden zwischen α_1 und β_3 sichtbar.

3. Allgemein kann gesagt werden, dass die Seren der Tumorratten im Gegensatz zu den Seren der Normal- und Immunratten nur sehr wenig γ-Globulin enthalten. Dagegen treten in den Seren der Tumorratten Zwei Komponenten zwischen α_1 und β_3 hervor, die in den Seren den Normal- und der Immunratten nicht erscheinen.

Versuchsreihe IV (Norwegische Ratte, grosser Tumor)

Elektrophorese wie in Versuchsreihe II.

Ergebnis: Auch bei dieser sarkomtragenden Ratten war das γ-Globulin nur in sehr geringer Menge vorhanden. Es zeigte sich eine Komponente X zwischen α_1 und β_3. (Bei BDI waren *zwei* Komponenten deutlich sichtbar.)

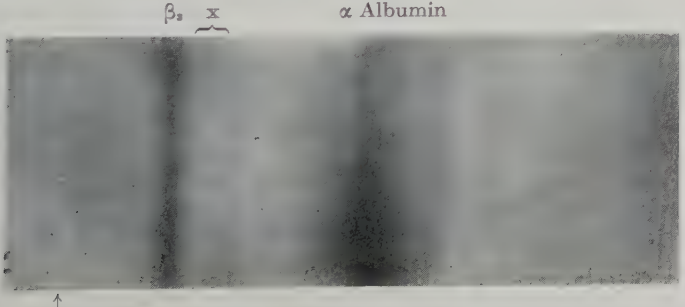

Fig. 4.

Unser Befund, dass das Blutserum sarkomtragender Ratten wenig γ-Globulin — weniger als normales Blutserum — enthält, bedeutet, dass die Abwehrkraft des normalen Serums, wenigstens zum Teil, auf der Gegenwart von γ-Globulin beruht. Bei *Ueberschuss* von γ-Globulin im Blut eines mit Tumor implantierten Tieres kann der Tumor nicht angehen, es tritt (in einem gewissen Grad) Immunität ein.

Nach Pillemer [11] und nach Linder [12] verhält sich das Properdin wie γ-Globulin. In Anwesenheit genügender Mengen von Properdin kommt ein in Ratten implantiertes Sarkom nicht zur Wirkung bzw. zum Wachsen. Im Blutserum normaler Ratten ist u.a. ein Tumor-Abvehrstoff wirksam, der im Serum sarkomtragender Ratten ganz oder teilweise fehlt.

Über den Properdin-Nachweis mittels des wasserunlöslichen Polysaccharides *Zymosan* sei auf die Zusammenfassungen von Hans Schmidt [13] von W. Maassen [14] und von G. Heymann [15] verwiesen.

Andererseits kann im Blut sarkomtragender Ratten auch eine *cancerogene* Substanz wirksam sein. Dass es bis jetzt nicht gelungen ist, in Ratten durch Injektion zellfreien Blutserums Tumoren hervorzurufen beruht vermutlich auf der gleichzeitigen Anwesenheit von Properdin oder eines anderen γ-Globulins.

Herrn Ing. Alf Larsen danken wir für die Mitarbeit bei der Ausführung der Elektrophorese-Versuche.

Stockholm, Universität, Vitamin-Institut.

LITERATUR

1. H. v. Euler, Kem. Arbeten Ny följd B. 19.1.1959. — Vortrag Lindau 1960. — Deut. med. Wochschr. *85*, 1911 (1960). — Compt. rend. acad. sci. (Paris) *250*, 2796 (1960).
2. H. v. Euler u. Leo Heller, Attempts to provoke karyolysis by active immunisation. Arkiv Kemi *1*, 425 (1949). — H. v. Euler, L. Heller u. Chr. Curman, Arkiv Kemi *1*, 299 (1949).
3. N. Waterman, Bull. Cancer *45*, 360 (1958).
4. L. A. Zilber, 7th Intern. Congr. Cancer Abstr. 46 (1958).
5. E. Weiler, Z. Naturforsch. *7 b*, 324 (1952).
6. H. Druckrey u. Mitarb., Z. Krebsforsch. *63*, 28 (1960).
7. H. v. Euler, H. Hasselquist, D. Nomura u. H. Erret, Arkiv Kemi *15*, 525 (1960).
8. H. v. Euler, Arkiv Kemi *16*, 239 (1960). — Krebsarzt *14*, 343 (1959),
9. H. v. Euler, H. Hasselquist u. H. Erret, Arkiv Kemi *16*, 327 (1960).
10. W. Grassmann, K. Hannig u. M. Knedel, Deut. med. Wochschr. *76*, 334 (1951).
11. L. Pillemer, Trans. New York Acad. Sci. *17*, 526 (1955).
12. E. Linder, Strahlentherapie *103*, 91 (1957).
13. Hans Schmidt, Fortschritte d. Immun.Forsch. Verlag Steinkopff, Darmstadt (1959).
14. W. Maassen, Z. Immun.Forsch. *119*, 405 (1960).
15. G. Heymann, Zblt. f. Bakt. I. Referate. Band *176*, 305 (1960).

Tryckt den 18 april 1961

Uppsala 1961. Almqvist & Wiksells Boktryckeri AB

ARKIV FÖR KEMI Band 17 nr 32

Communicated 11 January 1961 by Arne Ölander and Ole Lamm

An approach to the study of the chemical reactions of thermal gaseous ions with liquids and some notes on their possible biological effects

By T. Westermark and H. Lindroth

SUMMARY

The neutralization of a positive gaseous ion of radical character involves a very large energy release in comparison with all known chemical bond energies. The postulate is therefore put forward that such ions act radiation-like (radiomimetic)—for example if brought into contact with condensed substances. The possibility that the fundamental rôle of ions in radiation chemistry might be studied with ions produced by corona discharge is evident from briefly described experiments in which gaseous ions are brought into contact with aqueous solutions. Positive helium or argon ions are produced near a thin tungsten loop and moved to the top of a liquid surface using a four-cell quartz apparatus with a geometry that excludes to a large extent the action of UV-light. The formation of iodine in aqueous KI solutions of various concentrations has been studied. The yield was found to increase to a saturation level at high concentrations and is of an order that compares well with radiation chemical yields. The formation of H_2O_2 in water, the oxidation of Fe^{2+} ions and the decomposition of chloroform are briefly described. Although no biological evidence is available, it is physically and chemically reasonable to postulate that gaseous ions might play a rôle in the etiology of human lung cancer. It is known that there occur, in air, gaseous ions caused by electrical discharges, flames, glowing bodies, etc. Free charges of as yet unknown nature are present in cigarette smoke. According to findings published elsewhere, such free charges are also present in the exhaust gases from cars and often in high concentrations. Reasonable assumptions lead to equivalent radiation doses for the mucous membrane which correspond to the incidence rate for human lung cancer. It is assumed for these calculations that the loss occurring in the potential energy of the gaseous ions in the inhaled air due to aging is relatively small. This point, as well as the aggregation and capture of molecular ions by dust and droplets, is important for the validity of the lung cancer hypothesis put forward and has to be further studied.

I. Introduction

As is well-known, ionizing radiation is characterized by the production of ions. excited states, free electrons, free radicals, etc. In a gas, gaseous ions are formed and can be easily detected. It occurred to the senior author [39] (1957) that problems in radiation chemistry and radiation biology might be fundamentally approached by producing gaseous ions separately and subsequently bringing them into contact with the medium—liquid, gel or solid—to be studied. It cannot be excluded that gaseous ions may contribute to cause part of the lung cancer incidence in man. The

basis of this supposition is the well-verified circumstance that large radiological doses cause lung cancer in man. If it turns out that gaseous ions in inhaled air also act radiation-like, i.e. radiomimetic, then such ions must in consequence be seriously considered as a public hazard. Some studies concerning these problems will be discussed below.

Energy considerations

To produce a gaseous ion, energy has to be applied:

$$A \rightarrow A^+ + e^- - J. \tag{1}$$

J is the ionization potential, generally of the order 8–25 eV. (A^+ stands for any ion here.)

Now, if a gaseous ion that is already formed is brought into a (possibly condensed) medium where a free electron is available, then the reverse reaction of (1) will occur and the energy (J) will be evolved in some way. This thought, it seems clear, was expressed by S. C. Lind 30–40 years ago [2], but the present authors have not found its consequences expressed in the form that the positive ions might accordingly be termed *radiation equivalent* or, after C. Auerbach, *radiomimetic*. (Of course, the penetrating power of the radiation is lost.) The justification of this standpoint should be founded on a discussion of what is the real characteristic of ionizing radiation (to distinguish it from non-ionizing, for instance) from a chemical and thus also biological point of view. If we choose to say that the criterion is the indiscriminate breaking of covalent chemical bonds, we find that the positive gaseous ions should, energetically, be able to break all known chemical bonds including the biologically important O–H (5.1 eV in water), C–H (3.8 eV), C–C (2.5 eV), C–O (3.0 eV) etc. [3]. (The strongest bond listed by Pauling is Si–F 6.2 eV.) Free radicals will, of course, be thereby formed. If we choose to consider electronic excitation, which, usually requires less energy, we find that also this process is energetically possible. Negative ions should also be considered (for one example, see below). The discussion presumes that there are allowed reaction mechanisms which can be followed when the energy supplied is sufficient. The rôle of ionic species in radiation chemistry was an important point in Lind's work [2] and was re-emphasized later. For example, Burton *et al.* [1] in 1952 expressed the view that the ions M^+ formed in a liquid recapture an electron very quickly or within 10^{-13} sec:

$$M^+ + e^- \rightarrow M^\dagger,$$

where $M^\dagger$ represents a highly excited state.

Ions have also been assigned a rôle in some polymerisation processes [40, 41]. According to some British investigators [42], the ion CO_2^+ plays an important part in the destruction of reactor graphite in nuclear reactors.

Supposing now that we distribute N ions, with an ionization potential J (hence $-J$ is the electron affinity of the positive ion) in m grams of some material, we can express the radiation-equivalent dose by means of the equation:

$$D = \frac{N \times |J|}{m} \times 1.6 \times 10^{-14} \text{ rad}. \tag{2}$$

Some processes will tend to decrease the dose below this value. One such process is *charge transfer:*

$$A^+ + B \rightarrow B^+ + A + (J_A - J_B). \tag{3}$$

J_A should be larger than J_B but, in order to permit a high reaction probability in the gas, these potentials should not be too dissimilar. In a liquid or gel, the deposited ion may be assumed to act according to (3) (for one example, see reaction (5) below) and thus not according to (1) (backwards) because free electrons are seldom available in such cases. Secondly, positive and negative ions can recombine:

$$A^+ + B^- \rightarrow A + B + Q \tag{4}$$

(Q is the energy evolved), following the rate law $dn/dt = -\alpha \cdot n_+ \cdot n_-$, where the recombination coefficient $\alpha \sim 10^{-6}$ for gases. Q is very high compared with all chemical bond energies. (It can be roughly assumed to be equal to J minus the electron affinity of B. This process may also occur in liquids.) Other processes, e.g. the ion-molecule reactions [5, 27], may lead to bond breaking *already in the gas phase.*

In many cases of experimental interest, the presence of moisture must be taken into account. The following reaction seems probable:

$$A^+ + H_2O \rightarrow A + H_2O^+, \tag{5}$$

where A stands for any molecule or atom statisfying $J_A > J_{H_2O}$ ($J_{H_2O} = 12.52$ eV), e.g. N_2 or argon in inhaled air.

In such cases, a positive water ion may reach a liquid water surface or a mucous membrane or it may be formed just at the top of the surface layer of the liquid or gel. According to our present knowledge concerning radiation chemistry (see, for instance, a series of papers by E. J. Hart [6] in the Geneva 1958 Proceedings), the fate of the positive ion is supposed to be:

$$H_2O^+ \rightarrow H^+_{aq} + OH. \tag{6}$$

(Positive ions thus act in an oxidizing and acidifying manner.)

If OH radicals are formed densely, the following reaction can be expected:

$$OH + OH \rightarrow H_2O_2. \tag{7}$$

The negative water ion gives H radicals:

$$H_2O^- \rightarrow H + OH^-_{aq}. \tag{8}$$

(Negative ions thus act in a reducing and alkalinity-forming manner.)

If O_2 is present, the reaction

$$H + O_2 \rightarrow HO_2 \tag{9}$$

is likely to occur. Thus negative ions play an important rôle. If unipolar ions are deposited, the above reactions should be expected. If, however, ions of both signs are deposited simultaneously on a liquid surface, cross-reactions may obviously be expected to occur (as in radiation chemistry), for instance:

$$H + OH \rightarrow H_2O$$

and

$$H_3O^+_{aq} + OH^- \rightarrow 2H_2O.$$

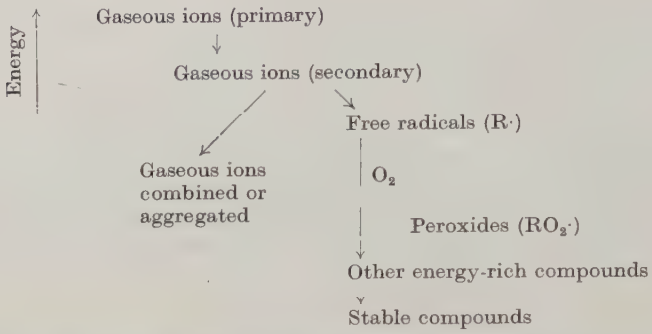

Fig. 1. Crude energy scheme for gaseous ions and some other entities in the gas phase.

Recently J. Weiss [26] has put forward several new points of view concerning the mechanisms involved in the radiation chemistry of water. The negative entity polarizes its neighbourhood and the polaron thus formed has a longer life than that previously assumed for H_2O^-. Two polarons may form hydrogen gas directly. Also a positive polaron is imagined. Two positive polarons may form H_2O_2 directly. These views do not change the main lines of reasoning here but the detailed mechanisms might have to be reconsidered. In fact, it seems possible to test many of Weiss' points just by means of gas ion chemistry.

In air, several processes are known to occur which make the above-mentioned reactions, which should be expected under clean laboratory conditions, less probable. The aging of ions in air [4] is an important phenomenon, but the detailed mechanisms are poorly known at present. Various sorts of aggregations (e.g. attraction of dipoles) may occcur, thus giving the ions a decreased mobility and perhaps longer life. A combining of the ions with small solid or liquid particles is also likely. Energy may be dissipated during these processes, thus yielding free radicals and less energetic charged entities.

Fig. 1 shows a crude energy scheme covering some of the entities discussed here. It should be noted that ozone, being of the RO_2 type, has been suggested to behave radiomimetically [24].

II. Experimental

Principles and apparatus

There are several ways of producing gaseous ions [4], e.g. by electrical discharges, heat, ionizing radiation, etc. In order to obtain basic experimental information which can be unambiguously interpreted, it was chosen to produce first of all unipolar positive ions of the noble gases helium and argon. The ionization potentials are 24.58 eV for He and 15.76 eV for A [4]. Although some success has been achieved with Po^{210} alpha sources, we have mainly used electrical discharges from very thin tungsten wires 0.002–0.1 mm diameter (procured from AB Lumalampan, Stockholm) in the form of loops.

The apparatus employed is shown in Fig. 2. The application of a high, gradually increasing positive voltage to the thin wire causes eventually a breakdown due to the high electrical field strength near the wire [18]. The latter effectively repels the

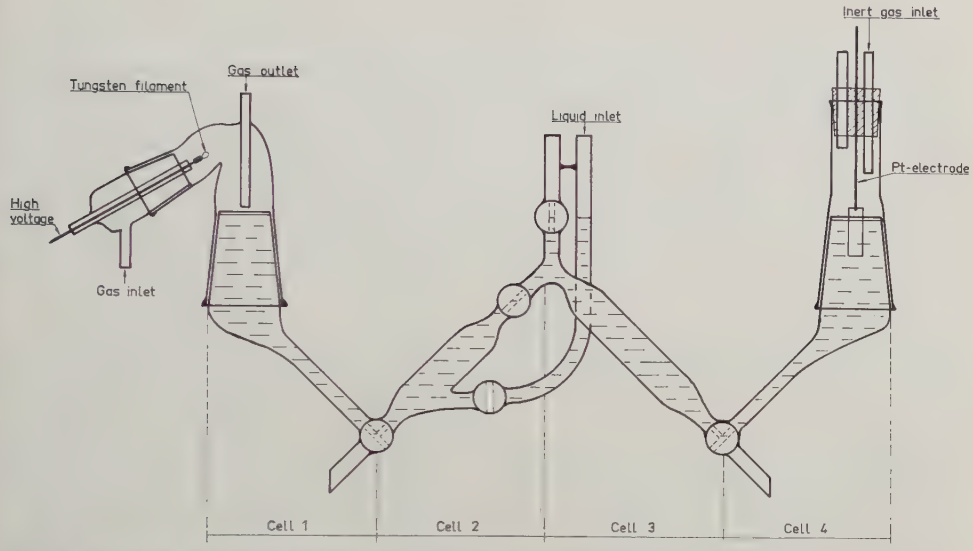

Fig. 2. Four-cell quartz apparatus for studying the chemical reactions in liquids initiated by gaseous ions. The latter are produced at the tungsten filament when the potential drop to the earthed liquid is high enough. The current to earth is recorded and the contents of the four cells are analyzed separately.

positive ions produced and retains the electrons. Light emission will be seen as a thin sheath around the wire. The positive gaseous ions produced will drift towards the negative electrode—in this case, a liquid surface. The direct current passing through the liquid should represent the flow of positive ions to the liquid. The liquid has to be sufficiently conducting and must be provided with a metal electrode and leads to close the circuit.

The apparatus was made completely of quartz glass and plastics, stopcock grease etc. were avoided in order to ensure rigorous purity. It has performed well and yielded sufficiently stable currents, in helium and argon at atmospheric pressure, of the order of some μA. Variations in current of about $\pm$ 10 % are regarded as quite normal. This might be partly due to the voltage variations of the H.T. unit (Brandenburg type S. 0530/R yielding up to 30 kV positive or negative) but has certainly also some connection with the gas flushing velocity and the discharge itself. The increase in current with applied voltage is very steep and, considering all factors involved, it might be very difficult to increase the current stability very much. The matter of interest here is the quantity of electricity or number of gaseous ions transferred to the liquid and this is readily obtained by integration of the recorder strips.

The products formed should be related to the total number of ions collected:

$$N_{\text{chem}} = \frac{G_{\pm} J i_{\pm} \cdot t}{z e_0 \cdot 100} \tag{10}$$

(z = ion charge, N_{chem} = number of molecules produced or destroyed, $i_{\pm}$ = average current representing the collection of positive or negative ions). This equation might be said to be a Faraday law for the action of gas ions on liquids or gels. It thus connects this sort of electrochemistry with radiation chemistry by means of an equiva-

lent G-value (G_+ or G) which should be formulated to include possible losses of energy in the gas and the deviations from exact equivalence. It follows that the ion current is connected to the dose rate in radiation chemistry and thus of great basic interest. Of course the yield can be expressed in accordance with Lind's classical M/N figure which is the number of molecules destroyed per reacted ion or in the case of unipolar ions the number of moles yielded per Faraday transported to the liquid surface. A similar expression is used by Hickling *et al.* [35] and by Dewhurst *et al.* [36] in their studies of "glow discharge electrolysis". Thus our experiments may yield equivalent G or M/N figures which can be compared with the corresponding figures from radiation chemistry and hence might enable basic conclusions to be drawn.

There are many causes of faulty operation. If too high a voltage is applied, sparking occurs and the current becomes quite unstable. It has been our practice to operate the apparatus in a dark-room. During normal operation, the anode glow is visible around the wire and no light is visible elsewhere, i.e. not even near the cathode. Sparking, which is seen as irregular threads to some part of the tube, must, of course, be avoided. This can be easily done by changing to a lower voltage. The choice of quartz glass is motivated by the high resistivity of this material. At the steady state, current should flow only to the liquid and not to the tube. The direction of the gas stream is designed both to flush the zone near the anode with fresh gas in order to prevent any condensation of moisture on the walls which may produce trivial creep currents and also to diminish the extent to which charge transfer to the vapour of the liquid may occur before the ions encounter the liquid surface. It is estimated that encounters with water vapor, for instance, will not occur until 3–5 mm above the surface.

According to Loeb [4], "it has experimentally been established that, in inert gases below values of $X/p = 5$, and in other gases, such as H_2 and N_2, up to $X/p = 10$ to 20, the ion does not gain much energy from the electrical field" (X = field strength in volts/cm, p = pressure in mm Hg). The experiments reported here were all performed at atmospheric pressure and low current densities were used (of the order of 1 μA/cm^2). Since most of the voltage drop occurs in the immediate vicinity of the corona wire about 2 cm from the liquid surface, the X/p-values obtained by simply dividing the voltage by distance times pressure should lead to an upper limit. X/p calculated in this way was usually found to be lower than 5, the only execptions being some of the first observations ($X/p \simeq 20$). The effective X/p-values for the space over the liquid should be much lower than the figures mentioned. Consequently any chemical action ascribable to the gaseous ions should be due to their potential energy. The kinetic energy of the ions should not be much higher than what corresponds to the thermal energy.

As has often been pointed out (see Loeb [4], for instance), the gas must be extremely pure before one can be sure that the ions under investigation are the expected ones. Charge transfer to impurities with lower ionization potentials is a process that has to be seriously considered. The gases used were helium and argon with the following possible impurities in mole percent: O_2 0.0005, H_2 0.0005, N_2 0.01 and 0.02 respectively. However, even this degree of purity might not be enough. The low oxygen content was removed by using a heated (~ 170°C) packed Cu column.[1] The packing material was prepared from sintered copper oxide reduced by flushing

[1] We are indebetd to Mr. F. Ericsson, Inorganic Division of this Institute, for the preparation of this column.

with hydrogen to a red colour. Although low, the nitrogen content might still cause some charge transfer giving rise to positive nitrogen ions ($J = 15.55$ eV) [4].

The encounters with water vapour just above the liquid surface might produce H_2O^+ ions ($J = 12.5$ eV), which would then constitute the charge carrier reaching the liquid surface. Even this supposition is not certain, however, since Lampe [27] gives, from mass-spectrometric evidence, a half-life of only 3×10^{-12} sec in water vapour of low pressure. A decomposition of the H_2O^+ would then lead to H^+ and the OH radical (cf. [6] above). The latter might be flushed out with the gas, since it is uncharged, or it might collide with the liquid surface and be captured. Analogous discussions might be applicable for other solvents.

It is clear that many conditions must be fulfilled in order to know with certainty that a specific ion species, say He^+ or A^+, is the only one reaching the liquid surface. The purity of the noble gas, conditions of gas flow, temperature, pressure and mobility of the ions are obvious factors involved. Not all these factors have been optimized in the experiments reported here.

The light emitted in the discharge is expected to be partly of very short wave-length, especially when helium is used (18–25 eV). Such light is known in itself to be very active photochemically—if water absorbs light of wave-length lower than 1800 Å, it is decomposed into radicals with high quantum yields [28]. Thus every effort must be made to reduce this contribution. If straight tubes are used with the anode wire at one end, large currents are obtained [39], but then the chemical response is probably partly due to the light. Comparisons of experiments with and without a grounded fine metal wire net placed just above the liquid surface should give the yields ascribable to the gaseous ions [39], provided the nature of the discharge is unchanged under such conditions. (This procedure has been used by Dewhurst *et al.* [36].) Probably a safer method would be to use a net of filter paper wetted with the cell liquid instead of the metal grid – the latter might be able to emit electrons which could neutralize the ions in the gas phase. From Fig. 2 it is seen that ions are guided along a curved path and so only scattered light can hit the liquid and thus the influence of the light is much reduced. (The reflection coefficents of the light involved are generally small.)

Common causes of failure in operation are often the creep currents apparently due to the moisture on the insulators. These are characterized by a linear current–voltage curve instead of a steep one with a virtual threshold. Good results have been obtained with Perspex cells but, since this material may obviously give off organic vapours, we have changed to quartz. Moreover, quartz seems better than Pyrex glass from the creep current point of view. However, such currents will be completely eliminated in a future modification of the apparatus in which the gas will be allowed to flow out between the two parts of the ground joint situated second from the left in Fig. 2, thus breaking the mechanical contact between the positive and negative parts of the apparatus.

The apparatus has been divided into four cells which are emptied after en experiment, and each sample is then analyzed. Thus the cell containing the earthing electrode is far from the cell (called cell 1) where the gaseous ions react and no confusion with electrochemical effects can take place.

Observations

Some preliminary observations indicated chemical yields of the order expected. The experiments were performed in an apparatus which resembles that of Fig. 2.

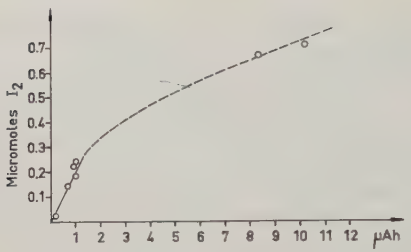

Fig. 3.

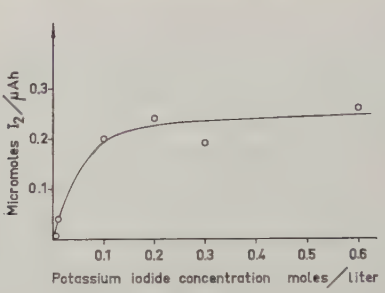

Fig. 4.

Fig. 3. Gas ion oxidation of 0.2 *M* KI. μMol I_2 as a function of the number of μAh given.
Fig. 4. Variation of iodine yield with concentration of KI (cf. text of Fig. 3). The runs (cf. both fig. 3 and fig. 4) were made with + 15kV on the anode, electrode distance 2 cm and using currents 0.2–1.1 μA.

The material used for the cell containing the anode wire was, however, Perspex (cf. above) and the solutions employed were prepared from distilled water from the laboratory supply without further purification. They certainly contained dissolved oxygen.

Fig. 3 shows the formation of iodine in an aqueous solution of potassium iodide and chloroform when gaseous ions are brought into contact with the liquid. (The chloroform seems to be a less important constituent of the solution.) When starch is present, a blue colour can be observed at the top of the liquid after a few minutes when using an ion current of about 1 μA.

As can be seen in Fig. 4, the yield is greatly dependent on the iodide concentration. From the initial slope of the curve in Fig. 3 or from the saturation level in Fig. 4, an equivalent *G*-value of about 40 can be calculated for the positive helium ions used in these experiments. But, as mentioned, charge transfer is likely to occur and so the chemical action might not necessarily be directly assigned to the helium ions without further considerations. The fact that the *G*-value depends on the concentration of the solute is a most interesting feature, since it indicates that the reaction takes place near the liquid surface in close analogy with the oxidation of Fe^{2+} ions by H-atoms [29]. Moreover, a competition of the two possible reactions

$$OH + I^- \rightarrow I + OH^- \tag{11}$$

and

$$OH + OH \rightarrow H_2O_2 \tag{12}$$

is very likely (expressed in terms of classical radiation chemistry). At low KI concentrations, a formation of H_2O_2 is probable.

Some experiments were devoted to the detection of H_2O_2 in the water treated in the apparatus without any KI added. The titanium reagent for H_2O_2 was used [30, 31] and a yield corresponding to about 3 H_2O_2 molecules per ion reaching the liquid was obtained. The M/N yields differed by a factor of 2 or 3 from experiment to experiment. While it is very gratifying to note that the yield is in the range expected from theoretical considerations (see above), the poor reproducibility is a disappointment. It might be noted here that the competitive formation of iodine and H_2O_2 has its close analogy in radiation chemistry (see, for example, Hart [6]). The oxidation of the Fe^{2+} radiation dosimetry system and the formation of HCl from water-saturated chloroform were also observed, the yield being of the order expected from

radiation chemical considerations. In all experiments, cell 1 contained most of the chemical reaction products. Some additional amounts, although of much smaller concentration, were found in cell 2, whereas cell 3 generally showed no products at all.

It was concluded from the preliminary observations that impurities may be very disturbing as is the case in the radiation chemistry of water [32]. In gaseous ion chemistry, this might be even more important since it seems reasonable that the reactions take place near the liquid surface. Ordinary distilled water most probably contains traces of organic compounds which might well be enriched in the surface and react with the OH radicals or positive polarons [26].

An alkaline permanganate solution was therefore prepared using distilled water from the laboratory supply and the water was distilled into a quartz apparatus (design BI 3, Heraeus, Hanau), where it was redistilled and degassed in two steps and thereafter collected in a flask under oxygen-free nitrogen. Preliminary results using this specially purified water and the much improved apparatus of Fig. 2 showed that the oxidation of iodide ions in 0.25 C KI to iodine corresponds to an M/N-value of 0.7 i.e. lower by more than a factor of ten than the result for aerated solutions. The reproducibility was still, however, not satisfactory. Although this is partly attributed to the low iodine concentrations, it is apparent that improvements are still necessary.

Using a 0.37 mC KI solution made from the high-purity water (i.e. about a thousand times more dilute), it was shown that H_2O_2 was formed. The yield obtained, M/N, was about 0.4.

Studies on polymerization by gaseous ions have been started. The apparatus used is a modification of that in Fig. 2 and is described elsewhere [33].

Discussion

The studies reported are, as seen, still of methodological character, although the present evidence indicates that the chemical yields obtained are in the range expected from transferring the ideas of radiation chemistry to the field of the chemical actions of gaseous ions in liquids. It has been demonstrated that the utmost purity of the gases and liquids is required. These requirements are perhaps even more stringent than in the radiation chemistry of water, because the reactions seem to take place near the liquid surface.

This suggestion concerning surface reactions is in itself interesting, since it might be possible to detect in some cases a fluorescence due to the high excitation energy of the neutralized ion. Substances which are fluorescent and at the same time surface active might emit light when present in solutions treated with positive gaseous ions. Such studies are in progress. (By applying similar ideas, a successful production of luminescence during the dissolution of irradiated solid alkali halides has been obtained [34]). It might be noted in this connection that Gorban and Solokov [38] have shown that the recombination of radicals on the surface of solid phosphorus produces luminescence.

For many years, the field of "glow discharge electrolysis" has been subjected to excellent investigations by A. Hickling and his associates at the University of Liverpool [35]. In a report from 1958, Denaro and Hickling [35*a*] state that "electrolysis is accompanied by oxidation arising from the breakup of water molecules due to the bombardment of the solution by gaseous ions and the chemical phenomena are

analogous to the effects produced by ionizing radiations". They have performed experiments with good reproducibility on several chemical systems. The shape of their curves relating yield and concentration and the order of magnitude of their yields are the same as those in Fig. 4 above. However, their point-to-plane corona discharge (600 V over 0.75 cm distance in H_2 at a pressure of 50 mm, 25–100 mA) yielded such high ion densities that a large fraction of the potential drop apparently occurred within a very short distance from the liquid surface (0.5 mm). Consequently the ions gained energy in the field and their kinetic energy was assumed by the authors to be about 100 eV. Moreover, their geometry does not exclude the action of UV light. (The same is certainly true for the work by Pavlov [43].) The bent tube technique described above is thought to be superior from this point of view. Dewhurst *et al.* [36], using essentially the same kind of apparatus as Hickling *et al.*, studied the oxidation of aqueous ferrous sulphate with ion currents varying from 4 μA to 4.2 mA and reported yields up to 25 oxidation equivalents per Faraday. (This quantity, of course, will be the same as the M/N-value used here.) The energy of the ions is not explicitly stated but it might be guessed that the kinetic energy gained is of the same order as in the studies of Hickling *et al.*

In a recent article [37], Kingdon describes the killing of bacteria by gaseous ions produced by a point to plane corona discharge and other ion sources. The currents used were several μA. The ions were assumed to possess an energy of 6 eV, i.e. about half their ionization energy (aged ions). No very detailed discussion was given about this energy estimation. Also here acceleration of ions near the cathode seems to occur. — We tentatively conclude that whereas our studies are made under conditions usually termed corona discharge [45] without "brushes" or "streamers", the work by Hickling *et al.*, Dewhurst *et al.* and Kingdon is made under typical glow discharge conditions, where an appreciable cathode fall and hence ion acceleration to tens of eV or more is present together with an appreciable light production. It might be questioned whether conclusions concerning chemical or biological actions of *thermal* gaseous ions can be made directly from such studies.

From the biological point of view and for discussions of fundamental mechanisms, the potential energy of the gaseous ions would seem to be of the greatest interest. Much evidence from studies of gaseous ion chemistry point to the equivalence between the chemical actions of electrical discharges and ionizing radiation. An application of this equivalence in a somewhat different manner is inherent in the acceleration methods for the Wilzbach labelling process developed in this laboratory [23] and by others.

Many of the statements concerning the radiation chemistry of water might have to be changed due to the concepts developed recently by Weiss [26]. Since we have observed experimentally that the application of high negative voltages in the apparatus described (Fig. 2) also produces sizable currents, we feel that it might be possible to produce both positive and negative entities which may lead to the polarons predicted by Weiss. The experimental studies initiated here might thus contribute to the testing of this and other theories concerning the radiation chemistry of aqueous systems.

III. A hypothesis of lung cancer induction by gaseous ions

The inhalation of ionized air is the most probable case in which living organisms are likely to be affected by the effects described above. A quantitative estimate of the

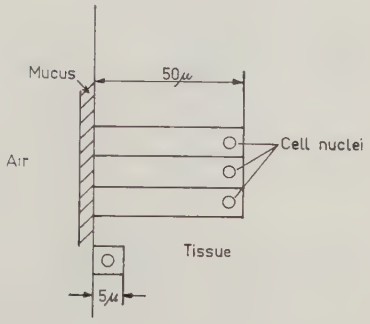

Fig. 5. Simplified picture for the discussion of ion deposition and energy transfer on trachea walls (cf. text).

radiation-equivalent dose, due to gaseous ions, for the mucous membranes of the nose, throat and lung must necessarily by very crude at present but would seem to be of interest. In this section, we shall make the as yet hypothetical assumption that the dose produced by the sorption of gaseous ions in tissue is radiation-equivalent. This assumption will thereafter be discussed.

It is probable that once a gaseous ion (at least a light one) collides with the wet walls of the air passages, it will react immediately. We might therefore be permitted to apply the ion deposition theory of Townsend [9], which has been tested by Chamberlain [10], for the charged daughter products of thorium and radon when discussing lung cancer in connection with the Schneeberg and Joachimstal uranium mine cases. The theory involves the diffusion coefficient of the ion and the gas velocity. The result, using parameters realistic for human beings,[1] is a roughly uniform deposition over about a 2 m path lenght.

We are thus justified, to a first approximation, in assuming that the distribution of the ions is rather uniform over the whole respiratory system (except the entrance, where turbulent flow seems to prevail [10]). An interesting problem is to consider the effective depth of penetration of the ions, or more likely, their reactive daughter products. Fig. 5 illustrates crudely this important point. In the superficial cell layer of the mucous membrane (which consists of cylindrical epithelial cells), the cell nuclei are rather deep-seated ($\sim 50\ \mu$). However, due to metaplasia to stratified epithelium, a process often preceding lung cancer development, there occur superficial cells[2] with less deep-seated nuclei from which malignancy starts and therefore it might be necessary to consider only a depth of, say, 5 μ. (It may be pointed out that the RaA α-particles, which were supposed to have caused the uranium mine lung cancer cases, only penetrate about 45 μ of tissue [10].) The depth is supposed to include the layer of mucus on top of the mucous membrane. However, it is known that positive ions and smoke decrease the ciliary activity and the mucus flow [25] and thus there may be some justification for neglecting this liquid layer in many cases.

For these reasons, we shall assume the ions to be distributed within about 6 g (assuming 50 μ depth) or 0.6 g (assuming only 5 μ depth) alternatively.

If the lung tissue is to be equally well protected against radiation or radiation-like

[1] The respiratory system has been approximated with a tube 18 mm diameter, 2 m length and, with an average breathing rate of 10 liters/minute.

[2] The authors thank Profs. N. Ringertz and T. Caspersson and especially Prof. B. Engfeldt for pointing out this circumstance.

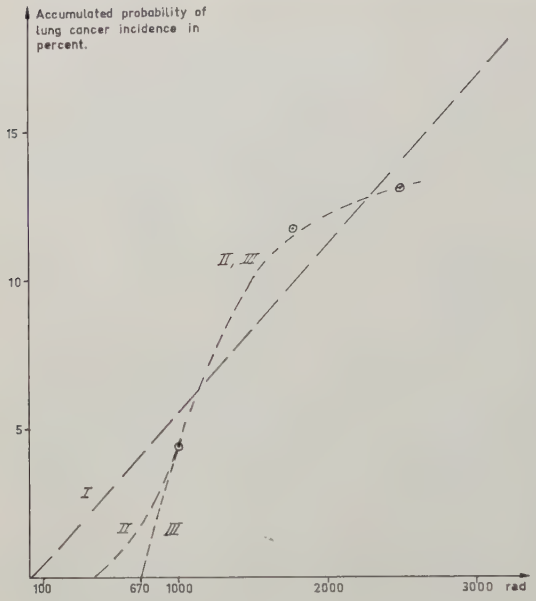

Fig. 6. Accumulated probability of lung cancer induction in mice as a function of dose. Figure obtained from data given by Stannard [15]. It should be noted that a certain incidence means that one or two animals out of 20–30 exposed got lung cancer within one year. Thus the data are statistically very uncertain. They are better known at higher dose values not shown in the figure. Such data are known also for man.

agents as the body as a whole should be against ionizing radiation, according to the recommendations of the International Commission of Radiological Protection [17] (100 mrad/week), we find that the highest allowable gaseous ion concentration is of the order of 12 000/cm³ for occupational exposure during working hours, assuming that no loss of potential energy by the ions occurs ($J = 10$ eV assumed). The figures arrived at, it should be pointed out, apply to molecular gaseous ions of radical character. The "light" ions, according to the classification of gaseous ion physics [4], are the closest ones to this definition.

It is very difficult to calculate the aerial ion inhalation of different persons or groups of persons. A further elaboration of this phase of the present lung cancer hypothesis meets with great difficulties, since we know at present too little about the state of the free charges detected in air and treated as gaseous ions (light, intermediate, Langevin or heavy [4, 11]). It seems evident that flames actually contain non-aggregated molecular ions. (See, for example, Fig. 1 in [12].)

There are many cases where human beings are exposed to flame combustion gases. Household gas for cooking is one example. It is likely that at least some part of the charges that have been detected [7, 8] in the exhaust gases of cars is, from the evidence of [12] and [13], of radiomimetic kind even if a rapid reaction with soot, droplets of oil or water is likely to occur. Welding, both gas and electrical, yields ions.

Smokers are, from the point of view of their constant habits, a good case for discussion. The number of free charges detected at the outlet of the cigarette is about 10^9/sec or about 10^{10} for one cigarette, according to our preliminary measurements. The figure obtained by Holmes *et al.* [14] is even higher but applies only to heavy particles. A smoker consuming 20 cigarettes/day would then get, if a 5 μ depth is assumed and supposing for the moment that all charges are radiomimetic ions, 20 rad/year. A non-smoker would get a natural background of 600–1000 ions/cm³ or 1

rad/year under the same assumptions. However, the nature of the charges detected in cigarette smoke is at present not at all clear. We have some indications that the ions are heavy. This discussion is admittedly hypothetical but it shows that further studies are of the greatest interest, both to reveal the nature of the charges detected and to find out the chemical reactivity of the various classes of gaseous ions.

Some material has been obtained concerning the probability of lung cancer induction due to ionizing radiation doses. This has been reviewed by Stannard at the 1958 Geneva conference [15].

Fig. 6 summarizes Stannard's data on mice at low doses. Several interpretations are, however, possible because of the meagreness of the data, e.g. a straight line case, a sigmoid one and one with a threshold. Stannard states 1000 r to be "effective" and this holds also for man (data from clinical experience). Using the threshold case (III), without discussing whether it is likely or not, we see that a certain induction period is to be expected. Thereafter the rise is 1 % incidence pro 80 rad. Should the charges in cigarette smoke turn out to be radiomimetic, which at present is an uncertain point, an incidence rate of 5 lung cancer cases among 1000 smokers is to be expected per year.

This figure agrees roughly with the statistical data [19] but this should at present be regarded as fortuitous. Other sources of ions than smoking are more likely to contain such radiomimetic entities, e.g. flames and car exhaust gases. A lot of sources are possible and many of them are more abundant in populated areas and connected with the increase in industrialization during the last few decades.

It should be pointed out that we have not included free radicals in this discussion. Some of them might possess sufficient potential energy (3–4 eV) to necessitate their inclusion among the radiation-like species. (The electron affinity of the radicals may be a method for including them in the quantitative estimation of radiomimetic action (cf. eq. 2), provided that the energy exceeds some critical value. The OH radical has, for instance, an electron affinity of 2.6 eV in the gas phase [20]. This might be sufficient to cause a radiomimetic action, but such an assumption is at present very uncertain.) We recall the figure of about 10^{15}/g given by Ingram *et al.* [21] for the free radicals in smoke, i.e. 10^5 times greater than the number of charges. Even if only a small fraction of these radicals is radiomimetic, they should be added to the above figures, thus giving even higher dose figures and lung cancer incidence rates. The rôle of ozone has already been touched upon above (cf. [24]).

The special problem of how the electronic energy is transferred from the mucus of the trachea wall to the cell nuclei was mentioned above (cf. Fig. 5). The most attractive theory here is the fluorescence[1] of the tar constituents. Smokers, of course, have such tar deposits in their lungs but the same should be true, to some extent at least, for people exposed to car exhaust or combustion gases. (Other fluorescent substances may also play a rôle.) We intend to investigate in detail whether these compounds have any UV-fluorescence in the "cancer region" around 2500 Å. (Reference is made to H. Blum's monograph [22].) Difficulties were found in correlating

[1] The potential energy of the gaseous ion should be large enough to excite fluorescence in the region 2000–3000 Å among others. It should be pointed out that the more general theory that ionizing radiation or radiation-like agents might, together with fluorescent substances, produce UV-light in the cancer region" has been considered independently to the senior author and Dr. Gunnar Ahnström, Stockholm University, in 1959. This effect would involve a considerable transfer of UV-energy to the cell nuclei. A few attempts in this direction seem to have been made earlier ([44] p. 73-74), but a new approach now would be most promising since much more basic knowledge has been collected e.g. on natural radiation doses (cf. ref. [16]).

quantitatively the ion hypothesis with the data of Blum. Even if one gas ion is supsed to give one quantum, the total number seems to be too low to explain the lung cancer incidence rate, but several factors are at present very poorly known. However, much can be performed experimentally in order to obtain more certain knowledge.

Present state of the hypothesis

The basic chemical part of the hypothesis can be considered, in the main, to correspond approximately to the experimental facts. More investigations are, however, necessary, e.g. one would have to study other ions with successively lower ionization potentials to see whether there is any lower limit to the radiation equivalence. Perhaps the main problem is the effect of aging in air under different conditions. If it is found that the potential energy of the gaseous ions is transferred to other species already in the gas phase, the above theory will not apply as it stands. However, free radicals may then turn out to be of central importance. On the other hand, it might turn out that some fraction of the ions retain their energy until deposition and this fraction would then have to be evaluated for various conditions.

The intriguing question concerning the energy transfer mechanism at the interface between inhaled air and tissue should be investigated experimentally. Physical and chemical work and also mutation studies on microorganisms[1] are planned. In addition, direct but more tedious studies on lung cancer incidence in animals will be performed.

If gaseous ions turn out to be of importance from the medical point of view, there are good prospects for reducing their concentration in inhaled air, e.g. by providing better ventilation and by the construction of ion-filters for cigarettes and exhaust pipes and fresh air intakes of cars etc. An interesting connection between the fields of air pollution and radiation biology would moreover occur if the effects discussed turn out to be real.

There are various applications of gaseous ion chemistry to certain fields including the origin of organic life on the earth, the rôle played in radiation chemistry, reactor technology, etc. which are not dealt with here.

As is seen, the evidence for the biological hypothesis is not very strong. On the other hand, virtually every link in it should be possible to test experimentally by the appropriate specialists. This might therefore justify a publication of the hypothesis at this stage of development.

ACKNOWLEDGEMENTS

The authors wish to express their gratitude to Professor O. Lamm for promoting this work and for providing a research atmosphere facilitating the extension of ideas from chemistry to biology and medicine. Thanks are also due to Dr. R. Siksna, Institute for High Tension Research, Uppsala, for generously making available his great experience on physical gas ion studies in air and for his pointing out to the authors the changes occurring in ions upon aging. The head of the same Institute, Professor D. M. Hillebrand, has contributed with constructive criticism which is hereby gratefully acknowledged. Professor E. Lindholm is gratefully thanked for positive criticism of the hypothesis in the early stages. Professors N. Ringertz, G. Klein, T. Caspersson, T. Teorell, A. Sjöberg, Drs. Å. Hanngren and S. Ullberg have all furnished us with

[1] Together with Prof. N. Fries and Dr. G. Zetterberg at Uppsala University, Department of Physiol. Botany.

valuable facts and points of view concerning the medical aspects. Dr. L. Ehrenberg, Dr. G. Ahnström and Dr. B. Larsson have provided valuable contributions especially with regard to radiation biology. The experiments presented in this paper have benefited from the undergraduate research work of Mr. L. Rennerfelt (now at the Dragon Project, Winfrith, Dorchester, England) in 1958. His work (unpublished) consisted of a series of trial experiments to achieve technical conditions suitable for observations of the chemical effects of gaseous ions.

We also wish to thank Mrs. M. Widell, Misses I. Andersson, M.-L. Walter, Messrs. P. Pedersen and A. de Ruvo for valuable assistance with the laboratory work. Valuable discussions with Mr B. Enander, the Division of Microwaves of this Institute and with Mr G. Eriksson of this Division are gratefully acknowledged.

Our experimental work has been sponsored by the Swedish Cancer Society, the Swedish Tobacco Company (AB Svenska Tobaksmonopolet) and the Swedish Council of Atomic Research.

Division of Physical Chemistry, The Royal Institute of Technology, Stockholm 70, Sweden.

REFERENCES

1. Burton, M., Magee, J. L., and Samuel, A. H., J. Chem. Phys. *20*, 760 (1952).
2. Lind, S. C., The chemical effects of alpha particles and electrons. Am. Chem. Soc. Monograph Series No. 2, New York (1928).
3. Pauling, L., Nature of the Chemical Bond, p. 53 (table 10-1). Cornell (1945).
4. Loeb, L. B., Basic Processes of Gaseous Electronics (aging of ions, see especially pp. 112–142). University of California Press, Berkeley (1955).
5. Stevenson, D. P., and Schissler, D. O., J. Chem. Phys. *23*, 1353 (1958); ibid. *24*, 926 (1956); ibid. *28*, 517 (1958) and later papers.
6. Hart, E. J., *et al.*, Proc. Sec. U.N. Intern. Conf. on the Peaceful Uses of Atomic Energy, Geneva 1958, Vol. *29*, p. 5, 13, 19 and 38.
7. Westermark, T., Detection of free charges from motor-car exhaust gases. Nature. *189*, 910 (1961).
8. Westermark, T., Gaseous ions as radiomimetic agents and their possible rôle in the etiology of lung cancer. Paper presented at the Symposium on Chemical and Biological Problems related to Smoking", May 2nd, 1960, in Stockholm. Acta Med. Scand. (in the press).
9. Townsend, J. S., Phil. Trans. *193A*, 129 (1900).
10. Chamberlain, A. C., and Dyson, E. D., Brit. J. Radiol. *29*, 317 (1956).
11. Siksna, R., Arkiv Fysik *5*, Nr. 25, 535 (1952); Siksna R., and Lindsay R., Arkiv Geofysik *3*, Nr. 8 and 9 (1959) and other papers by Siksna and Norinder.
12. Knewstubb, P. F., and Sugden, T. M., Nature *181*, 1261 (1958).
13. Deckers, J., and Tiggelen, A. van, Nature *181*, 1460 (1958).
14. Holms, J. C., Hardcastel, J. E., and Mitchell, R. I., Tobacco Science *149*, 20 (1959).
15. Stannard, J. N., Proc. Sec. U.N. Intern. Conf. on the Peaceful Uses of Atomic Energy, Geneva 1958, Vol. *23*, p. 306.
16. Burch, P. R. J., Nature *185*, 135 (1960).
17. Recommendations of the International Commission on Radiological Protection, Pergamon Press, London 1959 (adopted Sept. 9, 1958).
18. See, for instance, Rummel, T., Hochspannungsentladungschemie und ihre industrielle Anwendung. München 1951.
19. Ringertz, N., Statistical investigations into the connection between tobacco smoking and cancer. Report to the Council of Medical Research, Aug. 17, 1957 (in Swedish).
20. Page, F. M., Discussions Faraday Soc. No. 19, 87–96 (1955).
21. Lyons, M. J., Gibson J. F., and Ingram, D. J. E., Nature *182*, 1603 (1958).
22. Blum, H., Carcinogenesis of Ultra-violet Light. Princeton Univ. Press, 1959.
23. Westermark, T., Lindroth, H., and Enander, B., J. Appl. Rad. Isotopes *7*:4, p. 331 (1960).
24. Brinkman, R., and Lamberts, H. B., Nature *181*, 1202–3 (1958).
25. Kruger, A. P., and Smith, R. F., Proc. Soc. Exp. Med. *96*, 807 (1959); J. Gen. Physiol. *42*, No. 1, p. 69–82 (1958); Proc. Soc. Exp. Biol. Med. *98*, 412 (1958).
26. Weiss, J., Nature *186*, 751 (1960).

27. LAMPE, F. W., FRANKLIN J. L., and FIELD, F. H., J. Am. Chem. Soc. *79*, 6132 (1957).
28. MATHESON, G., Proc. Sec. U. N. Intern. Conv. on the Pecaeful Uses of Atomic Energy, Geneva 1958, Vol. *29*, p. 385.
29. CZAPSKI, G., and STEIN, G., J. Phys. Chem. *63*, 850 (1959).
30. EISENBERG, G. M., Ind. Eng. Chem. *15*, 327 (1943).
31. BONET-MAURY, P., Compt. Rend. *218*, 117 (1944).
32. ALLEN, A. O., *et al.*, J. Phys. Chem. *56*, 575 (1952).
33. WESTERMARK, T., WESTFELT L., LINDROTH, H., and GHANEM, N., Acta Chem. Scand. *14*, 1863 (1960).
34. WESTERMARK, T., and GRAPENGIESSER, B., Nature *188*, 395–396 (1960).
35*a*. DENARO A. R., and HICKLING, A., J. Electrochem. Soc. *105*, 265 (1958).
35*b*. DAVIES, R. A., and HICKLING, A., J. Chem. Soc. 1952, p. 3595.
35*c*. HICKLING, A., and LINACRE, J. K., J. Chem. Soc. 1954, p. 711.
36. DEWHURST, H. A., FLAGG, J. F., and WATSON, P. K., J. Electrochem. Soc. *106*, 366 (1959).
37. KINGDON, K. H., Phys. Med. Biol. *5*, 1 (1960).
38. GORBAN, A. N., and SOKOLOV, V. A., Opt. i Spektr. *7* (1959) 259.
39. WESTERMARK, T., Research plan and grant application to the Swedish Cancer Society, Sept. 26, 1958, and Dec. 29, 1959, and to the Swedish Atomic Committee, March 23, 1957. Reports to these Research Councils, Nov. 9, 1959 (report dated Oct. 30, 1959). These texts are all in Swedish and unpublished. Some experimental parts of them result from Mr. L. Rennerfelt's undergraduate research work.
40. CHAPIRO, A., and STANNETT, V., J. Chem. Phys. *57*, 35 (1960).
41. OKAMURA, S., and FUTAMI, S., Int. J. Appl. Rad. Isotopes *8*, 46 (1960).
42. ANDERSON, A. R., Proc. Sec. U.N. Intern. Conf. on the Peaceful Uses of Atomic Energy, Geneva 1958, Vol. *7*, p. 335.
43. PAVLOV, V. I., Comptes Rendus (Doklady) de l'Academie des Sciences de l'URSS 1944, Vol. XLIII, No. 6, p. 236, and No. 9, p. 383.
44. CLARK, G. L., Applied X-rays, McGraw Hill, New York, 1940.
45. MAXFIELD, F., and BENEDICT, R., Theory of gaseous conduction and electronics, McGraw Hill, New York, 1941.

Note added in proof: Recently K. H. Kingdon (Nature *189*, 180, Jan. 21, 1961) has put forward a lung cancer hypothesis with many features in common with the one described above. The arguments are qualitative and some details, e.g. the measuring techniques for small ions in cigarette smoke not described in full and so a complete discussion is not yet possible. It might be remarked that Kingdon's argument on the deposition of 0,5 μ droplets much deeper in the lung than the ions is most interesting. Further Kingdon considers the smokers' inhalation of ions from the cloud from the cigarette and not the ions passed through the cigarette. Kingdon holds the view that small ions cannot pass the unsmoked part of the cigarette to an appreciable extent. The same finding has been made by R. Siksna (private communication). Thus the charges found by us might be assigned to heavy ions. — Kingdon assumes that potassium ions might constitute the light ions detected. Such ions do not have radical character (cf. above) and might be assumed not to act radiomimetically. On the other hand their heat of hydration may be on the borderline to break strong chemical bonds but present data are uncertain: G. Kortüm, J. O. M. Bockris (Textbook of Electrochemistry, Vol. I, Elsevier, New York, 1951, p. 124, table 10) estimates the heat of hydration to be 92 kcal/mol or slightly higher.

Tryckt den 18 april 1961

Uppsala 1961. Almqvist & Wiksells Boktryckeri AB

ARKIV FÖR KEMI Band 17 nr 33

Communicated 25 January 1961 by The Svedberg

Photochemical depolymerization of cellulose nitrate in solution

By S. Claesson and G. Wettermark

With 5 figures in the text

Introduction

It is well-known that cellulose and cellulose derivatives depolymerize rapidly when exposed to ultraviolet light. Most of the studies in this field have been made by irradiating the substance in the solid state. The degradation has been followed by dissolving the substance in a suitable solvent and measuring the osmotic pressure, viscosity, copper number, etc. A review is given by Grassie [1]. By measuring the liberated products of cotton cellulose sheets in a vacuum when irradiated with light of 253.7 mμ wavelength, a mechanism for the degradation has been proposed [2].

Steurer made an investigation of the photochemical degradation of methylcellulose in dioxane [3]. He interpreted the results "so that" the scissions causing the change in the macromolecular behaviour of the solution, occurred at the oxygen linkages between the monomer units.

In this investigation the relation between chainlength and light dose has been observed by the irradiation of cellulose nitrate in solution. Irradiations have been made on extensively nitrated cellulose in ethylacetate and partially nitrated cellulose in methanol.

Effective light dose

When a system containing two components absorbs an infinitesimal light dose dD, the following relations are obvious:

$$dD = dD_1 + dD_2, \tag{1}$$

$$d = d_1 + d_2, \tag{2}$$

$$\frac{d_1}{d_2} = \frac{dD_1}{dD_2}, \tag{3}$$

where dD_1 and dD_2 are the doses absorbed by components 1 and 2, d the optical density of the system, and d_1 and d_2 the optical density of the components.

The optical density of the system is assumed to vary with the absorbed dose according to

$$d = f(D). \tag{4}$$

Assuming the optical density of the components to be a function only of the dose absorbed by the component (no energy transfer), we get

$$d_1 = f_1(D_1), \tag{5}$$

$$d_2 = f_2(D_2). \tag{6}$$

Combination of the equations (1)–(6) gives

$$\int_0^{D_1} \frac{d\,D_1}{f_1(D_1)} = \int_0^{D_2} \frac{d\,D_2}{f_2(D_2)} = \int_0^{D} \frac{d\,D}{f(D)}. \tag{7}$$

The relationship between viscosity and degree of depolymerization

When a polymer is depolymerized the number average chain length (P_n) is changed according to

$$P_n = \frac{P_0}{S+1}. \tag{8}$$

P_0 is the number average chain length before degradation, S/P_0 the ratio between the total number of linkages broken and the total number of linkages originally present. (Linkage means linkage between the monomers.)

As $P_n \approx P_n - 1$, the average number of links in a chain is put equal to the number average chain length.

Defining the quantum yield (ϕ) for the photochemical degradation as the ratio between the number of chain scissions and the number of absorbed quanta (D_a) and assuming ϕ to be constant, the following relation is valid,

$$\phi = \frac{\frac{S}{P_0} \cdot n}{D_a}, \tag{9}$$

where n is the number of bonds originally present.

A combination of equations (8) and (9) gives

$$\frac{1}{P_n} = \frac{1}{P_0} + \frac{\phi}{n} \cdot D_a. \tag{10}$$

This equation, which shows the relation between number average chain length and absorbed dose, is apparently valid, independent of the original chain length distribution.

Using equation (11) we get the viscosity average chain length:

$$[\eta] = K \cdot P_v^a. \tag{11}$$

With an exponential chain length distribution P_v and P_n are related in the simple way

$$P_v : P_n = [(1+a)\Gamma(1+a)]^{1/a} : 1 \tag{12}$$

and thus their ratio constant. In case of a random degradation, the distribution rapidly converges to an exponential and a straight line is obtained when plotting $1/P_v$ as a function of D_a (disregarding the initial stage where a deviation may occur).

In the case when the exponent in equation (11) is close to 1, equation (11) can be approximated by Staudinger's equation

$$[\eta] = K_1 \cdot P_v \tag{13}$$

and the degradation followed by plotting $1/[\eta]$ as a function of D_a, giving a straight line for a random degradation.[1]

Experimental

A suitable fraction of extensively nitrated cellulose was supplied by Dr. A. G. Chitale. Acetate grade cotton linters were nitrated according to Alexander and Mitchell [4]. A two-step fractionation in an acetone-water system was performed, yielding nine fractions.

Commercial partially nitrated cellulose (Kollodium bomull), Bofors Nobelkrut, VF 500) was fractionated as described above, and one of the middle fractions was used for the experiments.

The fractions had a nitrogen content of 13.87 and 12.12%, respectively. (The analyses were carried out at the Central Analytical Laboratory, Uppsala University.)

The solvents, ethylacetate, *pro analysi* (KEBO) and methanol, *pro analysi* (LKB), were distilled using an 80 cm long column, after drying with Drierite.

The irradiations were performed with "Apparatus 2" described by Moring Claesson [5]. It consists of two identical cylindrical glass cuvettes provided with circular quartz windows, mounted in front of a low-pressure mercury lamp (Hanovia Sc 2537). The cuvettes were kept in a water thermostate at 25°C. More than 99.5% of the light emitted at wavelengths shorter than 300 mμ is given off at 253.7 mμ. Shorter wavelengths were absorbed in a filter (1 cm, 21% acetic acid) in front of the cuvettes.

A slow stream of nitrogen was passed through the solution during the experiment. The nitrogen contained less than 0.002% oxygen. It was passed through sulfuric acid for the removal of ammonia and was then saturated with ethylacetate or methanol.

Two solutions were prepared, one containing 0.0879 g of extensively nitrated cellulose in 100 ml ethylacetate and the other containing 0.2812 g of partially nitrated cellulose in 100 ml methanol. Ten ml of the solutions were irradiated for

[1] By differentiation of equations (11) and (13), it is seen that the change in the viscosity average chain length, calculated by means of equation (13), should be multiplied by $1/a$ to give the correct value. If quantum yields are calculated by the combination of equations (10) and (13), this factor, which enters directly into the quantum yield, must be taken into consideration if a is not close to unity.

various times. The optical density of the solution was measured in a Beckman DU spectrophotometer immediately after the irradiation and with the same atmosphere as during the irradiation. The viscosity was measured at different concentrations in a capillary viscometer of the Ubbelohde type. A post-irradiation depolymerization took place and was complete within 24 hours. The solutions were thus kept for 24 hours before the viscosity measurements.

Pure ethylacetate was irradiated under the same conditions as for the solutions and the optical density measured at 253.7 mμ.

The light doses were measured with a uranyl oxalate actinometer. The solution was 0.001 *M* in uranyl oxalate and 0.004 *M* in oxalic acid. The amount of oxalate was determined by titration with ceric sulphate exactly as described by Claesson and Lindqvist [6]. A quantum yield of 0.62 was used in calculating the doses. The determination of the light doses was made simultaneously with the irradiation of the tested substances, one reaction vessel being filled with the tested solution and the other with actinometer solution. The ratio between the incident doses at the two cuvettes in a fixed time was determined separately.

Results and discussion

Ethylacetate has a notable absorption at 253.7 mμ, whereas methanol has no absorption at this wavelength. For the methanol solution the cellulose nitrate is thus responsible for the entire absorption. As the optical density at 253.7 mμ exceeds two and increases during irradiation, the absorbed dose can be put equal to the incident dose (Table 2).

Fig. 1 shows the wavelength dependence of the extinction coefficient $E^{1\,\%}_{1\,\mathrm{cm}}$ for different exposure times. $E^{1\,\%}_{1\,\mathrm{cm}}$ is the extinction coefficient in Beer's law ($\log (I_0/I) = E^{1\,\%}_{1\,\mathrm{cm}} \cdot c \cdot l$) for $c = 1\%$ and $l = 1$ cm.

For the ethylacetate solution the totally absorbed light dose must be divided into the dose absorbed by the solute and the dose absorbed by the solvent. Thus the theory presented above was applied. The reciprocal of the optical density was plotted as a function of absorbed dose for the solution, and the ethylacetate and the curves were integrated to give the same value. In this way the light absorbed by the ethylacetate was determined, and the difference in the two doses gives the light absorbed by the cellulose nitrate (D_n) (Table 1).

Table 1. Extensively nitrated cellulose in ethylacetate.

Exposure time, sec	Incident dose, $h\nu$	$E^{1\,\%}_{1\,\mathrm{cm}}$	D_n, $h\nu$	$[\eta]$, dl/g
0	0	2.29	0	10.32
30	0.76×10^{18}	2.44	0.17×10^{18}	9.72
60	1.57×10^{18}	2.79	0.36×10^{18}	9.37
120	3.04×10^{18}	3.05	0.77×10^{18}	8.51
240	6.08×10^{18}	3.45	1.66×10^{18}	6.40
480	12.2×10^{18}	4.22	3.65×10^{18}	4.01
960	24.3×10^{18}	4.93	8.00×10^{18}	2.35

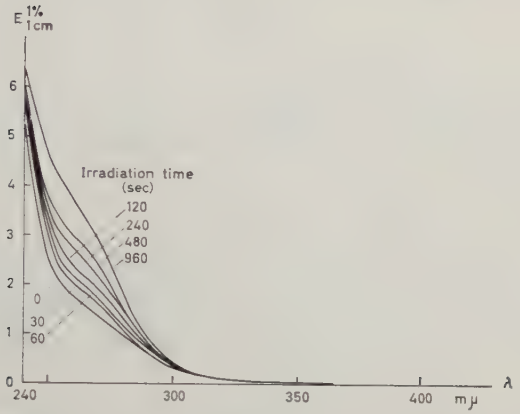

Fig. 1. Absorption spectra for partially nitrated cellulose in methanol after different exposure times.

Table 2. Partially nitrated cellulose in methanol.

Exposure time, sec	Incident dose, $h\nu$	$[\eta]$, dl / g
0	0	2.78
30	0.74×10^{18}	2.64
60	1.47×10^{18}	2.53
120	2.94×10^{18}	2.30
240	5.88×10^{18}	1.91
480	11.8×10^{18}	1.39
960	23.5×10^{18}	1.01

The intrinsic viscosities have been determined through straight line extrapolations (Figs. 2 and 3) and are collected in Tables 1 and 2.

When plotting the reciprocal intrinsic viscosities as a function of the dose absorbed by the cellulose nitrate, straight lines are obtained (Figs. 4 and 5). The degradation thus follows the theory for a random process.

In ethylacetate the molecular weight of both fractionated and unfractionated samples of cellulose nitrate have been calibrated against intrinsic viscosity by various investigators, using osmometric, sedimentation and diffusion data. By plotting the logarithm of the intrinsic viscosity against the logarithm of the molecular weight, values for the constants a and K have been determined in accordance with the viscosity equation (11). It must be stressed that these are *not* the correct constants; the obtained straight lines simply imply that the ratio of the two averages was fairly constant. (It is reasonable to assume that the distributions were essentially exponential.) The exponent a has been found to be close to unity (0.99, 1.03) [7, 8]. Using the osmometrical determinations in ref. [8], the quantum yield ϕ for the depolymerization of the extensively nitrated cellulose in ethyl acetate was calculated by setting

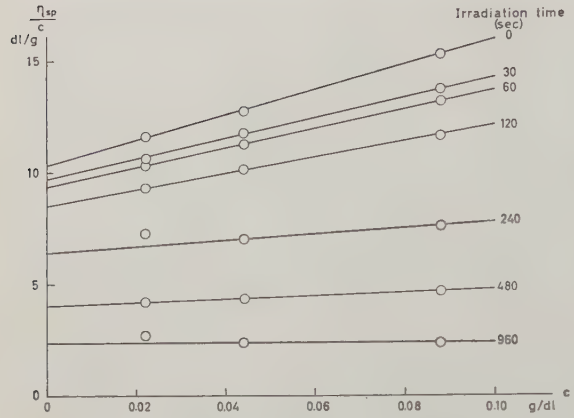

Fig. 2. Extrapolation of η_{sp}/c as a function of c for extensively nitrated cellulose in ethylacetate.

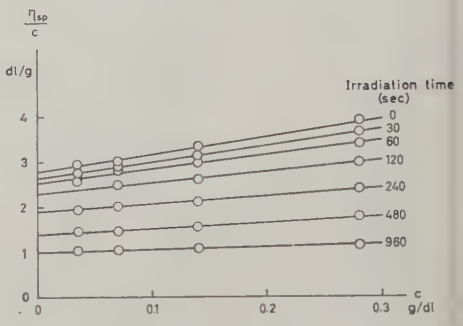

Fig. 3. Extrapolation of η_{sp}/c as a function of c for partially nitrated cellulose in methanol.

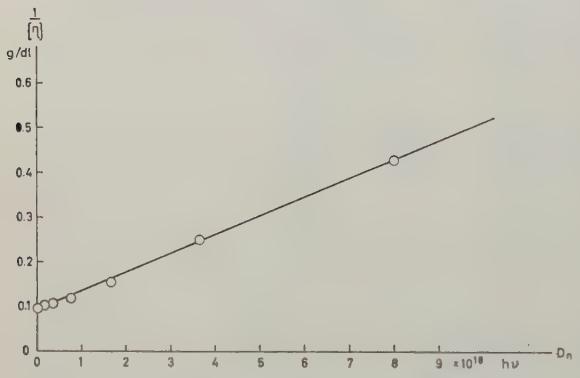

Fig. 4. $1/[\eta]$ as a function of the dose absorbed by the nitrocellulose (D_n) for the degradation of extensively nitrated cellulose in ethylacetate.

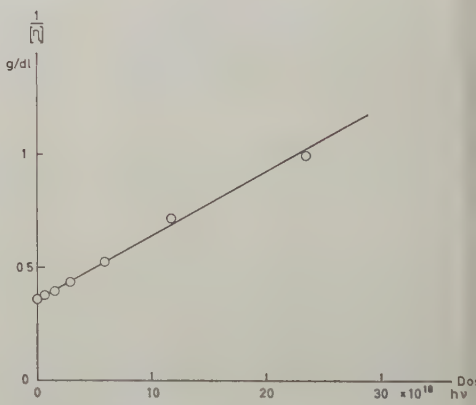

Fig. 5. $1/[\eta]$ as a function of the absorbed dose for the degradation of partially nitrated cellulose in methanol.

$$[\eta] = \frac{1}{62} \cdot P_n. \tag{14}$$

A quantum yield of 0.01_2 was obtained.

No thorough investigations on the relation between intrinsic viscosity in methanol and molecular weight have been found in the literature. In order to make an estimate of quantum yield for the partially nitrated cellulose in methanol, the intrinsic viscosity was determined for the initial fraction both in ethylacetate and methanol. Using equation (14), a corresponding relation for methanol was calculated

$$[\eta] = \frac{1}{83} \cdot P_n. \tag{15}$$

In this way the quantum yield for the depolymerization of partially nitrated cellulose in methanol was found to be 0.02.

SUMMARY

Cellulose nitrate, with a high and low degree of nitration has been dissolved in ethylacetate and methanol respectively, and irradiated with light of the wavelength 253.7 mμ. The depolymerization has been followed viscometrically, and the process was found to be random. The quantum yields for the chain scissions were found to be 0.01–0.02. A correction has been made for the absorption by the solvent and its variation with time.

ACKNOWLEDGEMENT

This work was supported by a grant from Swedish Technical Research Council which is gratefully acknowledged.

Institute of Physical Chemistry, University of Uppsala, Uppsala, Sweden.

REFERENCES

1. Grassie, N., Chemistry of High Polymer Degradation Processes. Butterworth, London, 1956.
2. Flynn, J. H., Wilson, W. K., and Morrow, W. L., J. Research Natl. Bur. Standards *60*, 229 (1958).
3. Steurer, E., Z. physik. Chem. *47*, 127 (1940).
4. Alexander, W. J., and Mitchell, R. L., Anal. Chem. *21*, 1497 (1949).
5. Moring Claesson, I., Arkiv Kemi *10*, 1 (1956).
6. Claesson, S., and Lindqvist, L., Arkiv Kemi *11*, 535 (1957).
7. Newman, S., Loeb, L., and Conrad, C. M., J. Polymer Sci. *10*, 463 (1953).
8. Immergut, E. H., Rånby, B. G., and Mark, H. F., Ind. Eng. Chem. *45*, 2483 (1953).

Tryckt den 27 april 1961

Uppsala 1961. Almqvist & Wiksells Boktryckeri AB

ARKIV FÖR KEMI Band 17 nr 34

Communicated 12 April 1961 by Erik Jorpes and Karl Myrbäck

On the metabolism of 7α-hydroxycholesterol in mouse liver homogenates

Bile acids and steroids 111

By Henry Danielsson

In a series of investigations on the metabolism in the bile fistula rat of different hypothetical intermediates in the degradation of cholesterol to bile acids, Lindstedt [1] found that 7α-hydroxycholesterol was transformed into cholic and chenodeoxycholic acid. This and other results [2] have suggested that one of the early steps in the formation of bile acids from cholesterol is the introduction of the 7α-hydroxyl group and that 7α-hydroxycholesterol might be an intermediary product.

In a recent study of the metabolism of cholesterol *in vitro* [3] it was found that both non-enzymatic and enzymatic oxidation occurred simultaneously. One of the main enzymatic products formed was shown to be converted by the bile fistula rat into chenodeoxycholic acid. When the autoxidation was reduced by carrying out the incubation of cholesterol in presence of 10^{-3} *M* EDTA,[1] the main metabolite formed was this same compound, which now has been identified as 26-hydroxycholesterol [4]. In view of the limited oxidation of cholesterol that so far has been achieved *in vitro*, it seemed of interest to study the metabolism *in vitro* of sterols that might be intermediates or structurally or metabolically related to intermediates between cholesterol and bile acids. As one of such sterols, 7α-hydroxycholesterol was chosen because of its ready conversion to bile acids *in vivo*.

While this work was in progress, Yamasaki and coworkers [5] reported on the oxidation of 7α-hydroxycholesterol by rat liver homogenates to a compound which on grounds of its ultraviolet spectrographic properties was suggested to be Δ^4-cholestene-7α-ol-3-one.

This communication describes the chromatographic separation and partial identification of the metabolites of 7α-hydroxycholesterol in mouse liver homogenates.

Experimental

Melting points are uncorrected. All rotations were taken in chloroform solutions except when otherwise stated.

Tritium labeled 7α-hydroxycholesterol. 50 mg cholesterol labeled with tritium according to the method of Bloch and Rittenberg [6][2] and 450 mg inactive cholesterol

[1] Abbreviations used: EDTA, ethylenediaminetetraacetic acid; Tris, tris(hydroxymethyl)-aminomethane; DPN, diphosphopyridine nucleotide.

[2] This material was a generous gift of Dr. S. Lindstedt of this laboratory.

were mixed to give cholesterol of a spec. act. of 200,000 cpm/mg. Benzoylation in the usual manner gave 515 mg of *cholesteryl benzoate*, spec. act. 175,000 cpm/mg. This material was brominated in the 7α-position according to the method of Bide *et al.* [7] by treatment with 250 mg *N*-bromosuccinimide in 10 ml boiling carbon tetrachloride for 5 min. Repeated crystallization afforded 105 mg of *7α-Br-cholesteryl benzoate* (spec. act. 137,000 cpm/mg) m.p. 135–136°; $[\alpha]_D^{20°} - 170°$ (*c*, 0.9); reported [7] m.p. 140°; $[\alpha]_D - 172°$. Conversion of 7α-Br-cholesteryl benzoate to 7α-hydroxycholesterol was performed according to Henbest and Jones [8]. The foregoing 7α-Br-cholesteryl benzoate was dissolved in 1 ml ether and treated with 100 mg sodium formate in 1 ml of formic acid for 24 h at room temperature. The reaction mixture was extracted with ether, washed until neutral with water and evaporated. The residue was then refluxed with methanolic potassium hydroxide for 1 h. The evaporated ether extract was chromatographed with phase system III [9]. The fractions containing the 7α-hydroxycholesterol were combined and evaporated. Crystallization from methanol/water afforded 37 mg of *7α-hydroxycholesterol* (spec. act. 155,000 cpm/mg) m.p. 181–182°; $[\alpha]_D^{20°} - 79°$ (*c*, 0.5); reported [8] m.p. 185°; $[\alpha]_D - 86.6°$.

Δ⁴-Cholestene-7α-ol-3-one. The synthesis of this compound has recently been described (10).

Δ⁵-Cholestene-3β, 7α, 26-triol and 3β, 7α-dihydroxy-Δ⁵-cholenic acid. 15 g *methyl-3β-acetoxy-Δ⁵-cholenate*, m.p. 156–157°, $[\alpha]_D^{21°} - 45°$ (*c*, 1.0); reported [11] m.p. 156–157°, $[\alpha]_D - 43°$, were refluxed for 8 h with *tert.* butyl chromate as described by Heusler and Wettstein [12]. Crystallization twice from ethanol yielded 8.5 g of *methyl 3β-acetoxy, 7 keto-Δ⁵-cholenate*, m.p. 177–179° $[\alpha]_D^{21°} - 122°$ (*c*, 1.0); reported [13] m.p. 177–178°. 5 g were dissolved in 400 ml methanol by warming and 5 g of sodium borohydride were added in portions over a period of 15 min. while the solution gradually reached room temperature. The solution was then stirred for an additional 3/4 of an hour. After dilution with water and acidification the solution was extracted with ether. The evaporated ether extract was chromatographed on a 400 g column of grade III Woelm aluminium oxide (Woelm, Eschwege, W-Germany) with increasing amounts of chloroform in benzene. 30 % chloroform in benzene eluted 2.723 g *methyl 3β-acetoxy, 7β-hydroxy-Δ⁵-cholenate*. Crystallization from acetone/water and methanol/water yielded 2.26 g, m.p. 121°$[\alpha]_D^{20°} - 5°$ (*c*, 1.0). Calculated for $C_{27}H_{40}O_5$: C, 72.6 %; H, 9.7 %. Found: C, 72.7 %; H, 9.5 %. Continued elution with 30 % chloroform in benzene gave 1.008 g *methyl 3β acetoxy, 7α-hydroxy-Δ⁵-cholenate*. Crystallization from acetone/water and methanol/water afforded 830 mg, m.p. 156–157° $[\alpha]_D^{22°} - 96°$ (*c*, 0.85). Calculated for $C_{27}H_{40}O_5$: C, 72.6 %; H, 9.7 %. Found: C, 72.9 %; H, 9.7 %. 500 mg methyl 3β-acetoxy, 7β-hydroxy-Δ⁵-cholenate were dissolved in 100 ml 75 % aqueous methanol containing 5 g potassium hydroxide and left at room temperature for 24 h. Dilution with water, acidification and extraction with *n*-butanol (extraction with ether was not possible due to gel formation by the precipitated acid) followed by crystallization from ethyl acetate gave 262 mg *3β, 7β-dihydroxy-Δ⁵-cholenic acid*, m.p. 223–5° (decomp.), $[\alpha]_D^{21°} + 28°$ (*c*, 1.46). Calculated for $C_{24}H_{38}O_4$: C, 73.8 %; H. 9.8 %. Found: C, 73.7 %; H, 9.8 %. 500 mg methyl 3β-acetoxy, 7α-hydroxy-Δ⁵-cholenate were saponified as above. Extraction with ether and crystallization from ethyl acetate gave 198 mg *3β, 7α-dihydroxy-Δ⁵-cholenic acid*, m.p. 210–4° (decomp.) $[\alpha]_D^{21°} - 97°$ (*c*, 0.98). Calculated for $C_{24}H_{38}O_4$: C, 73.8 %; H, 9.8 %. Found: C, 73.7 %; H, 9.7 %.

450 mg 3β, 7α-dihydroxy-Δ⁵-cholenic acid were dissolved in 50 ml methanol containing 4 g of methyl 2 DL-methyl-3-carboxypropanoate, prepared as described by

Ställberg [14], b.p. 108–110°/0.5 mm; m.p. 39–40°; reported [14], b.p. 101–103°/0.2 mm; m.p. 42.1–42.7°. 100 mg of sodium in 2 ml methanol was added and the solution electrolyzed with 1.6 A between platinum electrodes (5.2 cm^2) placed 0.2 cm from each other until a pH of about 8 was reached (30 min.) [15]. The solution was then diluted with water, extracted with ether and the ether extract washed with sodium carbonate and water and evaporated to dryness. The residual oil was chromatographed on a column of 100 g Woelm aluminium oxide, grade III, using increasing concentrations of ethyl acetate in benzene as eluent. The fractions collected were weighed and checked for chromogenicity in the Lifschütz color reaction [16], which gives a blue color with 7-hydroxy-Δ^5-sterols. Elution with 55 % ethyl acetate in benzene gave 110 mg of methyl 25 DL-*3β, 7α-dihydroxy-*Δ^5*-cholestenate*, which after crystallization from ethyl acetate/petroleum ether melted at 144–148°, $[\alpha]_D^{24°} - 92°$ (*c*, 0.9). Calculated for $C_{28}H_{46}O_4$: C, 75.3 %; H, 10.15 %. Found: C, 75.1 %; H, 10.3 %.

55 mg of foregoing ester were dissolved in 20 ml dry ether and reduced with 55 mg of lithium aluminium hydride for 3 h at room temperature. The mixture was acidified and extracted with ether, washed with sodium carbonate and water and evaporated. The residue was crystallized from ethyl acetate/petroleum ether yielding 36 mg of 25 DL-Δ^5-cholestene-3β, 7α, 26-triol, m.p. 168–172°, $[\alpha]_D^{24°} - 79$ (*c*, 0.73).

Preparation of homogenates. White male mice of the Danish State Serum Institute strain weighing approx. 25 g were used. 33 % (liver wet weight/volume) homogenates were prepared in 0.25 *M* sucrose containing 3.6 mg nicotinamide/ml with a tight-fitting Teflon pestle. 1 ml 0.05 *M* Tris buffer, pH 7.4, was added per 3 ml whole homogenate. Each mg of 7α-hydroxycholesterol was dissolved in 0.1 ml ethanol and diluted with 2 ml of a solution of 1 % serum albumin in water. DPN was purchased from the Sigma Chemical Co., St. Louis, Mo., USA. Incubations were run at 38° for 2 hours.

Analysis of incubation mixtures. The incubation mixtures were poured into 20 volumes of chloroform/methanol 2:1 and filtered into a separatory funnel. 0.2 volumes of 0.9 % sodium chloride were added, the mixture shaken and the phases allowed to separate for at least 4 h. The chloroform phase was evaporated and the residue chromatographed on columns of hydrophobic Hyflo Supercel (Johns Manville Co., USA) with phase system III [9]. The methanol/water phase was acidified and extracted with ether. Less than 2 % of the total activity was present in the ether extract.

The following phase systems were used:

	Moving phase	Stationary phase
III [9]	150 ml *iso*propanol	10 ml chloroform
	150 ml water	40 ml heptane
C 1 [17]	150 ml methanol	15 ml chloroform
	150 ml water	15 ml *iso*octanol
F 1 [17]	165 ml methanol	45 ml chloroform
	135 ml water	5 ml heptane
F 2 [17]	180 ml methanol	45 ml chloroform
	120 ml water	5 ml heptane

The stationary phase was supported on hydrophobic Hyflo Supercel.

Bile fistula rats. The strain of animal and the procedures for analysis of bile were the same as those recently described (10).

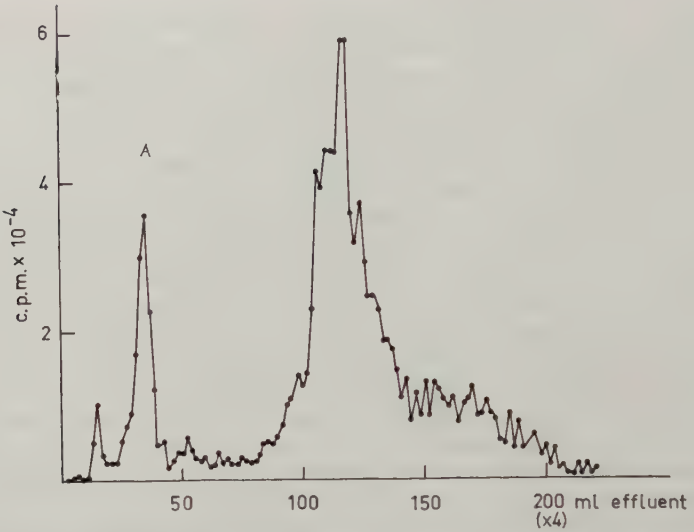

Fig. 1. Chromatogram of the chloroform extract of an incubation of 5 mg tritium labeled 7α-hydroxycholesterol with 30 ml of whole homogenate of mouse liver with 10 mg DPN added. 18 g column. Phase system III.

Results

Incubation of tritium labeled 7α-hydroxycholesterol with whole homogenates of mouse liver resulted in an appreciable (20–30 %) conversion into several different metabolites, mainly more polar than 7α-hydroxycholesterol. Addition of DPN to the incubations led to an increased formation of the metabolite that was less polar than 7α-hydroxycholesterol (the material eluted between 150–200 ml, Fig. 1). The elution volume of this metabolite was such as to indicate the presence of a keto-group instead of one of the hydroxyls. As the compound was not identical with 7-ketocholesterol it appeared likely that the 3β-hydroxyl in 7α-hydroxycholesterol had been oxidized to form Δ^4- or Δ^5-cholestene-7α-ol-3-one. Cochromatography of the metabolite with synthetic Δ^4-cholestene-7α-ol-3-one showed that the radioactivity was eluted together with this compound, which was measured by its ultraviolet absorption at 242 mμ (Fig. 2), and the identity of the labeled compound with Δ^4-cholestene-7α-ol-3-one was established by crystallization to constant specific activity with unlabeled material both as free sterol and after conversion to the acetate.

As one of the primary aims of this investigation was to identify and isolate labeled Δ^4-cholestene-7α-ol-3-one for studies of its further metabolism in the bile fistula rat [10], most incubations were performed in presence of DPN, which enhances the formation of this compound. Thus, the analyses of the other metabolites of 7α-hydroxycholesterol in mouse liver homogenates have been performed on material isolated from incubations with DPN added. Fig. 1 shows a chromatogram of the chloroform extract of an incubation of 5 mg 7α-hydroxycholesterol with whole homogenate. The radioactive material with its peak at 110 ml effluent represents unchanged 7α-hydroxycholesterol and the labeled compound eluted after 7α-hydroxycholesterol was, as mentioned before, identified as Δ^4-cholestene-7α-ol-3-one.

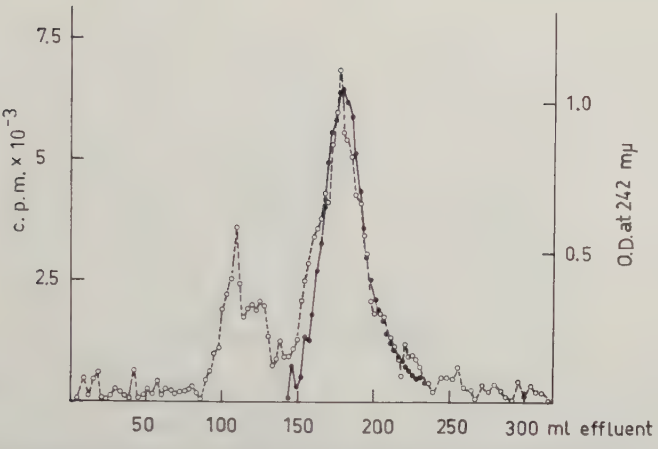

Fig. 2. Rechromatography of 135–200 ml effluent of the chromatogram shown in Fig. 1 with 5 mg unlabeled Δ^4-cholestene-7α-ol-3-one, measured by its absorption at 242 mμ (solid line). Broken line: radioactivity. 4.5 g column. Phase system III.

The other main metabolite of 7α-hydroxycholesterol appearing at 35 ml of effluent (A, Fig. 1) is more polar than 7α-hydroxycholesterol and shows chromatographic properties similar to those of a neutral C_{27}-sterol with three hydroxyl groups. In absence of DPN this compound, designated A, or a compound(s) with similar chromatographic behaviour, accounted for more of the amount of 7α-hydroxycholesterol metabolized than did Δ^4-cholestene-7α-ol-3-one.

Fractionation of homogenates by differential centrifugation and incubation of the subcellular fractions without any additions except buffer showed that the conversion of 7α-hydroxycholesterol into Δ^4-cholestene-7α-ol-3-one occurred in mitochondria to which 100,000 × g supernatant had been added, and also, though to a lesser degree, in 100,000 × g supernatant alone. The formation of compound A or compound(s) with similar chromatographic mobility was effected by mitochondria and addition of supernatant did not show any marked stimulatory effect. The formation of "acidic" material, i.e. the radioactivity eluted before compound A, Fig. 1, required the presence of both the mitochondrial and the 100,000 × g supernatant fractions.

Compound A. The structure of compound A has not yet been established. At first it seemed possible that this metabolite was a 26-hydroxylated derivative of 7α-hydroxycholesterol, i.e. Δ^5-cholestene-3β, 7α, 26-triol. However, when compound A and synthetic Δ^5-cholestene-3β, 7α, 26-triol were chromatographed together, they separated completely (Fig. 3), compound A being the less polar of the two. When the ultraviolet absorption of the chromatographic fractions was examined, it was found that concomitant with the radioactive peak, absorption with λ_{max} at 246 mμ was present. The ultraviolet spectrum of the peak fractions was then recorded in ethanol and was found to have the appearance typical of an α,β-unsaturated ketone with λ_{max} at 242 mμ. The molar extinction coefficient was calculated to be approx. 8000 by measuring the total activity in these fractions and correlating the figure obtained with the original specific activity of the 7α-hydroxycholesterol.

To obtain more information on the structure of this compound the further metabolism was studied in the bile fistula rat. When injected intraperitoneally into a bile

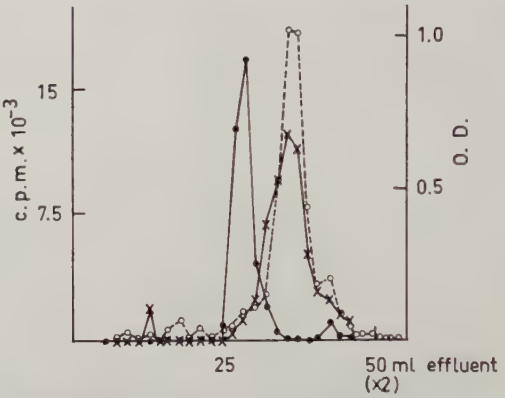

Fig. 3. Chromatography of compound A, cf. Fig. 1, with unlabeled Δ^5-cholestene-3β, 7α, 26-triol, measured by the Lifschütz color reaction at 620 mμ (solid line). Broken line: radioactivity. Crossed line: optical density at 246 mμ. 9 g column. Phase system III.

fistula rat it was rapidly excreted in bile as bile acids, 40 % of injected dose during the first 24 h. Preliminary fractionation of the saponified bile showed that 70 % of the excreted activity was present in the cholic acid fraction and the remainder in the chenodeoxycholic fraction. Upon rechromatography of the cholic acid fraction with phase system C 1, only a smaller part of this radioactivity was found within the titration peak of cholic acid (Fig. 4), while the main part was eluted after cholic acid at the place of 3α, 6β, 7β-trihydroxycholanic acid. Although this labeled acid was not conclusively identified by isotope dilution, the postulated identity of the labeled acid with 3α, 6β, 7β-trihydroxycholanic acid seems strengthened by the presence of a titration peak which very likely is due to this same acid. The main part of the radioactive material appearing within the cholic acid peak was identified as cholic acid by rechromatography followed by isotope dilution. Most of the radioactivity in the

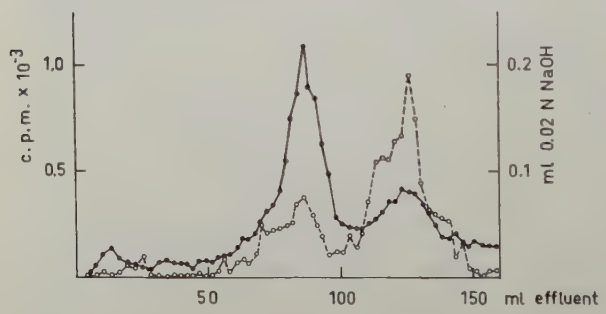

Fig. 4.

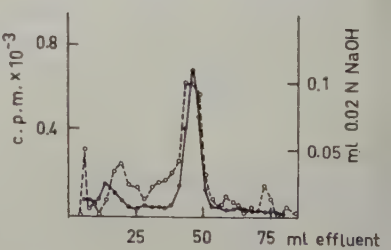

Fig. 5.

Fig. 4. Chromatography of the cholic acid fraction of the first 24 h portion of bile from bile fistula rat injected with compound A. Solid line: titration values. Broken line: radioactivity. 4.5 g column. Phase system C 1.

Fig. 5. Chromatography of the chenodeoxycholic acid fraction of the first 24 h portion of bile from bile fistula rat injected with compound A. Solid line: titration values. Broken line: radioactivity.

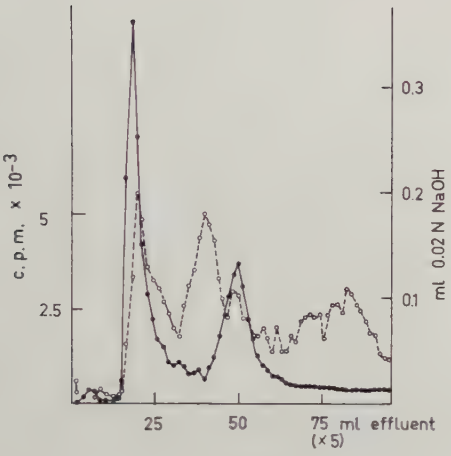

Fig. 6.

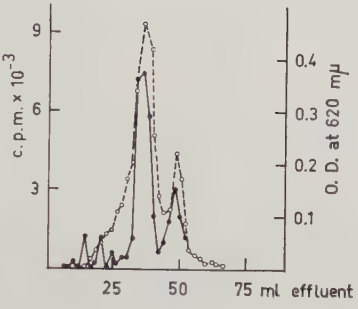

Fig. 7.

Fig. 6. Chromatography of "acidic" material from incubation of 7α-hydroxycholesterol (12–28 ml of effluent, Fig. 1) together with 10 mg of unlabeled chenodeoxycholic acid (peak at 50 ml of effluent). Solid line: titration values. Broken line: radioactivity. 22.5 g column. Phase system F 1.

Fig. 7. Rechromatography of radioactive material eluted between 65 and 90 ml of effluent in the chromatogram shown in Fig. 6 together with unlabeled Δ^5-cholestene-3β, 7α, 26-triol (peak at 36 ml of effluent), measured by the Lifschütz color reaction at 620 mμ (solid line) Broken line: radioactivity. 4.5 g column. Phase system III.

chenodeoxycholic acid fraction was shown to be chenodeoxycholic acid by rechromatography (Fig. 5) and isotope dilution.

"Acidic" material. All radioactive material appearing before the main peak of compound A (10–28 ml of effluent in Fig. 1) was pooled from several incubations and chromatographed with phase system F 1 together with unlabeled chenodeoxycholic acid (Fig. 6).

The radioactivity eluted between 65 and 90 ml of effluent was rechromatographed with unlabeled Δ^5-cholestene-3β, 7α, 26-triol and the major part of the label was found to be eluted together with this compound which was measured by the Lifschütz color reaction (Fig. 7), and the identity was established by crystallization to constant specific activity. The structure of the minor peak present in this chromatogram is unknown. Δ^5-Cholestene-3β, 7α, 26-triol is eluted with phase system III just before compound A, and can be separated from compound A (cf. Fig. 3), but it appeared easier to isolate it by chromatography with phase system F 1 as it was present in small amounts compared to compound A.

Rechromatography of the chenodeoxycholic acid peak (Fig. 6) demonstrated that the radioactivity present within this peak was not identical with chenodeoxycholic acid but represented partly the remainder of the radioactive acid eluted before chenodeoxycholic acid in Fig. 6 and partly another acid that was eluted very close to, but distinctly later than chenodeoxycholic acid.

The labeled acid eluted between 30 and 45 ml effluent (Fig. 6) was rechromatographed with unlabeled 3β, 7α-dihydroxy-Δ^5-cholenic acid (Fig. 8) but was found to be somewhat less polar than this acid. Recordings of the ultraviolet absorption of these fractions showed only a strong end absorption.

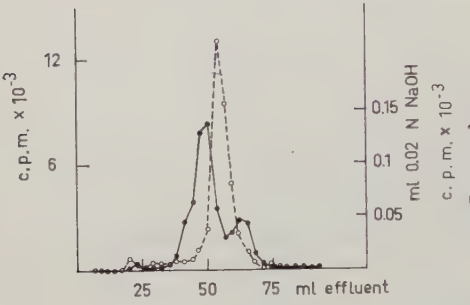

Fig. 8.

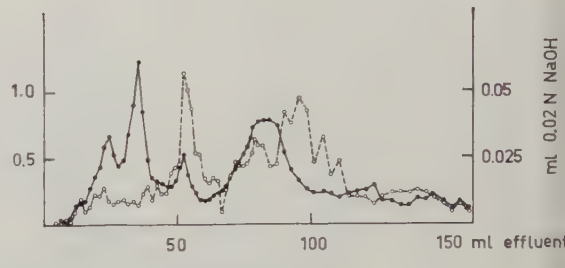

Fig. 9.

Fig. 8. Rechromatography of the radioactive material eluted between 30 and 45 ml of effluent in the chromatogram shown in Fig. 6 together with unlabeled 3β, 7α-dihydroxy-Δ^5-cholenic acid (peak at 50 ml of effluent). Solid line: titration values. Broken line: radioactivity. 4.5 g column. Phase system F 1.

Fig. 9. Rechromatography of radioactive material eluted between 12 and 30 ml of effluent in the chromatogram shown in Fig. 6 together with unlabeled cholic acid (peak at 85 ml of effluent). Solid line: titration values. Broken line: radioactivity. 4.5 g column. Phase system C 1.

The radioactivity eluted before above-mentioned acid (12–30 ml effluent, Fig. 6) was rechromatographed with unlabeled cholic acid using phase system C 1. As is seen in Fig. 9, none of the radioactivity coincided with the titration peak of cholic acid.

The radioactivity retained in the stationary phase of the column on which the "acidic" material originally was chromatographed (Fig. 6), was run on phase system F 2 with unlabeled 3β, 7α-dihydroxy-Δ^5-cholestenic acid obtained by saponification of the methyl ester. The radioactivity present in this fraction was found to be somewhat less polar than the added carrier acid.

Discussion

The present investigation on the metabolism of 7α-hydroxycholesterol in mouse liver homogenates fortified with DPN establishes the formation of Δ^4-cholestene-7α-ol-3-one, which had been suggested by Yamasaki and coworkers [5] on basis of presence of absorption at 240 mμ in chloroform extracts of incubations with 7α-hydroxycholesterol and of a parallel reduction of DPN. In addition, however, one other main metabolite, here designated A, is formed in whole homogenates of mouse liver. Also in rat liver homogenates this compound or compound(s) with similar chromatographic mobility is formed. The structure of compound A is not known but it is tempting to suggest a structure like Δ^4-cholestene-7α, 26-diol-3-one. The compound was somewhat less polar than Δ^5-cholestene-3β, 7α, 26-triol but much more polar than 7α-hydroxycholesterol. It exhibited an ultraviolet absorption spectrum characteristic of an α,β-unsaturated ketone. The calculated molar extinction coefficient was, however, fairly low, 8000, but this low value can be explained to some extent by an expected lower content of tritium in this compound as compared to 7α-hydroxycholesterol, the specific activity of which formed the basis for the calculation of the ε. The formation of labeled Δ^4-cholestene-7α-ol-3-one and in smaller

amounts of labeled Δ^5-cholestene-3β, 7α, 26-triol together with the presence of large amounts of DPN in the incubation mixture seem to favour the possibility of a structure similar to Δ^4-cholestene-7α, 26-diol-3-one for compound A. The manner in which compound A was metabolized in the bile fistula rat, yielding mainly chenodeoxycholic acid and 3α, 6β, 7β-trihydroxycholanic acid (a metabolite of chenodeoxycholic acid), agrees well with such a structure, as the presence of a hydroxyl in the side chain of a sterol lacking a 12α-hydroxyl group is oxidized to only a limited extent to cholic acid by the bile fistula rat (cf. ref. 2).

The "acidic" material formed in incubations of 7α-hydroxycholesterol with mouse liver homogenates accounted for about 5 % only of the total amount of 7α-hydroxycholesterol metabolized. However, it was found to consist of a complex mixture of acids none of which was identical with cholic or chenodeoxycholic acid.

In contrast to the considerable number of different acids formed from 7α-hydroxycholesterol, coprostane-3α, 7α-diol, when incubated with mouse liver homogenates, gives rise to only a few acidic products, among others chenodeoxycholic acid [18]. It appears possible, therefore, that some of the acids formed from 7α-hydroxycholesterol represent different stages in the epimerization of the 3β-hydroxyl and the saturation of the 5-double bond. If the oxidation of the side-chain of 7α-hydroxycholesterol followed the same pattern as that of coprostane-3α, 7α, 12α-triol, i.e. hydroxylation of carbon atom 26 and subsequent oxidation to a carboxyl group [19], 3β, 7α-dihydroxy-Δ^5-cholestenic acid or a derivative thereof would be formed. No evidence could, however, be obtained for the presence of 3β, 7α-dihydroxy-Δ^5-cholestenic acid among the acidic products, but an unknown acid of similar polarity was indeed formed. The isolation of labeled Δ^5-cholestene-3β, 7α, 26-triol and of compound A, which has been suggested to have the structure Δ^4-cholestene-7, 26-diol-3-one, appears to confirm the suggested pathway [19] for the degradation of the side-chain of C_{27}-steroids to C_{24}-bile acids.

SUMMARY

The metabolism of 7α-hydroxycholesterol in mouse liver homogenates has been studied and the metabolites formed have been separated by chromatography and partly identified.

The two main metabolities in incubations fortified by addition of DPN were Δ^4-cholestene-7α-ol-3-one and a compound that was more polar than 7α-hydroxycholesterol, compound A. Compound A for which the structure Δ^4-cholestene-7α, 26-diol-3-one has been suggested, was metabolized by the bile fistula rat to chenodeoxycholic acid and to some extent to cholic acid.

Δ^5-Cholestene-3β, 7α, 26-triol was identified as a minor metabolite of 7α-hydroxycholesterol.

Chromatographic separation of the acidic compounds formed in the incubations showed that these represented a complex mixture of unknown acids not identical with cholic or chenodeoxycholic acid.

ACKNOWLEDGEMENTS

The skilful technical assistance of Miss Birgitta Holmberg and Miss Marie-Louise Reinius is very gratefully acknowledged.

This work is part of investigations supported by *The National Institutes of Health, U.S. Public Health Service*, Bethesda, Md., USA (Grant H-2842) and has also been supported by a grant from *Karolinska Institutets Reservationsanslag.*

Department of Chemistry, Karolinska Institutet, Stockholm, Sweden.

REFERENCES

1. LINDSTEDT, S., Acta Chem. Scand. *11*, 417 (1957).
2. BERGSTRÖM, S., DANIELSSON, H., and SAMUELSSON, B., In Lipide Metabolism, ed. K. Bloch. Page 295–303. John Wiley and Sons, Inc., New York, 1960.
3. DANIELSSON, H., Acta Chem. Scand. *14*, 846 (1960).
4. DANIELSSON, H., Arkiv Kemi, 1961, in press.
5. YAMASAKI, K., NODA, F., and SHIMIZU, K., J. Biochem. Tokyo *46*, 739, 747 (1959).
6. BLOCH, K., and RITTENBERG, D., J. Biol. Chem. *149*, 505 (1943).
7. BIDE, H. E., HENBEST, H. B., JONES, E. R. H., PEEVERS, R. W., and WILKINSON, P. A., J. Chem. Soc. *1948*, 1783.
8. HENBEST, H. B., and JONES, E. R. H., J. Chem. Soc. *1948*, 1792.
9. DANIELSSON, H., Biochim. et Biophys. Acta *27*, 401 (1958).
10. DANIELSSON, H., Acta Chem. Scand. *15*, 242 (1961).
11. GREENHALGH, C. W., HENBEST, H. B., and JONES, E. R. H., J. Chem. Soc. *1952*, 2375.
12. HEUSLER, K., and WETTSTEIN, A., Helv. Chim. Acta *35*, 284 (1952).
13. HASLEWOOD, G. A. D., J. Chem. Soc. *1938*, 224.
14. STÄLLBERG, G., Arkiv Kemi *12*, 79 (1957).
15. BERGSTRÖM, S., and KRABISCH, L., Acta Chem. Scand. *11*, 1067 (1957).
16. BERGSTRÖM, S., Arkiv Kemi, Mineral. Geol. *16A* (1942) No. 10.
17. NORMAN, A., and SJÖVALL, J., J. Biol. Chem. *233*, 872 (1958).
18. BERSÉUS, O., and DANIELSSON, H., to be published.
19. DANIELSSON, H., Acta Chem. Scand. *14*, 348 (1960).

Tryckt den 3 maj 1961

Uppsala 1961. Almqvist & Wiksells Boktryckeri AB

ARKIV FÖR KEMI Band 17 nr 35

Communicated 12 April 1961 by Karl Myrbäck and Erik Jorpes

Formation and metabolism of 26-hydroxycholesterol

Bile acids and steroids 112

By Henry Danielsson

While the quantitative aspects of the degradation of cholesterol to bile acids and the metabolism of individual bile acids have been studied intensively, much less information is available concerning the sequence and detailed mechanisms of the reactions in the formation of bile acids from cholesterol. Bergström and Lindstedt [1] have concluded on the basis of investigations of the metabolism of hypothetical intermediates in the bile fistula rat that the modifications of the steroid nucleus precede the completion of the degradation of the side-chain and that one of the early steps is the introduction of the 7α-hydroxyl group.

The metabolism of cholesterol in liver homogenates has been studied mainly with respect to the ability of such preparations to oxidize the terminal methyl groups of cholesterol to carbon dioxide [2–4]. In a study of the metabolism of 4-^{14}C-cholesterol in fortified liver mitochondrial preparations, Fredrickson [5] and Fredrickson and Ono [6] found that in addition to acidic products of unknown structure, which were the main metabolites, labeled 25- and 26-hydroxycholesterol were formed. In a recent investigation of the oxidation of 4-^{14}C-cholesterol of high specific activity in liver mitochondrial preparations [7] it was found that both enzymatic and non-enzymatic oxidation of the added cholesterol occurred simultaneously. Two major enzymically formed compounds were isolated. The less polar of these two, compound III [7], was later found to be converted by the bile fistula rat into several unknown acids not identical with either cholic or chenodeoxycholic acid, and the structure of this compound has therefore not been further investigated. The other enzymic product, compound Ia [7], which was found to be somewhat more polar than 25-hydroxycholesterol and in chromatographic behaviour more similar to a saturated neutral C_{27}-sterol with three hydroxyl groups, was shown to be converted by the bile fistula rat into chenodeoxycholic acid [7–8]. Compound Ia has now been identified as 26-hydroxycholesterol corroborating the findings of Fredrickson and Ono [6]. However, no evidence could be obtained for the formation of 25-hydroxycholesterol in incubations of 4-^{14}C-cholesterol with fortified liver mitochondria. This communication also describes some preliminary studies on the metabolism of 26-hydroxycholesterol in mouse liver homogenates.

Experimental

Reference compounds. 25-Hydroxycholesterol, m.p. 179–181°, reported [9–10] 181.5–182.5° and 177–179°, was a generous gift of Dr. M. G. Horning. *26-Hydroxycholesterol,* m.p. 173–175°, reported [11] 177–178°, was generously supplied by Dr. E. Mosettig. *Cholestane-3β,5α,6β-triol,* m.p. 228–231°, reported [12–13] 229–233° and

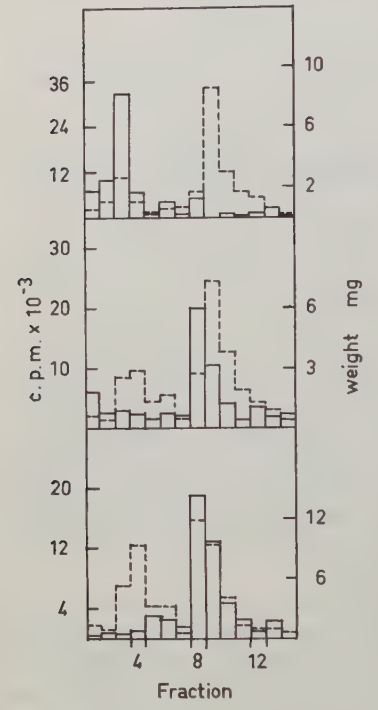

Fig. 1. Chromatography on 10 g columns of aluminum oxide, Woelm, grade II, of "trioxy neutral" fractions (cf. ref. 7) acetylated together with 26-hydroxycholesterol (uppermost), 25-hydroxycholesterol (middle) and cholestane-3β,5α,6β-triol (lower diagram). 25 ml fractions. Fraction 1, benzene, fractions 2–5, 1 % ethyl acetate in benzene and fractions 6–14, 3 % ethyl acetate in benzene. Solid bars, weight. Broken bars, radioactivity.

237–239°, was synthesized as described by Fieser and Rajagopalan [13]. *3β,7α-Dihydroxy-Δ^5-cholenic acid* and *25DL-Δ^5-cholestene-3β,7α,26-triol* were those described in the preceding paper [14].

Preparation of homogenates. 33 % homogenates (liver wet weight/volume) of mouse liver were prepared as described previously [7, 14].

Analyses of incubation mixtures. The procedures used were those described in the preceding paper [14], where also the phase systems used for reversed phase partition chromatography are listed.

The separation of 25-hydroxycholesterol, 26-hydroxycholesterol and cholestane-3β,5α,6β-triol by chromatography on aluminum oxide, Woelm grade II, was performed as described in a previous communication [7].

Results

Identification of 26-hydroxycholesterol as a metabolite of 4-^{14}C-cholesterol. Compound Ia, isolated by chromatography on aluminum oxide after conversion to the acetate and subsequent hydrolysis (7), was diluted with unlabeled 26-hydroxycholesterol and crystallized to constant specific activity both as free sterol and as the diacetate. In both cases the specific activity of the crystals remained constant after the first crystallization.

Absence of 25-hydroxycholesterol among the metabolites of 4-^{14}C-cholesterol. At an early stage [8] it was shown that from incubations of 4-^{14}C-cholesterol one main metabolite could be isolated that was somewhat more polar than 25-hydroxycholes-

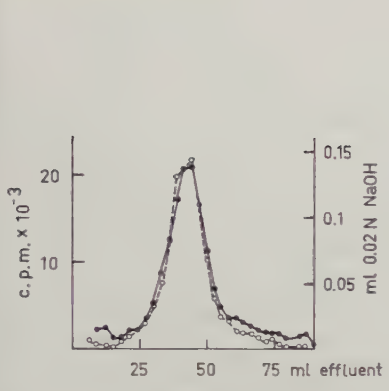

Fig. 2.

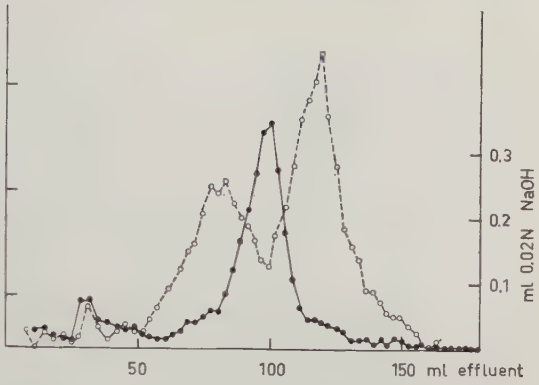

Fig. 3.

Fig. 2. Chromatography of the chenodeoxycholic acid fraction of the first 18 h of saponified bile from bile fistula rat injected with 4-^{14}C-26-hydroxycholesterol. Solid line: titration values. Broken line: radioactivity. 4.5 g column. Phase system F1.

Fig. 3. Chromatography of the cholic acid fraction of the same bile mentioned in legend to Fig. 2. 4.5 g column. Phase system C1.

terol and similar to a neutral saturated trihydroxylated C_{27}-sterol in chromatographic behaviour. Later it was found [7] that this metabolite was a mixture of cholestane-3β,5α,6β-triol and another compound Ia, which now has been identified as 26-hydroxycholesterol. To confirm these findings the "trioxy neutral" fraction (cf. ref. 7), in which any 25-hydroxycholesterol formed should be present, was isolated from an incubation of 20 μC 4-^{14}C-cholesterol with a fortified mouse liver mitochondrial preparation. This fraction was divided into three equal parts and 25-hydroxycholesterol, 26-hydroxycholesterol and cholestane-3β,5α,6β-triol respectively were added as carriers and the fractions acetylated.

Each fraction was then chromatographed on a 10 g column of aluminum oxide, Woelm grade II (Fig. 1). As is seen in Fig. 1, two main radioactive peaks were obtained, one in fractions 2–6 and the other in fractions 8–12. The first radioactive peak was eluted at the same place as the diacetate of 26-hydroxycholesterol (uppermost diagram, Fig. 1) and the identity was established by crystallization to constant specific activity. The second radioactive peak appeared together with the diacetate of cholestane-3β,5α,6β-triol (lower diagram, Fig. 1) and the identity was confirmed by crystallization to constant specific activity. The fractions containing the monoacetate of 25-hydroxycholesterol (middle diagram, Fig. 1) which was eluted somewhat earlier than the diacetate of cholestane-3β,5α,6β-triol, were combined and crystallized four times, after which the specific activity of the crystals had fallen to a value corresponding to the presence of 2 % of labeled monoacetate of 25-hydroxycholesterol in this material.

Metabolism of 26-hydroxycholesterol in the bile-fistula rat. When injected intraperitoneally into a bile fistula rat 4-^{14}C-labeled 26-hydroxycholesterol was rapidly excreted in bile as bile acids, 64 % of injected dose during the first 18 h after administration. Fractionation of the saponified bile into a cholic acid and a chenodeoxycholic acid fraction by chromatography on phase system F1 showed that 53 % of the

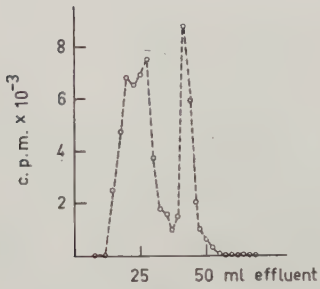

Fig. 4.

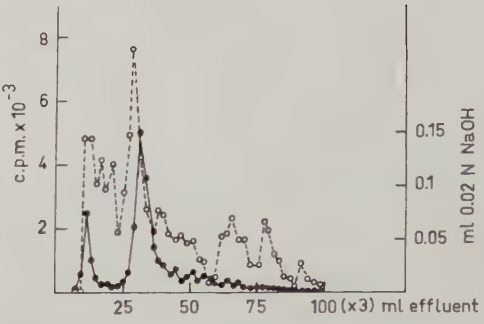

Fig. 5.

Fig. 4. Chloroform extract of an incubation of 4-^{14}C-26-hydroxycholesterol with mouse liver mitochondria and boiled liver juice. 4.5 g column. Phase system III.

Fig. 5. Chromatography of pooled incubations of 4-^{14}C-26-hydroxycholesterol with fractionated and unfractionated homogenates of mouse liver. 5 mg unlabeled chenodeoxycholic acid added (peak at 31 ml of effluent). Solid line: titration values. Broken line: radioactivity. 13.5 g column. Phase system F2.

labeled acidic products was present in the cholic acid fraction and the remainder in the chenodeoxycholic acid fraction. Rechromatography of the chenodeoxycholic acid fraction (Fig. 2) showed that the radioactivity coincided with the titration peak of chenodeoxycholic acid and the identity was established by isotope dilution. The cholic acid fraction was rechromatographed with phase system C1 and the radioactivity was found to be distributed mainly in two peaks appearing before and after the titration peak of cholic acid (Fig. 3). Although these labeled acids have not been identified conclusively, they have the same elution volumes as the two 6β-hydroxylated metabolites of chenodeoxycholic acid, 3α,6β,7α- and 3α,6β,7β-trihydroxycholanic acid respectively.

Metabolism of 26-hydroxycholesterol in vitro. Incubations of 4-^{14}C-labeled 26-hydroxycholesterol in quantities of a few μg with whole homogenates of mouse liver led to an extensive transformation of 26-hydroxycholesterol, 50–70 % of added label, into more polar products. Isolated mitochondria fortified by addition of boiled liver extract (cf. ref. 7) effected the same conversion and into the same products as judged by the chromatographic pattern of these. Fig. 4 shows a chromatogram of a chloroform extract of an incubation of 4-^{14}C-26-hydroxycholesterol (peak at 41 ml of effluent) with mitochondria and boiled liver juice. The radioactivity appearing before the peak of 26-hydroxycholesterol was shown by chromatography with phase system F2 to be a mixture of several different compounds and in subsequent experiments this phase system was therefore used instead of phase system III for analysis of the products formed.

For the purpose of a preliminary analysis of the products formed from 26-hyxycholesterol *in vitro*, material from incubations of both unfractionated and fractionated homogenates were pooled and subjected to chromatography with phase system F2 (Fig. 5). As is seen in Fig. 5, a number of different labeled compounds, more polar as well as less polar than chenodeoxycholic acid (peak at 31 ml of effluent), were present. About 40 % of the total radioactivity put on the column was retained in the stationary phase. This material was chromatographed with phase system III

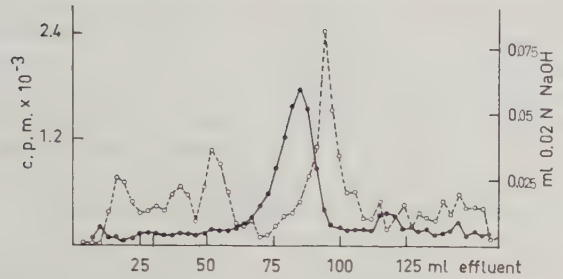

Fig. 6. Chromatogram of the early fraction, 10–20 ml of effluent, of chromatogram shown in Fig. 5, with 5 mg unlabeled cholic acid (peak at 85 ml of effluent). Solid line: titration values. Broken line: radioactivity. 4.5 g column. Phase system C1.

and was found to be eluted as a single peak with maximum at 39 ml of effluent, i.e. at the place where 26-hydroxycholesterol normally is eluted. The different radioactive peaks in the chromatogram shown in Fig. 5 were then chromatographed with known compounds.

The radioactive material appearing before 20 ml of effluent was pooled and chromatographed together with unlabeled cholic acid (peak at 85 ml of effluent, Fig. 6) on phase system C1. No radioactive peak was present that coincided with the titration peak of cholic acid (Fig. 6).

The labeled acid appearing somewhat earlier than the added unlabeled chenodeoxycholic acid, 25–35 ml of effluent (Fig. 5) was rechromatographed with unlabeled 3β,7α-dihydroxy-Δ^5-cholenic acid and was found to be slightly less polar than this acid (Fig. 7). This unknown metabolite or one with identical chromatographic properties, is formed also in incubations of 7α-hydroxycholesterol with mouse liver homogenates [14].

On chromatography of the labeled material eluted between 37 and 60 ml (Fig. 5) with synthetic Δ^5-cholestene-3β,7α,26-triol (Fig. 8), it was found that part of the radioactivity was associated with the carrier added, which was measured by the

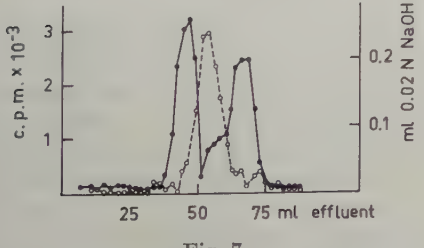

Fig. 7.

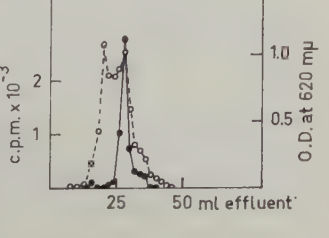

Fig. 8.

Fig. 7. Chromatogram of radioactive material from 25–35 ml effluent of chromatogram shown in Fig. 5 together with 8 mg unlabeled 3β,7α-dihydroxy-Δ^5-cholenic acid (peak at 47 ml of effluent). Solid line: titration values. Broken line: radioactivity. 4.5 g column. Phase system F1.

Fig. 8. Chromatogram of labeled material eluted between 37 and 60 ml of effluent of chromatogram shown in Fig. 5 together with 3 mg unlabeled Δ^5-cholestene-3β,7α,26-triol (peak at 28 ml of effluent) measured by the Lifschütz color reaction (14), solid line. Broken line: radioactivity. 4.5 g column. Phase system III.

Lifschütz color reaction [14]. Additional chromatography on a larger column and crystallization to constant specific activity established the presence of labeled Δ^5-cholestene-3β,7α,26-triol among the metabolites of 26-hydroxycholesterol.

The two radioactive bands with peaks at 65 and 78 ml of effluent respectively, were each chromatographed with unlabeled Δ^5-cholestene 3β,7α,26-triol on phase system III and both were found to be eluted close to, but distinctly after this compound. No clue to the structure of these two metabolites is at present available except that radioactive material of similar chromatographic mobility was present among the metabolites of 7α-hydroxycholesterol.

Discussion

In the present investigation the finding of Fredrickson and Ono [6] that labeled 26-hydroxycholesterol is formed from 4-^{14}C-cholesterol in a mouse liver mitochondrial system has been confirmed. However, in contrast to the results of these workers, it was not possible to isolate any labeled 25-hydroxycholesterol among the metabolites of 4-^{14}-C-cholesterol. The reason for this discrepancy is not known. Gurin and co-workers [15] have recently described the degradation of the side-chain of cholesterol *in vitro* to acetone by direct cleavage of the C_{24}-C_{25} bond. Likely intermediates in such a reaction would be compounds with hydroxyl groups at C_{24}, C_{25} or both. A similar type of reaction, i.e. hydroxylation(s) and subsequent cleavage of a C–C bond, has been postulated as the mechanism for the formation of pregnenolone and isocaproic aldehyde from cholesterol in the adrenal cortex [16–18].

The failure to isolate labeled 25-hydroxycholesterol as a metabolite of cholesterol could have a bearing on the possible mechanism of the degradation of the side-chain of cholesterol in the formation of bile acids. In an earlier communication [19] it was reported that coprostane-3α,7α,12α-triol *in vitro* was hydroxylated at C_{26} and subsequently converted to the C_{27}-acid. It was suggested that these two steps represented the initial mechanism in the degradation of the C_{27}-steroid side-chain to a C_{24}-bile acid. Very recently, Gurin and co-workers [20] have confirmed these findings concerning the metabolism of coprostane-3α,7α,12α-triol *in vitro*. The formation of 26-hydroxycholesterol from cholesterol is in agreement with such a formulation of the mechanism of the degradation of the side-chain of cholesterol in bile acid formation.

26-Hydroxycholesterol does not appear, however, to be any important intermediate in the formation of cholic acid in the bile fistula rat, but is metabolized predominantly to chenodeoxycholic acid and the two 6β-hydroxylated metabolites of chenodeoxycholic acid. In the experiment of Fredrickson and Ono [6] on the formation of bile acids from 26-hydroxycholesterol in the bile fistula rat, only one labeled bile acid was isolated which, as judged by paper chromatography, was very similar to, but not identical with cholic acid.

The results obtained on the further metabolism of 26-hydroxycholesterol *in vitro* indicate that this compound is readily hydroxylated in the 7α-position. The only metabolite so far identified was found to be Δ^5-cholestene-3β,7α,26-triol, which has been shown to be formed also from 7α-hydroxycholesterol *in vitro* [14]. Other evidence, although only circumstantial, for the ready 7α-hydroxylation of 26-hydroxycholesterol is the striking similarity in chromatographic properties of several metabolites of 26-hydroxycholesterol and 7α-hydroxycholesterol. This applies to the labeled compounds of polarity similar to that of cholic acid (Fig. 6, and Fig. 9 in

the preceding paper [14]) as well as to the radioactive compound, which had chromatographic mobility intermediate to that of 3β,7α-dihydroxy-Δ^5-cholenic acid and chenodeoxycholic acid (Fig. 7 and Fig. 8 [14]). In this connection it is worth mentioning that Usui and Yamasaki [21] recently have shown that 3β-hydroxy-Δ^5-cholenic acid is readily hydroxylated by rabbit liver in the 7-position, likely the 7α-position, but no configuration of the resulting acid was given.

SUMMARY

26-Hydroxycholesterol has been identified as a metabolite of 4-^{14}C-cholesterol in incubations with mouse liver mitochondrial preparations. The formation of 25-hydroxycholesterol from cholesterol under the same conditions could not be demonstrated.

4-^{14}C-26-hydroxycholesterol was found to be metabolized by the bile fistula rat predominantly to chenodeoxycholic acid and to the two 6β-hydroxylated metabolites of chenodeoxycholic acid.

Incubation of 4-^{14}C-26-hydroxycholesterol with unfractionated and fractionated homogenates of mouse liver yielded a number of different products. One of these was identified as Δ^5-cholestene-3β,7α,26-triol.

ACKNOWLEDGEMENTS

The very valuable technical assistance of Miss Birgitta Holmberg and Miss Marie-Louise Reinius is gratefully acknowledged.

This work is part of investigations supported by *The National Institutes of Health, U.S. Public Health Service*, Bethesda, Md., USA (Grant H-2842) and has also been supported by *Karolinska Institutets Reservationsanslag.*

Department of Chemistry, Karolinska Institutet, Stockholm, Sweden.

REFERENCES

1. Bergström, S., Danielsson, H., and Samuelsson, B., in Lipide Metabolism, ed. K. Bloch. Page 296 ff. John Wiley and Sons, Inc., New York, 1960.
2. Horning, M. G., Fredrickson, D. S., and Anfinsen, C. B., Arch. Biochem. Biophys. *71*, 266 (1957).
3. Whitehouse, M. W., Staple, E., and Gurin, S., J. Biol. Chem. *234*, 276 (1959).
4. Kritchevsky, D., Kolman, R. R., Whitehouse, M. W., Cottrell, M. C., and Staple, E., J. Lipid. Res. *1*, 83 (1959).
5. Fredrickson, D. S., J. Biol. Chem. *222*, 109 (1956).
6. Fredrickson, D. S., and Ono, K., Biochim. et Biophys. Acta *22*, 183 (1956).
7. Danielsson, H., Acta Chem. Scand. *14*, 846 (1960).
8. Danielsson, H., and Horning, M. G., Biochim. et Biophys. Acta *34*, 596 (1959).
9. Ryer, A. I., Gebert, W. H., and Murrill, N. M., J. Am. Chem. Soc. *72*, 4247 (1950).
10. Dauben, W. G., and Bradlow, H. L., J. Am. Chem. Soc. *72*, 4248 (1950).
11. Scheer, I., Thompson, M. J., and Mosettig, E., J. Am. Chem. Soc. *78*, 4733 (1956).
12. Dauben, W. G., and Payot, P. H., J. Am. Chem. Soc. *78*, 5657 (1956).
13. Fieser, L. F., and Rajagopalan, S., J. Am. Chem. Soc. *71*, 3938 (1949).
14. Danielsson, H., Arkiv Kemi, 1961 (in press).
15. Whitehouse, M. W., Staple, E., and Gurin, S., J. Biol. Chem. *236*, 68 (1961).
16. Shimizu, K., Dorfman, R. I., and Gut, M., J. Biol. Chem. *235*, PC 25 (1960).
17. Tchen, T. T., and Constantopoulos, G., J. Biol. Chem. *236*, 65 (1961).
18. Halkerston, I. D. K., Eichhorn, J., and Hechter, O., J. Biol. Chem. *236*, 374 (1961).
19. Danielsson, H., Acta Chem. Scand. *14*, 348 (1960).
20. Sulo, H. M., Staple, E., and Gurin, S., Fed. Proc. *20*, 284 a (1961).
21. Usui, T., and Yamasaki, K., J. Biochem. Tokyo, *48*, 226 (1960).

Tryckt den 3 maj 1961

Uppsala 1961. Almqvist & Wiksells Boktryckeri AB

ARKIV FÖR KEMI Band 17 nr 36

Communicated 12 April 1961 by K. Myrbäck and E. Jorpes

Synthesis and metabolism of Δ^5-cholestene-3β,12α-diol

Bile acids and steroids 113

By Henry Danielsson

With 2 figures in the text

According to current concepts [1] of the sequence of reactions in the formation of bile acids from cholesterol, the modifications of the steroid nucleus precede the completion of the side-chain degradation and one of the early steps is the introduction of the 7α-hydroxyl group, possibly with 7α-hydroxycholesterol as an early intermediate. These views are based on results of the metabolism of hypothetical intermediates in the bile fistula rat. Recently, the metabolism of 4-^{14}C-cholesterol [2], 7α-hydroxycholesterol [3] and 26-hydroxycholesterol [4] in mouse liver homogenates has been studied. The main enzymatic product formed from cholesterol was identified as 26-hydroxycholesterol [4]. Hydroxylation at C_{26} was one of the major reactions that took place also in incubations of 7α-hydroxycholesterol. Similarly, one of the main metabolites formed from coprostane-3α,7α-diol *in vitro* is the C_{26}-hydroxylated derivative, coprostane-3α,7α-26-triol [5]. These C_{26}-hydroxylated sterols lacking a 12α-hydroxyl group are metabolized predominantly to chenodeoxycholic acid in the bile fistula rat and yield cholic acid only in small amounts. It would seem that the introduction of the 12α-hydroxyl group is a crucial step which does not lend itself to easy reproduction *in vitro*. In fact, no evidence for the formation of a metabolite containing a 12α-hydroxyl group has been obtained in the above-mentioned *in vitro* studies.

The possibility that the introduction of the 12α-hydroxyl group could be one of the early steps did not seem entirely remote on account of the above-mentioned findings. Thus, it appeared of interest to study the metabolism of 12-hydroxycholesterol, i.e. Δ^5-cholestene-3β,12α-diol.

The present communication describes the synthesis of this compound labeled with tritium and its metabolism in the bile fistula rat.

Experimental

Melting points are uncorrected. All rotations were taken in chloroform solutions.

Coprostane-3α,12α-diol, m.p. 106–107°, reported [6] 108–110° (corr.), was prepared by electrolytic coupling of deoxycholic acid and *iso*valeric acid as described by Bergström and Krabisch [6]. About 10 mg of this material were labeled with tritium ac-

cording to the method of Wilzbach [7] in the apparatus described by Bergström and Lindstedt [8]. The labeled coprostane-3α,12α-diol was diluted with unlabeled diol and purified by repeated chromatography on aluminum oxide, Woelm, grade III (M. Woelm, Eschwege, W. Germany). The purified tritium-labeled coprostane-3α,12α-diol was diluted with more unlabeled diol to give 1.5 g of specific activity 138,000 c.p.m./μmole.

Coprostane-12α-ol-3-one. 1.5 g tritium-labeled coprostane-3α,12α-diol was refluxed for 21 h in 60 ml benzene and 24 ml acetone with 1.8 g aluminum *tert.*-butoxide, as described by Jones *et al.* [9]. The reaction mixture was then washed with 2 *N* sulfuric acid, sodium carbonate and water. The benzene layer was evaporated and the residue chromatographed on a 150 g column of Woelm, grade III, eluting with increasing concentrations of ethyl acetate in benzene. 20 % ethyl acetate in benzene eluted 1.26 g of coprostane-12α-ol-3-one. Crystallization twice from petroleum ether yielded 977 mg *coprostane-12α-ol-3-one* (specific activity 77,000 c.p.m./μmole), m.p. 122°, $[\alpha]_D^{24°} + 51°$ (*c*, 1.0). Calculated for $C_{27}H_{46}O_2$: C, 80.5 %; H, 11.5 %. Found: C, 80.8 %; H, 11.6 %.

Δ^4*-Cholestene-12α-ol-3-one dinitrophenylhydrazone.* 500 mg coprostane-12-α-ol-3-one were dissolved in 7 ml acetic acid and 0.5 ml of a solution of 0.26 ml bromine in 2 ml acetic acid was added [10]. The solution was then evaporated *in vacuo*. The residue was dissolved in 20 ml acetic acid and 300 mg dinitrophenylhydrazine added while the solution was warmed [11]. The dinitrophenylhydrazone started to precipitate after a few minutes and heating was interrupted after an additional 2 minutes. Cooling of the solution gave crystalline dinitrophenylhydrazone. Recrystallization from chloroform/ethanol yielded 261 mg Δ^4*-cholestene-12α-ol-3-one dinitrophenylhydrazone* (specific activity 73,000 c.p.m./μ mole), m.p. 237–239°, $\lambda_{max}^{CHCl_3}$ 390 mμ, $\varepsilon = 29{,}400$. Calculated for $C_{33}H_{48}N_4O_5$: C, 68.25 %; H, 8.3 %; N, 9.6 %. Found: C, 67.9 %; H, 8.4 %; N, 9.4 %.

Δ^4*-Cholestene-12α-ol-3-one.* 250 mg of the foregoing dinitrophenylhydrazone were treated in 12.5 ml chloroform with 18.8 ml pyruvic acid (Riedel–de Haën, Hannover, W. Germany) and 1.5 ml 4 *N* hydrogen bromide in acetic acid, as described by Djerassi [11]. This pyruvic acid yielded one layer with the chloroform. After 3 hours of warming at about 60° the solution was diluted with chloroform and washed with sodium carbonate and water. The chloroform extract was taken to dryness and the residue chromatographed on a 10 g column of Woelm, grade III. Δ^4-Cholestene-12α-ol-3-one was eluted with 10 % ethyl acetate in benzene. In spite of chromatography the material was colored and therefore treated with Norit in ethyl acetate. After this treatment 106 mg of the ketone was recovered. Crystallization from methanol/water yielded 85 mg Δ^4*-cholestene-12α-ol-3-one* (specific activity 67,000 c.p.m./μmole), m.p. 142–143°, $[\alpha]_D^{24°} + 86°$ (*c*, 0.8), λ_{max}^{EtOH} 241 mμ, $\varepsilon = 17{,}500$.

Δ^5*-Cholestene-3β,12α-diol.* The enol-acetate of Δ^4-cholestene-12α-ol-3-one was prepared as described by Djerassi *et al.* [12]. 60 mg of Δ^4-cholestene-12α-ol-3-one were dissolved in 5 ml benzene containing 7.5 mg *p*-toluene sulfonic acid and 0.2 ml *iso*-propenyl acetate and the solution slowly concentrated to about two-thirds of its volume by distillation over a period of 3 h. After the first and second hour an additional 0.1 ml *iso*propenyl acetate was added. The solution was evaporated to dryness, the residue taken up in ether containing one drop of pyridine and the ether was washed with sodium carbonate and water. The residue had an ultraviolet absorption maximum at 236 mμ in ethanol, i.e. a shift of 5 mμ compared with the starting ketone and an ε of approximately 17,000. This material was then dissolved in 30 ml methanol and

reduced at room temperature for 2 h with 120 mg sodium borohydride in 4 ml of 70 % aqueous methanol as described by Belleau and Gallagher [13]. After acidification and extraction with ether the ether extract was evaporated and the residue dissolved in 40 ml dry ether and reduced with 60 mg lithium aluminum hydride for 2 h at room temperature to remove the acetoxy group at C_{12}. The reaction mixture was worked up as above and the residue chromatographed on a 20 g column of Woelm III, eluting with increasing concentrations of ethyl acetate in benzene. Δ^5-Cholestene-3β,12α-diol (39 mg) was eluted with 15 % ethyl acetate in benzene. Crystallization from acetone/water yielded 19 mg as needles of *Δ^5-cholestene-3β,12α-diol* (specific activity 59,000 c.p.m./μmole), m.p. 149–150°, $[\alpha]_D^{24°} - 27°$ (c, 0.69). Calculated for $C_{27}H_{46}O_2$: C, 80.5 %; H, 11.5 %. Found: C, 80.7 %; H, 11.45 %.

Animal experiments. The procedures used in the analysis of bile from bile fistula rats have recently been described [14].

Results and discussion

When injected intraperitoneally into a bile fistula rat, randomly tritium-labeled 12-hydroxycholesterol (Δ^5-cholestene-3β,12α-diol) was excreted rapidly in bile, 32 % of a 2 mg dose during the first 24 h after injection, mainly as bile acids. Chromatography of the saponified bile on phase system F1 (Fig. 1) showed that the radioactivity eluted was present in two main peaks, one appearing together with the cholic acid present in bile, peak at 27.5 ml of effluent, and one of a polarity intermediate to that of cholic and chenodeoxycholic acid, which has its peak at 60 ml of effluent. 26 % of the total radioactivity put on the column was retained in the stationary phase. The main part of the radioactive material present in the cholic acid fraction was shown to be identical with cholic acid by rechromatography on phase system C1 (Fig. 2) and by subsequent isotope dilution. No further work has yet been done on the structure of the labeled acid that was eluted between cholic and chenodeoxycholic acid in the chromatogram shown in Fig. 1.

Two possible mechanisms for the formation of cholic acid from 12-hydroxycholesterol can be visualized. On the one hand, 12-hydroxycholesterol could be hydroxylated

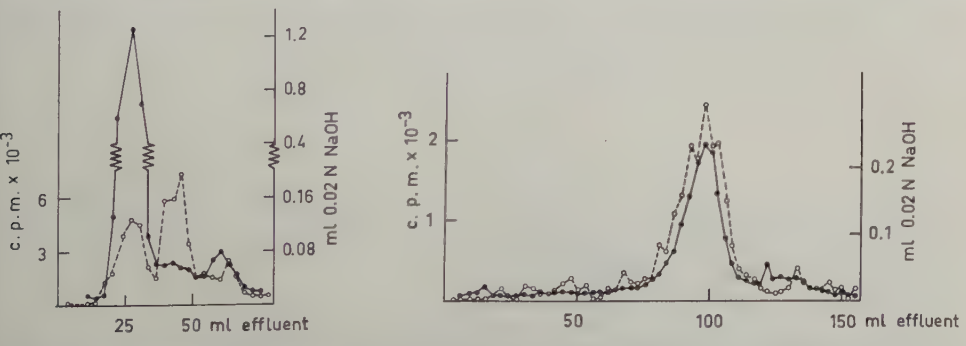

Fig. 1. Chromatography of the first 24 h portion of saponified bile from bile fistula rat injected with Δ^5-cholestene-3β,12α-diol. Solid line: titration values. Broken line: radioactivity. 4.5 g column. Phase system F1.

Fig. 2. Rechromatography of the cholic acid fraction from chromatogram shown in Fig. 1. Solid line: titration values. Broken line: radioactivity. 4.5 g column. Phase system C1.

in the 7α-position before the side-chain is degraded. On the other hand, the side-chain of 12-hydroxycholesterol might be oxidized prior to the introduction of the 7α-hydroxyl group, possibly with the intermediate formation of deoxycholic acid. In the case of the latter mechanism, discussions of the possible bearing of the present results on the sequence in the formation of bile acids from cholesterol must take into account the fact that deoxycholic acid is rapidly hydroxylated at C_7 by rat liver [15]. Hence, the labeled cholic acid formed from labeled 12-hydroxycholesterol would represent only a metabolite of initially formed deoxycholic acid. However, in the chromatogram shown in Fig. 1 there is no appreciable amount of radioactivity eluted at the place of deoxycholic acid, which does not separate from chenodeoxycholic acid with this phase system. It is possible, though, that the 7α-hydroxylation of deoxycholic acid is so rapid that this acid does not accumulate. If the labeled cholic acid is formed from 12-hydroxycholesterol with deoxycholic acid as an intermediate, it would mean that the rat liver is able to synthesize deoxycholic acid from a suitable precursor. According to present knowledge deoxycholic acid is formed only by microbial action on cholic acid during the enterohepatic circulation of bile, in rat [16] as well as in other species [1].

To establish the direct formation of cholic acid from 12-hydroxycholesterol, the rabbit would be a suitable experimental animal, as in this species, deoxycholic acid cannot be hydroxylated by the liver to cholic acid [17].

SUMMARY

A method of synthesis of Δ^5-cholestene-3β,12α-diol (12-hydroxycholesterol) is described.

The metabolism of tritium labeled Δ^5-cholestene-3β,12α-diol in the bile fistula rat has been investigated, and it has been shown that this compound in part is converted to cholic acid.

ACKNOWLEDGEMENTS

The very valuable technical assistance of Miss Birgitta Holmberg and Miss Marie-Louise Reinius is gratefully acknowledged.

This work is part of investigations supported by a grant (H-2842) from *The National Institutes of Health, U.S. Public Health Service*, Bethesda, Md., USA, and has also been supported by a grant from *Karolinska Institutets Reservationsanslag.*

Department of Chemistry, Karolinska Institutet, Stockholm, Sweden.

REFERENCES

1. Bergström, S., Danielsson, H., and Samuelsson, B., In Lipide Metabolism, ed. K. Bloch, page 296 ff. John Wiley and Sons, Inc., New York, 1960.
2. Danielsson, H., Acta Chem. Scand. *14*, 846 (1960).
3. Danielsson, H., Arkiv Kemi, 1961 (in press).
4. Danielsson, H., Arkiv Kemi, 1961 (in press).
5. Berséus, O., and Danielsson, H. (to be published).
6. Bergström, S., and Krabisch, L., Acta Chem. Scand. *11*, 1067 (1957).
7. Wilzbach, K. E., J. Am. Chem. Soc. *79*, 1013 (1957).
8. Bergström, S., and Lindstedt, S., Acta Chem. Scand. *11*, 1275 (1957).
9. Jones, A. S., Webb, M., and Smith, F., J. Chem. Soc. *1949*, 2164.
10. Burckhardt, V., and Reichstein, T., Helv. Chim. Acta *25*, 821 (1942).
11. Djerassi, C., J. Am. Chem. Soc. *71*, 1003 (1949).

12. DJERASSI, C., MANCERA, O., VELASCO, M., STORK, G., and ROSENKRANZ, G., J. Am. Chem. Soc. *74*, 3321 (1952).
13. BELLEAU, B., and GALLAGHER, T. F., J. Am. Chem. Soc. *73*, 4458 (1951).
14. DANIELSSON, H., Acta Chem. Scand. *15*, 242 (1961).
15. BERGSTRÖM, S., ROTTENBERG, M., and SJÖVALL, J., Z. physiol. Chem. *295*, 278 (1953).
16. NORMAN, A., and SJÖVALL, J., J. Biol. Chem. *233*, 872 (1958).
17. LINDSTEDT, S., and SJÖVALL, J., Acta Chem. Scand. *11*, 421 (1957).

Tryckt den 3 maj 1961

Uppsala 1961. Almqvist & Wiksells Boktryckeri AB

ARKIV FÖR KEMI Band 17 nr 37

Mitgeteilt am 25. Januar 1961 durch Arne Fredga

Beiträge zur Chemie α-substituierter Sulfide. IV*

Über in 3-Stellung aliphatisch substituierte 4-Thiaisochroman-1-one

Von Alexander Senning und Sven-Olov Lawesson

In zwei früheren Mitteilungen [1, 2] berichteten wir über die Umsetzung von Thiosalizylsäure mit Aldehyden in siedendem Eisessig in Gegenwart von Chlorwasserstoff, die in durchschnittlich 50%iger Ausbeute das in der Methylengruppe substituierte Methylen-bis-(*o*-karboxyphenylsulfid) (I) und in durchschnittlich 25%iger Ausbeute das in 3-Stellung substituierte 4-Thiaisochroman-1-on (II) liefert.

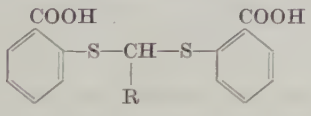

I

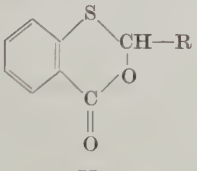

II

Diese Umsetzung, deren Ausführung einer von Bistrzycki [3] für die Darstellung substituierter 1,3-Thioxolan-4-one gegebenen Vorschrift folgt, ist, wie aus den Ausbeuteverhältnissen hervorgeht, besser für die Darstellung der Merkaptale als für die der 4-Thiaisochroman-1-on-derivate geeignet. Bei der Suche nach einer günstigeren Darstellungsmöglichkeit für die 4-Thiaisochroman-1-one spielte auch eine Rolle, dass es, um einerseits ungesättigte und andererseits empfindlichere Aldehyde in dieser Reaktion einsetzen zu können, wünschenswert war, ohne Chlorwasserstoff und gleichzeitig bei einer niedrigeren Temperatur zu arbeiten.

Modellversuche mit Benzaldehyd zeigten, dass die Ausbeute an 3-Phenyl-4-thiaisochroman-1-on auf rund 50 % steigt, wenn man die Umsetzung in Abwesenheit von Chlorwasserstoff durchführt, während die sauren Produkte ein schwer zu trennendes Gemisch verschiedener Säuren darstellen (die experimentellen Daten werden in unserer nächsten Mitteilung enthalten sein). Besonders günstige Bedingungen für die Bildung von 4-Thiaisochroman-1-on-derivaten erhielten wir, als wir Thiosalizylsäure in Benzollösung mit einem geringen Überschuss an Aldehyd in Gegenwart einer katalytischen Menge *p*-Toluolsulfonsäure am Rückfluss kochten (ohne Zusatz von *p*-Toluolsulfonsäure erhält man das Ausgangsmaterial unverändert zurück) und das entstehende Wasser mit Hilfe eines Veresterungsaufsatzes aus dem Reaktions-

* III. Mitteilung siehe Literaturzitat [2].

gemisch entfernten. Auf diese Weise gelang es uns in den meisten Fällen, gute Ausbeuten der 4-Thiaisochroman-1-on-derivate zu erhalten. Im Falle des Paraldehyds gelingt die Umsetzung unter diesen Bedingungen nicht, dagegen erhält man das 3-Methyl-4-thiaisochroman-1-on in guter Ausbeute, wenn man die Umsetzung in Eisessig durchführt. Im Versuchsteil soll über eine Reihe derartiger Umsetzungen von Thiosalizylsäure mit aliphatischen Aldehyden berichtet werden.

Ein kurzer Überblick über die in der Literatur beschriebenen 4-Thiaisochroman-1-on-derivate zeigt, dass vor unseren Untersuchungen kein einfacher und allgemein gangbarer Weg zu in 3-Stellung aliphatisch substituierten 4-Thiaisochroman-1-on-derivaten bekannt war. Spezielle Reaktionen, die zu kompliziert substituierten 4-Thiaisochroman-1-on-derivaten führen, sind von Kaufmann [4] und Chandra [5] beschrieben worden. Die von Mowry [6] gefundene Reaktion von Thiosalizylsäure mit Vinylazetat, die über Addition an die Doppelbindung und anschliessende Abspaltung von Essigsäure zum 3-Methyl-4-thiaisochroman-1-on führt, eignet sich nicht zur Einführung homologer Substituenten in 3-Stellung und die Umsetzung von Thiosalizylsäure mit Aldehyddiazetaten nach Mowry [7] ist nur auf aromatische Aldehyde anwendbar. Böhmes [8] Darstellung des 3-Trichlormethylderivates durch Zusammengeben und Erwärmen der Komponenten Thiosalizylsäure und Chloral stellt einen Spezialfall dar, der durch die wasserabspaltende Wirkung des Chlorals zu erklären ist. Beim Arbeiten nach Böhmes Vorschrift konnten wir die angegebene Ausbeute nicht erreichen. Wir fanden es günstig, einen grösseren Überschuss an Chloral oder ein anderes Lösungsmittel, z. B. Benzol, zu verwenden (arbeitet man nach der von uns beschriebenen Methode, kann man selbstverständlich statt von Chloral auch von Chloralhydrat ausgehen).

Während in Mowrys Arbeiten [6, 7] stillschweigend eine weitgehende Analogie der Reaktionen der Salizylsäure und der Thiosalizylsäure vorausgesetzt wird, zeigt ein Vergleich des Verhaltens bei der säurekatalysierten Reaktion mit Aldehyden, dass die Sulfhydrylgruppe im Gegensatz zur Hydroxylgruppe keinen nennenswerten substitutionserleichternden Einfluss auf die Parastellung ausübt. Während Aldehyde Salizylsäure in Gegenwart katalytischer Mengen Säure zu Triphenylmethanderivaten substituieren (Mowry [7] gibt eine eingehende Darstellung derartiger Reaktionen mit zahlreichen Literaturhinweisen) wird der Benzolkern der Thiosalizylsäure bei derselben Reaktion nicht merklich angegriffen. Entsprechende Verhältnisse wurden im Falle des Anisols und des Thioanisols beobachtet. Im Gegensatz zum Anisol, das ohne weiteres im Kern substituiert wird, lässt sich beim Thioanisol auch bei langzeitiger Einwirkung eines Überschusses von Chlor nur wenig Trichlormethyl-*p*-chlorphenylsulfid isolieren [9].

In der Patentliteratur sind einige 4-Thiaisochroman-1-on-derivate zusammen mit den homologen 1,3-Benzdioxan-4-on-derivaten als Insektizide beschrieben worden [10]. Eine Untersuchung der von uns dargestellten Derivate auf ihre biologische Aktivität ist im Gange. Wir werden zu einem späteren Zeitpunkt über die Ergebnisse dieser Untersuchung berichten.

Auch Aldehyde, mit denen sich nach anderen Methoden das 4-Thiaisochroman-1-on-derivat gar nicht oder nur in geringer Menge gewinnen lässt, liefern nach der hier beschriebenen Methode gute Ausbeuten der Ringschlussverbindung. 2-Thiophenaldehyd z. B. liefert das 2-Thienylderivat in 71 % Ausbeute, während die Umsetzung in Eisessig nur 2 % Ausbeute ergab [2]. Eine Untersuchung der Umsetzungen ähnlicher Aldehyde (u. a. Furfurol und Vanillin) ist in Arbeit und soll Gegenstand unserer nächsten Mitteilung sein.

Beschreibung der Versuche

Alle Schmelz- und Siedepunkte sind unkorrigiert. Die Analysen wurden im Institut für Analytische Chemie der Universität Uppsala ausgeführt.

Die Thiosalizylsäure wurde von der Firma Schuchardt, München bezogen und schmolz zwischen 161° und 164° (Literatur: F: 164°).

Versuchsanordnung

Methode A. In einem 1-*l*-Kolben, der mit einem Rührer und einem Veresterungsaufsatz versehen war, wurde ein Gemisch von 0,10 Mol Thiosalizylsäure, 0,12 Mol Aldehyd, 1 g *p*-Toluoslulfonsäure und 500 ml Benzol etwa 3 Stunden am Rückfluss gekocht, wobei sich das gebildete Wasser im Veresterungsaufsatz ansammelte. Bei verhältnismässig niedrig siedenden Aldehyden wurde ein grösserer Überschuss an Aldehyd verwendet. Nach beendigter Umsetzung wurde die erkaltete Lösung von eventuellen Trübungen abfiltriert und nach Zusatz von etwa 150 ml Äther solange mit verdünnter Sodalösung ausgeschüttelt, bis die alkalische Reaktion der wässrigen Phase bestehen blieb. Anschliessend wurde die organische Phase mit Wasser neutral gewaschen, getrocknet und eingeengt. Flüssige Produkte wurden durch Destillation gereinigt, feste durch Umkristallisieren.

Methode B. In einem 1-*l*-Kolben mit Rückflusskühler und aufgesetztem Chlorkalziumrohr wurden äquivalente Mengen Thiosalizylsäure und Aldehyd in 300 bis 500 ml Eisessig 3 Stunden am Rückfluss gekocht. Anschliessend wurde auf ein kleines Volumen eingeengt, abfiltriert und die Lösung in einen Überschuss kaltes Wasser gegossen. Feste Produkte wurden abfiltriert und mit verdünnter Sodalösung digeriert. Flüssige Produkte wurden mit Äther aufgenommen und weiterbehandelt wie bei Methode A.

4-Thiaisochroman-1-on

Methode B. Ausgangsmaterial: 46,2 g (0,3 Mol) Thiosalizylsäure und 9,0 g (0,3 Mol) Paraformaldehyd. Rohausbeute 31,8 g = 64 % der Theorie. F: 34°–42° (Literatur [1]: F: 45°–47°). Nach Umkristallisieren aus leichtsiedendem Petroläther F: 45°–47°.

3-Methyl-4-thiaisochroman-1-on

Methode B. Ausgangsmaterial: 30,8 g (0,20 Mol) Thiosalizylsäure und 57,2 g (1,30 Mol) Paraldehyd. Bei der Destillation gingen zwischen 125°/5 mm und 141°/5 mm 17,4 g = 48 % der Theorie über (F: 45°–46°). Nach einmaligem Umkristallisieren aus Alkohol schmolz die Substanz zwischen 54° und 56° (Literatur [6]: F: 57°). Nach Methode A wurde kein Produkt erhalten.

3-Trichlormethyl-4-thiaisochroman-1-on

Methode B. Ausgangsmaterial: 23,1 g (0,15 Mol) Thiosalizylsäure und 22,1 g (0,15 Mol) Chloral (Firma Schuchardt, $n_D^{20} = 1{,}4622$; Literatur $n_D^{20} = 1{,}45572$). Das Rohprodukt schmolz zwischen 95° und 100° und wog 32,4 g = 77 % der Theorie. Nach einmaligem Umkristallisieren aus Essigester schmolz die Substanz zwischen 98° und 100° (Literatur [8]: F: 98°).

Methode A. Ausgangsmaterial: 15,4 g (0,10 Mol) Thiosalizylsäure und 19,8 g (0,12 Mol) Chloralhydrat. Rohprodukt 13,0 g = 46 % der Theorie (F: 96°–100°).

3-Tribrommethyl-4-thiaisochroman-1-on

Methode A. Ausgangsmaterial: 15,4 g (0,10 Mol) Thiosalizylsäure und 33,7 g (0,12 Mol) Bromal (ein Präparat der Firma Schuchardt ohne Angabe des Reinheitsgrades, das trotz einer leichten Färbung ohne weitere Reinigung verwendet wurde. Während der Umsetzung war eine leichte Bromwasserstoffentwicklung zu beobachten). Rohausbeute 19,5 g = 47 % der Theorie (F: 156°–158°). Mehrmals aus Alkohol umkristallisiert schmolz das 3-Tribrommethyl-4-thiaisochroman-1-on (farblose dünne Tafeln) zwischen 158° und 159°.

$C_9H_5Br_3O_2S$ gef. Br 57,28 %; S 7,58 %
ber. Br 57,50 %; S 7,69 %

3-n-Propyl-4-thiaisochroman-1-on

Methode A. Ausgangsmaterial: 15,4 g (0,10 Mol) Thiosalizylsäure und 28,8 g (0,40 Mol) *n*-Butyraldehyd. Zwischen 120°/0,1 mm und 127°/0,1 mm gingen 12,9 g = 62 % der Theorie Rohprodukt über (n_D^{20} = 1,5745). Die analysenreine Substanz hatte Kp. 164°/2 mm und n_D^{20} = 1,5766.

$C_{11}H_{12}O_2S$ gef. C 63,40 %; H 5,85 %; S 15,25 %
ber. C 63,43 %; H 5,81 %; S 15,40 %

3-i-Propyl-4-thiaisochroman-1-on

Methode A. Ausgangsmaterial: 15,4 g (0,10 Mol) Thiosalizylsäure und 18,0 g (0,25 Mol) Isobutyraldehyd. Zwischen 127°/0,1 mm und 129°/0,1 mm gingen 12,0 g = 58 % der Theorie über (n_D^{20} = 1,5767). Die analysenreine Substanz hatte Kp. 170°/12 mm–171°/12 mm und n_D^{20} = 1,5774.

$C_{11}H_{12}O_2S$ gef. C 63,35 %; H 5,90 %; S 15,21 %
ber. C 63,43 %; H 5,81 %; S 15,40 %

3-(β-Styryl)-4-thiaisochroman-1-on

Methode A. Ausgangsmaterial: 15,4 g (0,10 Mol) Thiosalizylsäure und 15,8 g (0,12 Mol) Zimtaldehyd (n_D^{20} = 1,6215; Literatur: n_D^{20} = 1,6195). Rohausbeute 18,0 g = 69 % der Theorie (F: 88°–96°). Nach mehrmaligem Umkristallisieren aus Alkohol schmolz das 3-(β-Styryl)-4-thiaisochroman-1-on (farblose Nadeln) zwischen 100° und 102°.

$C_{16}H_{12}O_2S$ gef. C 71,62 %; H 4,51 %; S 11,92 %
ber. C 71,62 %; H 4,51 %; S 11,95 %

3-(1-Propenyl)-4-thiaisochroman-1-on

Methode A. Ausgangsmaterial: 15,4 g (010 Mol) Thiosalizylsäure und 8,4 g (0,12 Mol) frisch destillierter Krotonaldehyd. Destillation unter Stickstoffatmosphäre lieferte zwischen 123°/0,1 mm und 133°/0,1 mm 2,9 g Produkt (=14 % der Theorie). Die analysenreine Substanz hatte Kp. 125°/0,1 mm–126°/0,1 mm und n_D^{20} = 1,6011.

$C_{11}H_{10}O_2S$ gef. C 64,17 %; H 4,91 %; S 15,42 %
ber. C 64,05 %; H 4,89 %; S 15,55 %

3-n-Undezyl-4-thiaisochroman-1-on

Methode A. Ausgangsmaterial: 15,4 g (0,10 Mol) Thiosalizylsäure und 22,0 g (0,12 Mol) Laurinaldehyd (F: 36°–38°; Literatur: F: 44,5°). Nach einem Vorlauf von

Laurinaldehyd lieferte die Destillation zwischen 204°/0,1 mm und 210°/0,1 mm 18,3 g Produkt (=57 % der Theorie). Das Destillat wurde in Äther gelöst und bei −14° aufbewahrt. Auf diese Weise wurde die Verbindung kristallin erhalten. Nach mehrmaligem Umkristallisieren aus Äther schmolz das 3-n-Undezyl-4-thiaisochroman-1-on (farblose schmale Tafeln) zwischen 37° und 38°.

Nach Methode B wurden von 30,8 g (0,20 Mol) Thiosalizylsäure und 36,8 g (0,20 Mol) Laurinaldehyd ausgehend 18,5 g (27 % der Theorie) Produkt erhalten.

$C_{19}H_{28}O_2S$	gef. C 71,42 %;	H 8,87 %;	S 9,63 %
	ber. C 71,20 %;	H 8,81 %;	S 10,00 %

ZUSAMMENFASSUNG

In 3-Stellung aliphatisch oder aromatisch substituierte 4-Thiaisochroman-1-one, die man bei der Darstellung von in der Methylengruppe substituierten Methylen-bis-(*o*-karboxysulfiden) in durchschnittlich 25 %iger Ausbeute als Nebenprodukt erhält [1, 2], werden in guter Ausbeute erhalten, wenn man die Umsetzung des Aldehyds mit Thiosalizylsäure in Gegenwart von *p*-Toluolsulfonsäure in Benzol durchführt und das gebildete Wasser mit Hilfe eines Veresterungsaufsatzes aus dem Reaktionsgemisch entfernt. Auch die Umsetzung der Komponenten in siedendem Eisessig (in Abwesenheit von Chlorwasserstoff) liefert in vielen Fällen gute Ausbeuten. Nach diesen Methoden wurden sechs neue und drei bekannte 4-Thiaisochroman-1-on-derivate dargestellt.

Wir sind dem Institutsvorstand, Herrn Professor A. Fredga, für die Überlassung des Arbeitsplatzes und *Jordbrukets Forskningsråd* für die finanzielle Unterstützung unserer Arbeit zu Dank verpflichtet.

Laboratorium für Organische Chemie, Chemisches Institut der Universität Uppsala, Uppsala, Schweden.

LITERATUR

1. Senning, A. und Lawesson, S.-O., Acta Chem. Scand. *14*, 2230 (1960).
2. Senning, A. und Lawesson, S.-O., Arkiv Kemi *17*, 261 (1961).
3. Bistrzycki, A. und Brenken, B., Helv. chim. Acta *3*, 447 (1920).
4. Kaufmann, H. P. und Rossbach, E., Ber. *58*, 1556 (1925).
5. Chandra, K., Chakrabarty, N. K. und Mitra, S. K., J. Indian Chem. Soc. *19*, 139 (1942).
6. Mowry, D. T., Yanko, W. H. und Ringwald, E. L., J. Am. Chem. Soc. *69*, 2358 (1947).
7. Mowry, D. T., J. Am. Chem. Soc. *69*, 2362 (1947).
8. Böhme, H. und Schmidt, W., Arch. Pharm. *286*, 330 (1953).
9. Egen, R., Dissertation. Erlangen, 1951.
10. Monsanto Chemical Co., Brit. Pat. 640570, CA *45*, 8560 (1951); Monsanto Chemical Co. (Nason, H. K. und Mowry, D. T.), US Pat. 2496741, CA *44*, 5522 (1950); Monsanto Chemical Co. (Nason, H. K. und Mowry, D. T.), Brit. Pat. 645130, CA *45*, 5726 (1951).

Tryckt den 3 maj 1961

Uppsala 1961. Almqvist & Wiksells Boktryckeri AB